JOINT INTERNATIONAL CONFERENCE ON

Hyperfine Interactions

AND SYMPOSIUM ON

Nuclear Quadrupole Interactions 2014

hfi nqi
2014
Canberra

www.hfinqi.consec.com.au

SUNDAY 21 SEPTEMBER – FRIDAY 26 SEPTEMBER 2014

THE SHINE DOME CANBERRA AUSTRALIA

Conference Handbook
Program and Abstracts

magritek
Spinsolve Carbon

CONTENTS

Abstracts

PRESENTED BY:

Professional Conference Managers

consec

Consec – Conference Management
PO Box 3127
BMDC ACT 2617 Australia

Telephone: +61 2 6252 1200
Facsimile: +61 2 6252 1222
Email: hfinqi2014@consec.com.au
Website: www.hfinqi.consec.com.au

Conference Manager
Barry NeameCEM, PCO-DIR

Sponsorship/Exhibition Manager
Aaron Neame

Conference Coordinator
Charmaine Ogilvie BA (Comm&Media)

WELCOME

As Conference Chairs and on behalf of the international committee and the local organising committees, we would like to warmly welcome you to Canberra for the 5th Joint International Conference on Hyperfine Interactions and Symposium on Nuclear Quadrupole Interactions (HFI/NQI 2014).

Looking back on a successful conference tradition and the four recent meetings in Bonn, Iguassu Falls, CERN and Beijing, this year the conference is presented by the Australian National University and the University of New South Wales. We meet at the spiritual home of Australian Science, the uniquely designed Shine Dome of the Australian Academy of Sciences in, the Australian capital. HFI/NQI 2014 is the 17th International Conference on Hyperfine Interactions and the 21st International Symposium on Nuclear Quadrupole Interactions.

September is a beautiful time of year in Canberra, when spring tends to offer sunny days and a colourful palette of blooms. The conference venue is in the heart of the city making it easy for you to participate in conference events, while being within walking distance of accommodation, museums, sights and Canberra's entertainment venues. We hope that the social events of the conference will give you an impression of the modernity of our city, its hospitality and its beautiful surrounds.

In line with previous meetings, we have endeavoured to make HFI/NQI 2014 a forum for the discussion and publication of all aspects of hyperfine interactions, detected by nuclear radiations and of all facets of nuclear quadrupole interactions, detected by resonance methods. As you see from this booklet, the conference program also includes many and diverse associated applications.

The international committee has invited speakers presenting on topics on the forefront of our field and selected a diverse spectrum of oral contributions with presenters originating from all continents. The organisers have tried to interweave the two poster sessions with the oral program by including selected briefs on posters in the oral program and stage the poster sessions in the break-out area of the auditorium. We hope that the diverse and engaging program of the conference will stimulate lively debate and discussion.

Enjoy HFI/NQI 2014 and advancing your research!

Conference Chairs
Wayne Hutchison, Andrew Stuchbery, Heiko Timmers

THE HFI/NQI CONFERENCE SERIES

The four recent meetings in this series were held in Bonn (Germany), Iguassu Falls (Argentina/Brazil), CERN (Switzerland) and Beijing (China). The respective Conference-Chairs have kindly provided brief summaries of those symposia, which are printed below.

Beijing 2012

The 4th joint meeting of the International Conference on Hyperfine Interactions and the International Symposium on Nuclear Quadrupole Interactions (HFI/NQI 2012) was held on 10-14 September 2010 at the Beijing International Convention Centre, Beijing, China. The meeting was hosted jointly by China Institute of Atomic Energy (CIAE), Shanghai Institute of Applied Physics (SINAP) and Lanzhou University (LZU). The topics discussed at the meeting maintained its general spirit and intention of the previous conferences in the series. The scientific program covered a wide spectrum of the subjects in the hyperfine interactions and nuclear quadrupole interactions detected by nuclear radiation. The meeting consisted of the plenary sessions in which the invited talks and oral presentations were given and the poster session. The meeting was attended by 118 delegates from 25 countries. 108 abstracts were submitted. There were 13 invited talks selected by the International Program Committee (IPC) from the 40 candidates recommended by the International Advisory Committee (IAC) and 29 oral presentations picked up by the IAC, IPC and Local Organizing Committee (LOC) from the submitted abstracts. The rest of contributions were presented in the poster session.

During the meeting the International Advisory Committee meeting was held to review the on-going meeting, pick-up the host of the next meeting and to elect the new executive committee. After discussion the IAC decided to keep the current executive committee till the next conference.

The hyperfine interactions community felt acute distress at the passing way of two giants Robert Blinc (1933-2011) and Romain Coussement (1935-2012). They were warmly commemorated during the meeting and obituaries on them were included in the conference proceedings.

Conference Chair: Shengyun Zhu

CERN 2010

The third in the series of joint International Conference on Hyperfine Interactions/Nuclear Quadrupole Interactions (HFI/NQI2010) took place at CERN, Geneva, in September 2010. The conference was hosted by the ISOLDE Collaboration at CERN. The topics discussed at the conference followed those of the previous joint HFI/NQI conferences held at Bonn (2004) and Iguasu Falls (2007). The scientific program comprised 14 invited talks, which included a plenary talk on anticipated LHC physics and 13 oral presentations of which several were devoted to hyperfine interactions studies utilizing radioactive ion beams from the ISOLDE facility. The remainder of the 200 abstracts that were received by the program committee were selected for oral presentation.

The conference was attended by 122 delegates, 51 of them from developing countries. CERN proved to be an excellent venue due both to the excitement generated in the scientific community by the development of the Large Hadron Collider and the planned search for the Higgs boson when the LHC came online, as well as to the generous support of the CERN management.

The hyperfine interactions community was saddened by the passing way of two of its stalwarts, Hendrik de Waard and Ekkehardt Recknagel, obituaries on whom were included in the proceedings volume.

The International Advisory Committee decided to change the frequency of the joint HFI/NQI conference to be biennial, and to be held in alternate years to ICAME.

Joint Chairs: Krish Bharuth-Ram and Guido Langouche

Iguassu Falls 2007

The joint meeting of the XIV International Conference on Hyperfine Interactions and the XVIII International Symposium on Nuclear Quadrupole Interactions took place at Iguassu Falls in August 2007, on the Argentina–Brazil border, as a joint organisational effort of both countries.

The event was held at the Mabu & Thermas Resort in Foz de Iguaçu (Brazil). 130 delegates participated in the meeting. There were around 20 participants from Japan, 20 from Argentina, 20 from Brazil and 17 from Germany, the rest came from the USA, Russia, Israel, South Africa, Belgium, India, Peru, Poland, Australia and Denmark. There were 186 contributions distributed into 15 invited talks, 33 oral presentations and 138 poster presentations. Afterwards 103 manuscripts were accepted for publication.

Chairs:

AF Pasquevich (La Plata – Argentina)
E Baggio Saitovitch (Rio deb Janeiro – Brazil)
HM Petrilli (São Paulo – Brazil)

Bonn 2004

In August 2004 more than 200 scientists from 27 nations attended the first joint meeting of the XIIIth International Conference on Hyperfine Interactions and the XVIIth International Symposium on Nuclear Quadrupole Interactions. The conference was hosted by the Helmholtz - Institut für Strahlen- und Kernphysik of the Rheinische Friedrich - Wilhelms - Universität Bonn. The programme covered the theory of hyperfine fields in solids, as well as the traditional scientific subjects connected to hyperfine interaction detected by nuclear radiation. A major section was dedicated to nuclear quadrupole resonance measurements. 220 abstracts were submitted to the conference from which the joint programme committee selected 27 for oral presentation. Additionally 17 scientists were invited to present their latest results or give overviews of various new developments in the field.

During the meeting the late Professor Dr Erwin Bodenstedt (1926–2002) was warmly commemorated, who started this line of research in Bonn and made many important contributions to its development over more than 25 years.

Conference Chair: Reiner Vianden

SHINE DOME HISTORY

Our venue has special significance to the Australian scientific community and it is a unique architectural delight.

The Dome: The story of its construction

Completed in 1959 and reflecting some of the more adventurous architectural ideas of that time, the Shine Dome (previously known as Becker House) remains one of the most unusual buildings in Australia.

The dome – roof, walls and structure combined – dives down beneath the still water of its moat to give the sense that it is floating. From the walkway between the moat and the inner walls, the arches provide a 360° panoramic sequence of 16 views of the capital city and the hills beyond.

The Shine Dome was conceived before Canberra's Lake Burley Griffin existed, before microchips, and before manned space travel. It was created in the visionary scientific era of Sputnik, the first artificial satellite to orbit the Earth.

The dome came about because the Australian Academy of Science needed a home. In the early 1950s, under the founding Presidency of Sir Mark Oliphant, the new Academy and its 64 Fellows set about finding funds to create a building of its own. The Academy, which had been using offices in the Australian National University, recruited some eminent industrialists to its cause and received its first cheque (for £25,000) from BHP. Thus encouraged, Fellows both provided funds and encouraged their business associates to do the same. The dome, which cost a total of £260,000 to build, was completed in 1959 and named Becker House, recognising Sir Jack Ellerton Becker's £100,000 donation.

Once the Academy had found a suitable site, the next step was to select an architect. Six architects were invited to submit plans to a competitive process, and on 1 December 1956 the Academy's Building Design Committee met in Adelaide to look at them. The committee wanted a building that would be of a very high order aesthetically, judged from a non-traditional standpoint.

The committee settled upon the most radical design and their decision was unanimously approved by Council. Grounds, Romberg and Boyd were seen as the most influential Australian architects of their time. Roy Grounds was the sole architect on the Academy's building: it was his design that won the commission.

Unique features and challenges

The radically different building created radically different problems for the architects and engineers involved. Some doubted it could be built. Nobody knew how to calculate the stresses created by a 710 tonne concrete dome perched on 16 slender supports. This was vital, because if they got it wrong the whole dome might collapse when the building supports were taken away. In the end they grappled with the problem by building a one-fortieth scale model to see if it would work.

Those who trusted the model were proved right. When the massive concrete dome was built and the forest of wooden formwork and supports removed, the top of the dome dropped less than a centimetre as it took its own weight. It was a triumph for those who worked on the calculations and the model.

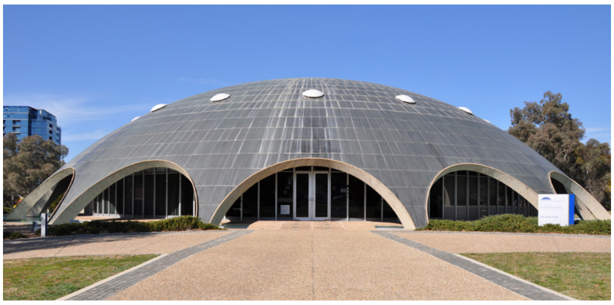

But getting the 'roof' on was only half the battle. In the centre of the dome was a lecture theatre for 150 people – and the big concrete umbrella did some strange things to sound. Again, the problems were new ones, and it took a great deal of work by acoustic engineers to get the sound right. The solution was to use a complex series of acoustic baffles to control the sound. Some were suspended from the ceiling and others built as part of long wooden panels on the walls. After much trial and error, the sound problem was solved.

Then a whole new and totally unexpected problem emerged. It became apparent that the elegant eucalyptus sound baffles gracing the walls created a form of optical interference, rendering about half of the people in the room nauseous. It took quite some time to find a solution, but eventually a Fellow, Dr Victor Macfarlane, who worked at the John Curtin School of Medicine at the ANU, came up with the idea of filling in the visually offending gaps with strings. This fixed the optical problem without spoiling the acoustics.

The concrete roof of the dome is sheathed in copper – and under the copper is a layer of vermiculite which partly insulates the interior from outside temperatures. This provides a degree of thermal inertia and the temperature of the dome's underside is roughly an average of the outdoor temperature of the previous 24 hours. It can become unpleasantly hot after a February heatwave or chilly after an August cold spell. However, a natural gas heating system helps keep the building warm in winter. In the summer the sloping roof shields the windows from direct sunlight.

Later additions

In 2000 the dome was completely restored and updated with a new cooling system. These major works were supported by a donation of $1 million from a Fellow, Professor John Shine, and a grant of $525,000 from the National Council for the Centenary of Federation. In recognition of this donation, the building is now named the Shine Dome.

A capital landmark

For its unique architecture and status as a landmark, the Shine Dome was included in the National Heritage List on 21 September 2005. For many years the Dome has been an iconic landmark of the national capital. It has featured in news backdrops, on posters, postcards, teatowels and even as a souvenir fridge magnet. The Shine Dome, which has won a number of national and international architecture awards and citations, continues to fascinate visitors to Canberra.

ORGANISATION OF HFI/NQI 2014

HFI/NQI Chairmen

- Wayne Hutchison
- Andrew Stuchbery
- Heiko Timmers

HFI/NQI 2014 Local Organising Committee

- Sean Cadogan (UNSW)
- Stewart Campbell (UNSW)
- Wayne Hutchison (UNSW)
- Tibor Kibedi (ANU)
- Petra Rickman (ANU)
- Mark Ridgway (ANU)
- Andrew Stuchbery (ANU)
- Glen Stewart (UNSW)
- Heiko Timmers (UNSW)

HFI/NQI 2014 International Advisory Committee

- Hisazumi Akai (Japan)
- Ercan Alp (USA)
- Tersuo Asaji (Japan)
- Tatyana Babushkina (Russia)
- Krish Bharuth-Ram (South Africa)
- Jon Billowes (UK)
- Gary S Collins (USA)
- Joao Martins Correia (Portugal)
- Stefaan Cottenier (Belgium)
- Pierre Dalmas de Reotier (France)
- Manfred Deicher (Germany)
- Haraldur Palloe Gunnlaugsson (Denmark)
- Lars Hemmingsen (Denmark)
- Wayne Hutchison (Australia)
- Herbert Jaeger (USA)
- Ryosuke Kadono (Japan)
- Ken Ichi Kumagai (Japan)
- Guido Langouche (Belgium)
- Jochen Litterst (Germany)
- Kensaku Matsuta (Japan)
- Andrew McFarlane (Canada)
- Takashi Ohtsubo (Japan)
- Alberto F Pasquevich (Argentina)
- Helena M Petrilli (Brazil)
- Mario Renteria (Argentina)
- Rudolf Rueffer (ESRF)
- Andrew Stuchbery (Australia)
- Heiko Timmers (Australia)
- Reiner Vianden (Germany)
- Ilan Yaar (Israel)
- Matthew Zacate (USA)
- Shengyun Zhu (China)

HFI/NQI 2014 Program Committee

- Krish Bharuth-Ram (South Africa)
- Stefaan Cottenier (Belgium)
- Pierre Dalmas de Reotier (France)
- Lars Hemmingsen (Denmark)
- Wayne Hutchison (Australia)
- Guido Langouche (Belgium)
- Kensaku Matsuta (Japan)
- Alberto F Pasquevich (Argentina)
- Helena M Petrilli (Brazil)
- Mark Ridgway (Australia)
- Andrew Stuchbery (Australia)
- Heiko Timmers (Australia)
- Reiner Vianden (Germany)
- Sheng-Yun Zhu (China)

INVITED SPEAKERS

JESS BREWER
University of British Columbia, Canada
μSR HOWTO

ARTUR CARBONARI
IPEN, Brazil
First principles calculations of the Cd-doped $ZrIn_2$: a study of electronic properties and electric field gradients

MANFRED DEICHER
Universität des Saarlandes, Germany
Structural and optical characterization of indium-antimony complexes in ZnO

YANN GARCIA
Catholic University of Louvain, Belgium
Spin Crossover Complexes – Muon Spin Relaxation and Mössbauer Studies

KHASHAYAR GHANDI
Mount Allison University, Canada
Muons as a Hyperfine Interaction Probe in Chemistry

MICHAEL JAMES
Australian Synchrotron
The Australian Synchrotron: Shining a Light on Australian Research

RAPHAEL HERMANN
FZ Juelich, Germany
Nuclear Resonance Scattering above 30 keV

GUIDO LANGOUCHE
University of Leuven, Belgium
Properties of Fe in dilute Magnetic Semiconductors after Ion Implantation Studied by ^{57}Fe Emission Mössbauer Spectroscopy

KEI MINAMISONO
NSCL Michigan State University, USA
Collinear Laser Spectroscopy and Beta NMR at NSCL/MSU

DOMINIC RYAN
McGill University, Canada
Phase-quantitative Studies of Magnetism and Valence using Mössbauer Spectroscopy

TILO SÖHNEL
The University of Auckland, New Zealand
Mössbauer Spectroscopy on Fe, Ru and Ir-Sn Cluster Compounds

MONIKA STACHURA
ISOLDE-CERN, Switzerland
Beta-NMR on Liquid Media for Biophysics Applications

NICHOLAS STONE
University of Tennessee, USA
New Table of Recommended Nuclear Electric Quadrupole Moments

KRISTIAAN TEMST
KU Leuven, Belgium
Probing the Influence of Spatial Confinement on Magnetic and Superconducting Properties by Nuclear Resonant Scattering

GERHARD WORTMANN
University of Paderborn, Germany
High-pressure Studies using Synchrotron-based Mössbauer Spectroscopies

SPONSORS

PRINCIPAL SPONSOR

UNSW AUSTRALIA
Canberra

PRIZE SPONSOR

magritek
www.magritek.com

CONFERENCE SPONSORS

Australian National University

CENGAGE Learning™

Nucletron

EXCURSION

HFI/NQI 2014 Excursion

Date: Wednesday 24 September 2014
Time: 12:00–17:30

A guided tour of the Tidbinbilla Nature Reserve that showcases Australian fauna and flora and a visit of the Canberra Deep Space Tracking Centre operated by NASA. Departure by coach is from The Shine Dome, this is also the point of return after the excursion.

Tidbinbilla Nature Reserve offers outstanding wildlife and natural experiences being nestled in a beautiful valley with typical Australian landscapes. Enjoy a walk in the sanctuary wetlands, photograph kangaroos, search for the shy platypus from the boardwalks, observe resident and migratory bird life, get up close to reptiles or find a sleepy koala in the eucalypt forest enclosure.

The Canberra Deep Space Centre is one of a network of tracking stations operated by NASA. It offers visitors the chance to learn about the role that Australia plays in the exploration of space.

SOCIAL FUNCTIONS

Welcome Reception

Date: Sunday 21 September 2014
Time: 17:00–19:00
Venue: The Shine Dome

Conference Dinner

Date: Thursday 25 September 2014
Time: 19:00–23:00
Venue: University House, The Australian National University

POSTER INSTRUCTIONS

As part of the program we will have two poster sessions. Information relating to these sessions is listed below:

Poster Session I

Tuesday 23 September
Time: 15:30–17:30

Requirements: Poster numbers are listed in this handbook, please refer to the correlating poster number on the poster boards for where to mount your poster. We encourage you to display your poster as early as practical to add to the scientific discourse. For Poster Session I posters should be placed on the poster boards as early as Sunday 21 September from 16:00 and need to be removed on Wednesday 24 September before morning tea to make space for the posters of Poster Session II.

Poster Session II

Thursday 25 September
Time: 13:30–15:30

Requirements: Poster numbers are listed in this handbook, please refer to the correlating poster number on the poster boards for where to mount your poster. Posters should be placed on the poster boards on Wednesday morning 24 September before or during morning tea break. In order to return the venue in a clean manner, we ask presenters to remove all posters by Friday lunch time.

Organisers expect poster presenters to attend their posters during the allocated poster session in order to facilitate discussions of their work with the conference delegates.

EXHIBITION

A small number of organisations will exhibit during the conference. Organisers ask and encourage delegates to interact with exhibitors and thus acknowledge the important contributions they are making to the staging of our event.

Exhibition Hours

HFI/NQI EXHIBITION HOURS

Sunday 21 September	17:00–19:00 (Welcome Reception)
Monday 22 September	08:30–16:00
Tuesday 23 September	08:30–16:00
Wednesday 24 September	No Exhibition
Thursday 25 September	08:30–15:30
Friday 26 September	No Exhibition

List of Exhibitors

TABLE 03
The University of New South Wales
Dr Wayne Hutchison
School of PEMS, UNSW Canberra
T +61 2 6268 8804
E w.hutchison@adfa.edu.au
W http://www.unsw.adfa.edu.au/

TABLE 04
Nucletron Pty Ltd
Rob Saunders
1b Little Commodore Street
NEWTOWN NSW 2042
T +61 2 9517 1300
E sales@au.nucletron.com

GENERAL INFORMATION

Welcome to Canberra

Canberra is modern city, set within extensive parks and gardens and enjoys four distinct seasons.

The nation's capital is the home of the Australian story. Discover the national attractions which showcase indigenous and Australian history, culture, flora, fauna, art and science with regular displays, tours and exhibitions.

The climate and geography of Canberra nourishes excellent food and wine which you may enjoy in modern and stylish restaurants, cafes, bars and shops.

An extensive network of parks and reserves with walking trails and cycle ways offer wonderful recreation, exploration and rejuvenation opportunities alongside the conference program.

With a bustling calendar of events, festivals, exhibitions and tours, Canberra is full of unexpected delights awaiting you www.visitcanberra.com.au. During the conference the annual Floriade Festival is being staged and might be worth a visit to get to know the Australian outdoor lifestyle.

Cafés

Listed below are recommended eateries within walking distance to the Shine Dome: The red numbers correspond to the map on the next page.

ON ANU CAMPUS

1. The Gods Cafe & Bar
Café style food
Building 16 ANU Arts Centre
University Ave
Mon–Fri: 07:30–17:00

2. University House – The Fellows Bar and Café
Well-priced food and drinks in a stylish and relaxed venue
1 Balmain Crescent
Breakfast Mon–Fri: 07:00–09:30
Sat–Sun: 07:30–10:00
Lunch Mon–Fri: 12:00–14:00
Dinner Mon–Fri: 18:00–20:00

2. University House – Boffins Restaurant
Elegant dining from fixed and à la carte menus
1 Balmain Crescent
Lunch Mon–Fri: 12:00–14:00

3. University General Store, Licensed Grocer on Balmain
For general grocery items and reasonable priced lunch items

Bldg 64b/Balmain Crs
Mon–Fri: 07:30–17:30

4. ANU Union
Union Circuit, Building 20

A range of eateries including: ANU Bar, Asian Bistro, Boost Juice, Campus Bakery, Degree Café, Functions & Conference Centre, Mee Sushi, Mini-Market (Union Shop), Pakenka's, Plowman's, Rosie's Chicken, Subway, Zambrero

5. National Film & Sound Archive Café
McCoy Circuit
Mon–Fri: 09:00–15:00
Open Friday nights for 19:30

Arc film screenings
Sat: 13:30–19:30
Sun: 13:30–16:30
Dinner Mon–Sun: 18:00–21:00

6. Biginelli Espresso
Childers Street
Level 5, Canberra School of Music
Mon–Thurs: 08:00–18:00
Fri: 08:00–16:00

7. Chat's Cafe
Ellery Crescent
ANU School of Art
Mon–Fri: 08:30–15:00

OUTSIDE ANU CAMPUS

8. Močan & Green Grout
Bistro/Cafe/Deli, Gourmet, Modern Australian, Seafood,
Mon & Sat: 07:00–18:00
Tues–Fri: 07:00–21:00
Sun: 08:00–16:00

9. Monster Kitchen and Bar
Breakfast, bar, shared and sweet
1/19 Marcus Clarke St (within Hotel Hotel)
06:30–13:00 every day

10. Bicicletta Provedore and Cellar
Italian
Diamant Hotel Canberra
15 Edinburgh Ave
Mon–Sun: 05:00–11:00

ATM

The closest ATMs are located at:

- Café 21 – Located on the corner of Marcus Clarke and Edinburgh Avenue
- Exchange on London – Located on the corner of Edinburgh Avenue and London Circuit

The following banking facilities are located near the conference venue:

ANZ
148 Bunda Street
Canberra City

National Australia Bank
Civic Square
Corner of London Circuit and Ainslie Avenue
Canberra City

St George
222 City Walk
Canberra City

Commonwealth Bank
Cnr London Circuit & Ainslie Avenue
Canberra City

Post Office

The nearest post office is located on the corner of Alinga and Moore Streets.

Car Parking

Car parking is located within walking distance from the Shine Dome at an approximate cost of $13.80 for all-day parking. Credit cards are accepted.

Program Changes

Session chairs will notify delegates of any changes made to the program.

Disclaimer

The information is correct at the time of provision. However, the organisers reserve the right to change the information where necessary without notice.

Liability Waiver

In the event of industrial disruptions or cancellation, the conference and the organisers accept no responsibility.

Mobile Telephone Policy

Mobile phones are not to be used while sessions are in progress. Please ensure they are switched to silent during these times.

MAP – DINING


Showing all results for restaurants near Marcus Clarke St, Canberra ...
CIVIC
NEW ACTON
ANU CAMPUS
The Shine Dome
Pedestrian Ramp to New Acton
1
2
3
4
5
6
7
8
9
10
Blu Ginger
Happy's Chinese Restaurant
Benchmark Wine Bar
Red Chilli Sichuan Restaurant
Tasuke
Iori Japanese Restaurant
Alice's
Tosolini's
Hog's Breath Cafe
ZenYai Thai
Thirst Thai Restaurant and Winebar
Mama's Trattoria
Roti House
Mezzalira Ristorante
Spicy Ginger Cuisine
The Golden Drum
Shalimar Indian Restaurant
Delhi 6 Authentic Indian Cuisine
Berroca Restaurant
Cafe Alibi
Xchange on London
Capitol Bar & Grill Restaurant
NewActon
A. BAKER
Monster Kitchen and Bar
Parlour Wine Room
Chicken Gourmet
BreakFree Capital Tower
Teatro Vivaldi Restaurant
Zambrero
Pearl City Asian Cuisine
Boffins
Academy of Science
Australian Academy of Science
National Film and Sound Archive
London Circuit
Parkes Way
Marcus Clarke St
University Ave
Canberra Theatre Centre
APEX Driving School
Acton Park
Fellows Oval
Menzies Library
Canberra School of Art
ANU School of Music
The Australian National University

Name Badges

Your name badge is your official pass to the conference sessions, the welcome reception, the exhibition and catering areas. Please ensure you wear your name badge at all times.

No Smoking Policy

All internal areas of the Shine Dome are non-smoking areas.

Personal Insurance

Delegates shall be regarded in every aspect as carrying their own risk for loss or injury to person or property, including baggage, during the conference. The organisers are in no way responsible for any claims concerning insurance.

Privacy Clause

In registering for this conference, relevant details have been incorporated into a delegate list for the benefit of all delegates (name, organisation and state only), and may have been available to parties directly related to the conference including Consec – Conference Management, HFI/NQI, the Organising Committee, venues and accommodation providers (for the purpose of room bookings and conference options), key sponsors (subject to strict conditions) and parties associated with related conference.

By completing the HFI/NQI 2014 registration, you have acknowledged that the details supplied by you may be used for the above purposes.

Registration Desk

The Conference Registration Desk will be staffed by Consec – Conference Management as follows:

Sunday 21 September 2014	16:00–17:00
Monday 22 September 2014	08:30–12:00

Outside of the hours listed above, the registration desk will be staffed with members of the local organising committee as required, who will be very happy to assist you with any questions or suggestions that you may have.

MAP – SHINE DOME PARKING

DAY 1 SUNDAY / DAY 2 MONDAY

Day 1 Sunday 21 September 2014

16:00–17:00 17:00–19:00	Registration (Foyer of The Shine Dome) Welcome reception (Jaeger Room of The Shine Dome)

Day 2 Monday 22 September 2014

8:30–12:00	Registration (Foyer)
9:00–10:00	Opening session (Ian Wark Theatre) *Session chair:* ***Wayne Hutchison****, University of New South Wales, Australia* **9:00 Welcome** *Conference chairs:* ***Wayne Hutchison****, University of New South Wales, Australia,* ***Andrew Stuchbery****, Australian National University, Australia and* ***Heiko Timmers****, University of New South Wales, Australia* **9:10 Official opening** **Aidan Byrne**, *Chief Executive Officer, Australian Research Council* **9:30 Invited presentation** **Monika Stachura**, *ISOLDE-CERN, Switzerland* Beta-NMR on liquid media for bio-physics applications
10:00–10:30	*Morning Tea (Jaeger Room)*
10:30–12:00	Session M1 (Ian Wark Theatre): Applications of HFI and NQI techniques *Session Chair:* ***Guido Langouche****, University of Leuven (KU Leuven), Belgium* **10:30 Invited presentation** **Khashayar Ghandi**, *Mount Allison University, Canada* Muons as a hyperfine interaction probe in chemistry **11:00 Oral presentation** **Tim Bastow**, *MSE, CSIRO, Australia* NMR measurement of NQI in metals: application to lightweight alloy development **11:20 Oral presentation** **David Stephenson**, *University of the West Indies, Trinidad and Tobago* ^{14}N NQR of sildenafil citrate **11:40 Oral poster presentation (Poster Session I)** **Mototsugu Mihara**, *Department of Physics, Osaka University, Japan* Spin-spin relaxation of the short-lived β-emitter ^{12}B in Si **11:45 Oral poster presentation (Poster Session I)** **Asif Ahmed**, *Australian National University, Australia* Time-dependent recoil in vacuum using the ANU plunger device–improved sensitivity to hyperfine fields and nuclear moments **11:50 Oral poster presentation (Poster Session I)** **Debashis Banerjee**, *Bhabha Atomic Research Centre, India* Short-range texture formation in anatase: a TDPAC study **11:55 Announcements** *Conference chair:* ***Wayne Hutchison****, University of New South Wales, Australia*
12:00–14:00	*Lunch* (Lunch will not be provided at The Shine Dome, however, quite a number of food outlets are located in walking distance and cater for a variety of tastes. The local organisers would be very happy to make suggestions. If in doubt, ask at the registration desk. This may be an opportunity to venture out in groups and catch-up with other conference participants.)

14:00–15:20

Session M2 (Ian Wark Theatre): Hyperfine interactions

Session chair: **Stefaan Cottenier**, *Center for Molecular Modeling, Belgium*

14:00 Invited presentation
Guido Langouche, *University of Leuven, Belgium*
Properties of Fe in dilute magnetic semiconductors after ion implantation studied by ^{57}Fe emission Mössbauer spectroscopy

14:30 Invited presentation
Tilo Söhnel, *The University of Auckland, New Zealand*
Mössbauer spectroscopy on Fe, Ru and Ir-Sn cluster compounds

15:00 Oral presentation
Kei Imamura, *RIKEN Nishina Center/Meiji University, Japan*
Measurement of the hyperfine splitting of ^{133}Cs atoms in superfluid helium

15:20–15:50 *Afternoon Tea (Jaeger Room)*

15:50–17:20

Session M3 (Ian Wark Theatre): Theory

Session chair: **Kristiaan Temst**, *KU Leuven, Belgium*

15:50 Invited presentation
Artur Carbonari, *IPEN, Brazil*
First-principles calculations of the Cd and Fe co-doped In_2O_3: a comparison to experimental results to determine the occupancy site of impurities

16:20 Oral presentation
Georgi Georgiev, *CSNSM/IN2P3/CNRS, France*
Electron–nuclear spin interactions for nuclear moment studies

16:40 Oral presentation
Qiaoli Zhang, *China Institute of Atomic Energy, China*
Ab initio calculations of electric field gradient and magnetic hyperfine field in Fe-doped SnO_2

17:00 Oral presentation
Matthew Zacate, *Northern Kentucky University, United States of America*
Fluctuating hyperfine interactions: an updated computational implementation

Day 3 Tuesday 23 September 2014

Early morning Optional balloon rides

8:30–10:00

Session Tu1: Mössbauer Spectroscopy (I)

Session chair: **Glen Stewart**, *The University of New South Wales, Australia*

8:30 Invited presentation
Gerhard Wortmann, *University of Paderborn, Germany*
High-pressure studies using synchrotron-based Mössbauer spectroscopies

9:00 Oral presentation
Michael Oshtrakh, *Ural Federal University, Russia*
The ^{57}Fe hyperfine interactions in the iron bearing phases in different fragments of Chelyabinsk LL5 meteorite: a comparative study using Mössbauer spectroscopy with a high velocity resolution

9:20 Oral presentation
Vadim Ksenofontov, *Institute of Inorganic and Analytical Chemistry, Johannes Gutenberg-University, Germany*
^{57}Fe-Mössbauer study of $LiNH_2$-intercalated FeSe: evidence for spin fluctuations connected with superconductivity at T_C = 43 K

9:40 Oral presentation
Sunghyun Yoon, *Department of Physics, Gunsan National University, South Korea*
Temperature dependence of magnetic anisotropy constant in $CoFe_2O_4$ nanoparticles examined by Mössbauer spectroscopy

10:00–10:30 *Morning Tea*

DAY 3 TUESDAY

10:30–12:00

Session Tu2: Mössbauer Spectroscopy (II)

Session chair: ***Krish Bharuth-Ram****, University of KwaZulu-Natal, South Africa*

10:30 Invited presentation
Dominic Ryan, *McGill University, Canada*
Phase-quantitative studies of magnetism and valence using Mössbauer spectroscopy

11:00 Oral presentation
Dariusz Malczewski, *University of Silesia, Faculty of Earth Sciences, Poland*
Correlations between changes of the select Mössbauer parameters and changes in electric conductivity for the annealed fully metamict $REE_2Fe^{2+}Be_2Si_2O_{10}$

11:20 Oral presentation
Itzhak Halevy, *NRCN, Israel*
Neutrons high pressure crystallographic structure and magnetic study of the Fe-Cr-H_x phase diagram

11:40 Oral poster presentation (Poster Session I)
Adurafimihan Abiona, *University of New South Wales, Australia*
Split-vacancy palladium defect complexes in silicon and germanium

11:45 Oral poster presentation (Poster Session I)
Hisazumi Akai, *ISSP, University of Tokyo, Japan*
Electronic structure and isomer shift of valence-fluctuating beta-$YbAlB_4$

11:50 Announcements
Conference chair: ***Andrew Stuchbery*** *Australian National University, Australia*

11:55 Conference photo in front of the Shine Dome

12:00–13:50

Lunch
(Lunch will not be provided at the Shine Dome, however, quite a number of food outlets are located in walking distance and cater for a variety of tastes. The local organisers would be very happy to make suggestions. If in doubt, ask at the registration desk. This may be an opportunity to venture out in groups and catch-up with other conference participants.)

13:50–15:00

Session Tu3: Lattice and defect dynamics

Session chair: ***Hisazumi Akai****, ISSP, University of Tokyo, Japan*

13:50 Invited presentation
Manfred Deicher, *Universität des Saarlandes, Germany*
Structural and optical characterization of indium-antimony complexes in ZnO

14:20 Oral presentation
Shintaro Yamaoka, *Van De Graaff Lab Faculty of Science, Osaka University, Japan*
Dynamical property of Li in Li-ion conductions studied by ^{8}Li β-NMR

14:40 Oral presentation
Patrick Kessler, *HISK, Bonn University, Germany*
Orientation of a defect induced electric field gradient in ZnO

15:00–15:30

Afternoon Tea

15:30–17:30

Session Tu4 (Corridor around the Ian Wark Theatre and Jaeger Room): Poster session I and exhibition

(Please refer to the contents section of the conference handbook for the list of posters).

17:00 onwards refreshments served, sponsored by the conference chairs.

17:30 Presentation of Abstract Submission Prizes sponsored by Magritek

18:00–19:00

18:00 Meeting of the International Committee (Becker Room of the Shine Dome)

DAY 4 WEDNESDAY

Day 4 Wednesday 24 September 2014

Early morning	Optional balloon rides
8:30–10:00	Session W2: Magnetism, magnetic materials, thermoelectricity and superconductivity (I) *Session Chair:* ***Itzhak Halevy**, NRCN, Israel* **8:30 Invited presentation** **Yann Garcia**, *Catholic University of Louvain, Belgium* Spin crossover complexes - Muon spin relaxation and Mössbauer studies **9:00 Invited presentation** **Kristiaan Temst**, *KU Leuven, Belgium* Probing the influence of spatial confinement on magnetic and superconducting properties by nuclear resonant scattering **9:30 Invited presentation** **Raphael Hermann**, *Forschungszentrum Juelich, Germany* Nuclear resonance scattering above 30 keV
10:00–10:30	*Morning Tea*
10:30–12:00	Session W2: Magnetism, magnetic materials, thermoelectricity and superconductivity (II) *Session chair:* ***Manfred Deicher**, Universität des Saarlandes, Germany* **10:30 Oral presentation** **Michael Reissner**, *Vienna University of Technology, Austria* FeSb$_2$–a still puzzling material **10:50 Oral presentation** **Hisazumi Akai**, *ISSP, University of Tokyo, Japan* Hyperfine fields and magnetic anisotropy in Nd$_2$Fe$_{14}$B and Sm$_2$Fe$_{17}$N$_3$ **11:10 Oral presentation** **SN Mishra**, *Tata Institute of Fundamental Research, India* Lattice location and magnetism of isolated Fe impurities in narrow band semiconductor InSb **11:30 Oral presentation** **Vasily Potapkin**, *Jülich Centre for Neutron Science JCNS and Peter Grünberg, Institut PGI, JARA-FIT, Germany* Magnetic interactions in NiO at ultra-high pressure **11:50 Announcements** *Conference Chair:* ***Heiko Timmers**, University of New South Wales, Australia*
10:00–12:00	*Pick-up your lunch packs for the bus trip at the registration desk*
12:00–17:30	HFI/NQI Excursion **12:00 Coach departure outside the Shine Dome** **12:50 Guided tour of the Tidbinbilla Nature Reserve** **15:20 Visit to the Canberra Deep Space Communication Complex** **17:30 Return to the Shine Dome**

DAY 5 THURSDAY

Day 5 Thursday 25 September 2014

Early morning	Optional balloon rides
9:00–10:20	Session Th1: Nuclear moments, nuclear polarization and nuclear models (I) *Session chair:* ***Andrew Stuchbery**, Australian National University, Australia* **9:00 Invited presentation** **Nicholas Stone**, *University of Tennessee, United States of America* New table of recommended nuclear electric quadrupole moments **9:30 Oral presentation** **Mototsugu Mihara**, *Department of Physics, Osaka University, Japan* Development of ^{129}Xe comagnetometer for precise measurement of neutron electric dipole moment **9:50 Oral presentation** **Tomoya Sato**, *Tokyo Institute of Technology, Japan* EDM measurement in ^{129}Xe atom using dual active feedback nuclear spin maser **10:10 Oral poster presentation (Poster Session II)** **Yu Sakamoto**, *Tokyo Institute of Technology, Japan* Development of high-homogeneity magnetic field coil for ^{129}Xe EDM experiment **10:15 Oral poster presentation (Poster Session II)** **Rakesh Dogra**, *Beant College of Engineering & Technology, India* Structural, magnetic and optical studies of ni-nanostructures embedded in Al_2O_3 matrix
10:20–10:50	*Morning Tea*
10:50–12:00	Session Th2: Nuclear moments, nuclear polarization and nuclear models (II) *Session Chair:* ***Tibor Kibedi**, Australian National University, Australia* **10:50 Oral presentation** **Ping Fan**, *China Institute of Atomic Energy, China* g-factor measurements of high spin states in ^{108}Cd **11:10 Oral presentation** **Debashis Banerjee**, *Variable Energy Cyclotron Centre, India* Measurement of lifetime and quadupole moments in neutron rich ^{131,132}I **11:30 Oral presentation** **Alan Gregorovic**, *Institute "Jozef Stefan", Slovenia* Correlations between ^{14}N NQR frequencies and ^{14}N local environment in molecular crystals **11:50 Oral poster presentation (Poster Session II)** **Darren Goossens**, *ANU, Australia* Chemical and magnetic ordering in $Fe_{0.5}Ni_{0.5}PS_3$ **11:55 Oral poster presentation (Poster Session II)** **Nihed Chaâbane**, *CEA Saclay, France* Damage accumulation in Au^{2+} irradiated SiC/SiC composites
12:00–13:30	*Lunch* (Lunch will not be provided at The Shine Dome, however, quite a number of food outlets are located in walking distance and cater for a variety of tastes. The local organisers would be very happy to make suggestions. If in doubt, ask at the registration desk. This may be an opportunity to venture out in groups and catch-up with other conference participants.)
13:30–15:30	Session Th 3 (Corridor around the Ian Wark Theatre and Jaeger Room): Poster session II and exhibition (Please refer to the abstract section of the conference handbook for the list of posters).
15:00–15:30	*Afternoon Tea*

DAY 5 THURSDAY / DAY 6 FRIDAY

15:30–17:00

Session Th 4 (Ian Wark Theatre): Large facilities

Session chair: ***Sean Cadogan**, University of New South Wales, Australia*

15:30 Invited presentation
***Jess Brewer,** University of British Columbia & TRIUMF, Canada*
μSR HOWTO

16:00 Invited presentation
***Kei Minamisono**, NSCL Michigan State University, United States of America*
Collinear laser spectroscopy and β NMR at NSCL/MSU

16:30 Invited presentation
***Michael James**, Australian Synchrotron, Melbourne*
The Australian synchrotron: shining a light on Australian research

17:00–19:00 *- break -*

19:00–23:00

HFI/NQI Dinner–University House

19:00 Pre dinner drinks

19:30 Guests seated

Day 6 Friday 26 September 2014

9:00–10:20

Session F1 (Ian Wark Theatre): Nano-particles and–structures

Session chair: ***Matthew Zacate**, Northern Kentucky University, United States of America*

9:00 Oral presentation
***Wataru Sato**, Kanazawa University, Japan*
Atomic level observation of Ag-ion hopping motion in AgI nanoparticles

9:20 Oral presentation
***Alexios Douvalis**, Physics Department, University of Ioannina, Greece*
Carbon nanotubes filled or decorated for advanced applications: properties insight through hyperfine interactions of ^{57}Fe and ^{119}Sn nuclei

9:40 Oral presentation
Vadim Ksenofontov
Application of the MIMOS II spectrometer in to study ductile Heusler alloys

10:00 Oral presentation
***David Stephenson**, University of The West Indies, Trinidad and Tobago*
^{14}N NQR and relaxation in ammonium nitrate

10:20–10:50 *Morning Tea*

10:50–12:40

Session F2 (Ian Wark Theatre): New developments and future directions

Session chair: ***Stewart Campbell**, University of New South Wales, Australia*

11:00 Oral presentation
***Takeshi Inoue**, Tohoku University, Japan*
Experimental search for the electron electric dipole moment with laser cooled francium atoms

11:20 Oral presentation
***Stefaan Cottenier**, Center for Molecular Modeling, Belgium*
Teaching hyperfine interactions in the 21st century

11:50 Acknowledgements and handing over of the flag
Conference chairs: ***Wayne Hutchison**, University of New South Wales, Australia,* ***Andrew Stuchbery**, Australian National University, Australia and* ***Heiko Timmers**, University of New South Wales, Australia*

12:00 Presentation from the hosts of the next conference
***Kristiaan Temst**, KU Leuven, Belgium*

12:20 Summary & Discussion
***Matthew Zacate**, Northern Kentucky University, United States of America*
Hyperfine interactions: Quo vadis?

12:40 End of conference

CONTENTS

ORAL PRESENTATIONS AND ORAL POSTER PRESENTATIONS

MONDAY 22 SEPTEMBER

TUESDAY 23 SEPTEMBER

WEDNESDAY 24 SEPTEMBER

THURSDAY 25 SEPTEMBER

FRIDAY 26 SEPTEMBER

Abstracts Contents

POSTER PRESENTATIONS

SESSION I
TUESDAY 23 SEPTEMBER

SESSION II
THURSDAY 25 SEPTEMBER

Beta-NMR on liquid media for biophysics applications

M. Stachura[1,2], A. Gottberg[1], M. Kowalska[1], M.L. Bissell[3], V. Arcisauskaite[2], K. Blaum[4], A. Helmke[5], K. Johnston[6], K. Kreim[4], F.H. Larsen[7], R. Neugart[8], G. Neyens[3], D. Szunyogh[9], P.W. Thulstrup[2], D.T. Yordanov[4], L. Hemmingsen[2]

[1] *CERN, Geneva, Switzerland. monika.stachura@cern.ch*
[2] *Kemisk Institut, Københavns Universitet, Thorvaldsensvej 40, 1871 Frederiksberg C, Denmark. lhe@chem.ku.dk*
[3] *Instituut voor Kern- en Stralingsfysica, KU Leuven, Celestijnenlaan 200 D, B-3001 Leuven, Belgium.*
[4] *Max-Planck-Institut für Kernphysik, Saupfercheckweg 1, 69117 Heidelberg, Germany.*
[5] *Humedics GmbH, Marie-Elisabeth-Lüders-Str. 1, 10625 Berlin, Germany.*
[6] *Universität des Saarlandes, Experimentalphysik, 66123 Saarbrucken, Germany.*
[7] *Institut for Fødevarevidenskab, Københavns Universitet, Rolighedsvej 30, 1958 Frederiksberg C, Denmark.*
[8] *Institut für Kernchemie, Universität Mainz, Fritz-Straßmann-Weg 2, 55128 Mainz, Germany.*
[9] *Szervetlen és Analitikai Kémiai Tanszék, Szegedi Tudományegyetem, Dom ter 7, 6720 Hungary.*

In August 2012 β-NMR spectroscopy was successfully applied for the world's first experiments on liquid samples - an achievement which opens new avenues of research in the fields of wet chemistry and biochemistry [1]. This project was motivated by the need for finding a new experimental approach to directly study biologically highly relevant metal ions, such as: Mg(II), Cu(I), Ca(II), and Zn(II).

The resonance spectrum recorded for Mg-31 implanted into a liquid sample shows two clear peaks, which originate from Mg ions occupying two different coordination geometries, illustrating that this technique can in fact discriminate between different structures - the first and the most important step towards the application of β-NMR spectroscopy in chemistry.

A prototype bio-β-NMR spectrometer, designed and constructed explicitly for this purpose using polarized ions at the ISOLDE-COLLAPS setup, allowed for testing different aspects, such as: different liquids, vacua and rest gases, showing that even aqueous solutions are within reach. In a future biochemical perspective, this proof-of-principle allows the application of β-NMR for studying metal ions, which are silent in most other spectroscopic techniques in their body-like environments.

In order to exploit the potential of this technique, a dedicated permanent bio β-NMR spectrometer is now planned at ISOLDE, while experiments at TRIUMF are under consideration.

[1] A. Gottberg *et al.* manuscript in preparation, 2014.

Electronic address: *monika.stachura@cern.ch*

Muons as a hyperfine interaction probe in chemistry

Khashayar Ghandi,[1]

[1] *Dept. Chemistry and Biochemistry Mount Allison University Sackville, Canada*

Muon spectroscopy is a powerful tool to measure hyperfine interactions in paramagnetic species in particular reactive free radicals. There are different varieties of muon spin spectroscopy that could be used to measure hyperfine interactions for different chemical systems. These spectroscopic studies have played a key role in the study of free radical and radiation chemistry. I set our recent investigations using the complementary techniques of muon spin spectroscopy and computational chemistry, exploring chemical systems relevant to green chemistry, nanotechnology and Energy. Such complementary computational and experimental muon studies are important since 1) they provide detailed information about electronic structure of free radicals; 2) they can be used to study free radicals structure, dynamics and kinetics almost under any condition relevant to chemistry; 3) they can be used to study free radicals bound to the surfaces and in the fluids.

Electronic address: *Presenting.kghandi@triumf.ca*

NMR measurement of NQI in metals; application to lightweight alloy development

Tim Bastow,

CSIRO Materials Science and Engineering, Private Bag 33, Clayton South 3169 Australia

NMR spectroscopy of metals is feasible provided at least one of the dimensions of the specimen aggregate is of order the classical electromagnetic skin depth. This generally means powders, produced by filing from the bulk material.

The high electrical conductivity of most metals drastically lowers the Q-factor ($\nu/\Delta\nu$) of the probe tuning curve, decreasing the detection sensitivity but with the advantage of increasing the bandwidth of the probe, so that short sub-$\pi/2$ pulses can be used to excite a larger spectral range than possible with insulating substances. Because the linewidths in the NMR spectra of metals are generally large, an echo pulse sequences is almost invariably employed for their detection to minimize contamination of the signal by transmitter breakthrough.

The determination of NQIs proceeds, as for insulators, by measurement of the first or second order perturbed NMR lineshapes. Examples of both are displayed in the figure at the foot of the page for ^{25}Mg (first order) and ^{67}Zn (second order).

An example of the application to lightweight alloy research is as follows. Two of the principal industrial construction metals, Al and Mg, are soft and easily malleable. They can be stiffened up, their Vickers hardness and ultimate tensile strength increased, by alloying with a few weight percent of other elements chosen, so that, after suitable heat treatment, intermetallic precipitates are formed which block the flow of dislocations responsible for the plasticity of the pure metal. These intermetallics can be identified by their NQI and their presence quantified as the heat treatment proceeds. This data can then be correlated with the approach to maximum Vickers hardness and ultimate tensile strength. Examples of the use of this technique will be outlined for **Al**(Cu), **Al**(Cu,Mg), **Al**(Zn,Cu,Mg) and **Mg**(Al) where the alloying elements, a few weight percent of the total, are indicated in brackets.

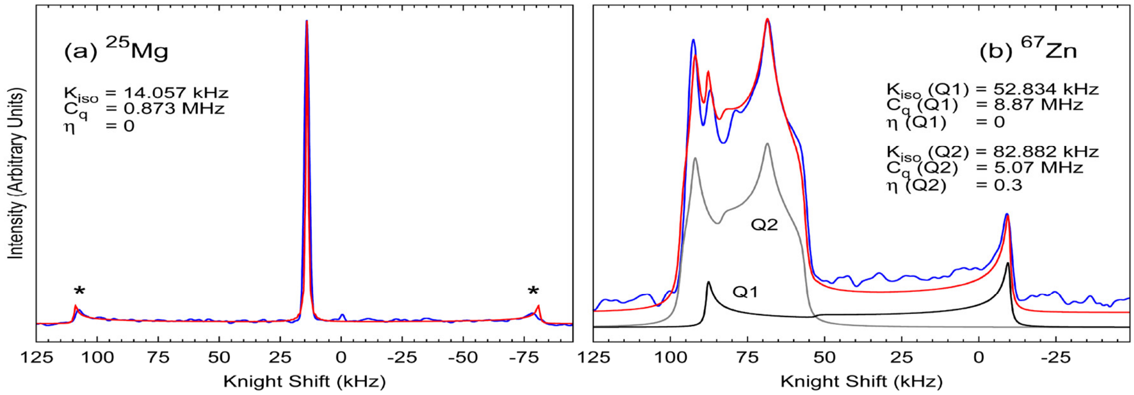

^{25}Mg and ^{67}Zn NMR spectra of a nominally pure sample of $MgZn_2$

Electronic address: *tim.bastow@csiro.au*

^{14}N NQR of Sildenafil Citrate

David Stephenson and Nadia Singh

Chemistry Dept., University of the West Indies, St. Augustine, Trinidad and Tobago.

Sildenafil citrate is marketed by Pzifer as Viagra. Its use, effectiveness and high price has made it one of the most counterfeited drugs. A recent study found that 77% of the samples they analyzed (from internet suppliers) were counterfeit [1]. Sildenafil contains six structurally unique nitrogen atoms so it should be possible to authenticate samples using ^{14}N NQR. ^{14}N NQR is advantageous because it is non-destructive and the resonances are very sensitive to molecular structure. As a first step to possible authentication of Viagra using NQR we have recorded the spectrum of Viagra tablets and made an assignment of the observed frequencies to the nitrogen atoms in its structure. The NQR spectrum (Figure 1) was recorded using Pzifer Viagra tablets which contain 100 mg of active ingredient and 520 mg of filler. Despite the large amount of filler (84 %) all but the lowest frequency lines were detected. This has allowed the 6 quadrupole couplings (Qcc) and asymmetry parameters (η) to be determined. Density functional calculations were carried out to assist the assignment using a 6-31+G-dp basis set and a B3LYP exchange/correlation function. Atom positions were obtained from an X-ray structure of the similar sildenafil citrate monohydrate [2]. The experimental values and calculated values are shown in Table 1. In all cases the calculated Qccs are some 10% larger than those obtained from the spectrum. This deviation can be attributed to intermolecular interactions (the calculations were done on an isolated molecule). The spectrum in Figure 1 was recorded using field cycling double resonance and consists of 1024 frequency points and has been processed using 3-point smoothing. The slope in the first and last 300 kHz is caused by the application of a polynomial baseline correction.

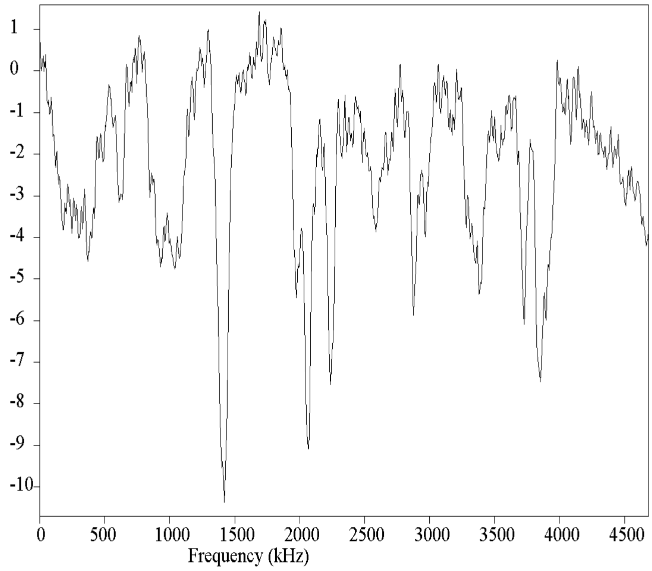

Figure 1. The NQR spectrum of sildenafil citrate. The Y-axis is recovered magnetization in arbitrary units the peaks show as a loss of proton signal.

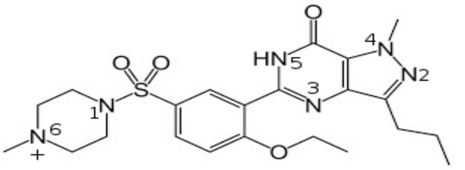

	Experimental		Calculated	
^{14}N	Qcc	η	Qcc	η
1	4813	.183	5174	.11
2	3977	.727	4445	.58
3	3697	.195	3960	.10
4	3229	.551	3481	.38
5	2327	.533	2611	.65
6	1347	.178	1428	.20

Table 1. Quadrupole couplings (in kHz) and asymmetry parameters. The numbering in the left column corresponds to the numbering on the structure above.

[1] N. Campbell et. al., J. Sex Med., **9(4)**, 248 (2012).
[2] H.S. Yathirajan et al., Acta Cryst., **E61,** 489 (2005).

Electronic address: david.stephenson@sta.uwi.edu

P28

Spin-spin relaxation of short-lived β-emitter ^{12}B in Si

M. Mihara,[1] Y. Kamisho,[1] J. Ohno,[1] M. Tanaka,[1] S. Shinozaki,[1] S. Yamaoka,[1] Y. Morita,[1] R. Kambe,[1] K. Watanabe,[1] T. Minamisono,[1] M. Fukuda,[1] and K. Matsuta[1]

[1]*Dept. Physics, Osaka Univ., 1-1 Machikaneyama, Toyonaka, Osaka 560-0043, Japan*

Diffusion of boron impurity in silicon has been studied for many years. According to the number of experimental and theoretical studies, the diffusion mechanism is now considered that a self interstitial Si (I) generates an intermediate mobile species from a substitutional B [1]. However, the experimental studies are mostly limited to the measurement of macroscopic B profiles in Si using chemical composition analysis like the secondary ion mass spectrometry (SIMS). The nuclear magnetic resonance (NMR), which is a promising tool to study the microscopic diffusion process, is indispensable to understand the diffusion mechanism of B in Si.

Recently, we have developed a pulse NMR technique for short-lived β-emitting nucleus ^{12}B (I = 1, $T_{1/2}$ = 20 ms) to detect spin-spin relaxation time T_2 using the spin-echo method [2], which allows us to observe the microscopic behavior of extremely dilute impurities in materials such as dopants in semiconductors. Using this technique, we have measured T_2 for ^{12}B implanted into non-doped Si between 230 K and 600 K. Figure 1 shows the spin-spin relaxation rates 1/T_2 plotted as a function of the reciprocal temperature 1/T. Above 370 K, 1/T_2 exponentially decreases with 1/T and the activation energy E_{a} = (0.11 ± 0.01) eV was deduced. Although, this value is much smaller than known diffusion barrier of about 3 eV for B in Si [1], it is quite in agreement with the SIMS result obtained under the condition that a number of Is are supplied by ion irradiation during the SIMS analysis [3]. The sample of our experiment was in similar situation because a scattered deuteron beam from a target backing was irradiated to the sample simultaneously with ^{12}B produced through the ^{11}B(d, p)^{12}B reaction. Our result suggests that the enhanced B diffusion under irradiation was also observed by the T_2 measurement.

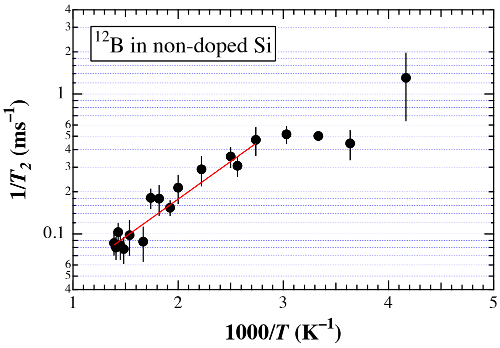

FIG. 1: Arrhenius plot of the spin-spin relaxation rate of ^{12}B in Si.

[1] S. Mirabella et al., J. Appl. Phys. **113**, 031101 (2005).
[2] Y. Kamisho et al., Hyperfine Interactions **222**, 121 (2013).
[3] E. Napolitani et al., Phys. Rev. Lett. **93**, 055901 (2004).

Electronic address: `mihara@vg.phys.sci.osaka-u.ac.jp`

P16

Time-Dependent Recoil in Vacuum using the ANU Plunger Device – Improved Sensitivity to Hyperfine Fields and Nuclear Moments

Asif Ahmed,[1] **Andrew Stuchbery**[1], **Greg Lane**[1], **Tibor Kibēdi**[1]

1 Department of Nuclear Physics, RSPE, Australian National University, Canberra ACT 0200, Australia

Motivated by applications to nuclear moment measurements on radioactive beams, the development of methods to measure the time dependence of hyperfine fields of free ions recoiling in vacuum using the ANU Plunger were investigated.

The so-called recoil in vacuum (RIV) method has proved powerful as a technique to measure the magnetic moments of short-lived excited states of exotic nuclei produced as radioactive beams [1-3]. When a recoiling ion from a nuclear reaction leaves the target and enters vacuum, the free-ion hyperfine fields couple the nuclear angular momentum, ***I***, to the atomic angular momentum, ***J***, and together they undergo a precession about the total, ***F***, at a frequency proportional to the nuclear moment times the strength of the hyperfine magnetic fields at the nucleus. The method can therefore be used either to study free-ion hyperfine interactions (if the nuclear moment is known) or measure nuclear moments (if the hyperfine fields are known). In principle, the hyperfine fields can be calculated by atomic physics methods such as Multiconfiguration Hartree Fock (MCHF), especially if the ions have simple electronic configurations (i.e. few electrons remain bound to the ion).

To date, the nuclear moment measurements performed on radioactive beams have used time-integral measurements, in which the effect of the hyperfine interactions of the free ions is averaged over the lifetime of the nuclear state. A potentially more sensitive method would be to measure the time dependence of the hyperfine interactions, and where feasible, the actual frequency of the precession. A time-dependent RIV method (TDRIV) applicable for radioactive beams has been proposed by Stuchbery, Mantica and Wilson [4]. In conventional TDRIV measurements the ions are stopped in a foil after flying a distance D through vacuum. At that point the hyperfine interactions are quenched and the orientation of the nuclear spin is frozen. By varying the distance D, the precession frequency of the ions in vacuum can be observed.

This paper describes the development of methods and apparatus at ANU for time-dependent RIV measurements (TDRIV) on ^{76}Ge. The aim is to illuminate puzzling differences observed in integral RIV measurements on Ge and Se isotopes under similar of experimental conditions [5]. Experimental results and calculations of hyperfine interactions for relevant ions will be presented. Results of a RIV experiment on ^{54}Fe and ^{56}Fe, with very different average charge states, will also be discussed.

[1] N.J. Stone et al., Phys. Rev. Lett. 100 (2005), 187.
[2] A.E. Stuchbery and N.J. Stone, Phys. Rev C. 76 (2007), 034307.
[3] A.E. Stuchbery et al., Phys. Rev C. 76 (2007), 034306.
[4] A.E. Stuchbery, P.F. Mantica and A.N. Wilson, N.J. Stone, Phys. Rev C. 71 (2005), 047302.
[5] R.F Leslie, PhD Thesis, in preparation. A.E. Stuchbery, Hyperfine Interactions 22(10B)29.

Asif.ahmed@anu.edu.au

P3

Short-Range Texture Formation in Anatase: A TDPAC Study

D. Banerjee,[1*] **S. K. Das**[1], **T. Bhattacharjee**[2] **and S. V. Thakare**[3]

[1] *Radiochemistry Division (BARC), VECC, 1/AF, Bidhan Nagar, Kolkata-700064, India.*
[2] *Variable Energy Cyclotron Centre, 1/AF Saltlake, Kolkata – 700 064, India*
[3] *Radiopharmaceutecal Division, BARC, Mumbai-400085, India.*

Titanium dioxide is the naturally occurring oxide of titanium with chemical formula TiO_2. Its prominent modifications are anatase and rutile. Anatase and Rutile, both have tetragonal lattice structure with different lattice parameters (a = b = 4.5845 Å; c = 2.9533 Å for Rutile and a = b = 3.7842 Å; c = 9.5146 Å for Anatase). As the anatase modification is elongated along the c-axis, its crystal structure might be more susceptible to temperature effect than the rutile structure. As there is no experimental measurement for anatase with ^{181}Hf/^{181}Ta probe either at room temperature or at any other temperature except our work [1], we have pursued the low temperature study of anatase from 20K to room temperature (295K) using the nuclear hyperfine technique Time Differential Perturbed Angular Correlation (TDPAC). The sample has been prepared by coprecipitation method described elsewhere [2]. Data acquisition was carried out by electronic setup based on CAMAC electronics [1] coupled to $LaBr_3$(Ce) detectors and a closed circuit refrigeration system.

A_2G_2 spectra and their cosine transforms for anatase sample at two different temperatures are shown in Fig1. The change of TDPAC parameters with temperature is shown in Fig 2. From the present work, it has been observed that some of the anatase microcrystals in the polycrystalline sample get oriented as indicated by the ratio of the intensity of the frequency components which does not follow 3:2:1 trend [3]. The increase in the anisotropy value with lowering temperature in Fig 2 also indicates such preferential orientation of the anatase microcrystals. A plot of Ln(anisotropy) vs. 1/T has also been shown in the inset of first layer in Fig 2 from which the activation energy of crystal orientation can be calculated. The other parameters did not show a very prominent change in their values with temperature. But, the trend indicates similar phenomena. The XRD measurements at those temperatures did not show any significant indication of the texture formation. So, it is concluded that the preferential orientation only occurs in a short range distance. The TDPAC parameters indicate the present phenomenon by their behavior with temperature.

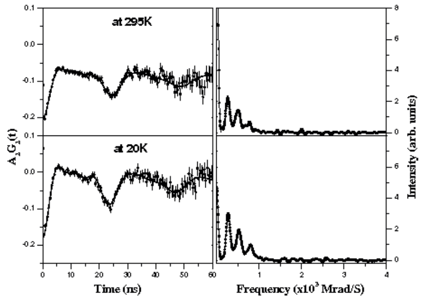

Fig. 1. TDPAC spectra for anatase at RT and 20K

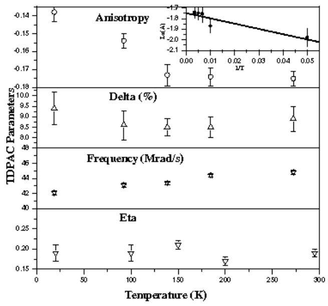

Fig. 2. Change of TDPAC parameters with temperature

[1] S K Das et al., *Journal of Physics and Chemistry of Solids* **778-781**, 70 (2009).
[2] Seung baek Ryu et al., *Physical Review* **094124**, *B* 77 (2008).
[3] R. Govindaraj et al., Pramana-J. Phys., **535-546**, 49(5) (1997).

---

*Electronic address: dbanerjee@vecc.gov.in

Properties of Fe in dilute magnetic semiconductors after ion implantation studied by 57Fe emission Mössbauer spectroscopy

Guido Langouche

Oxides (among them ZnO) doped with 3d-metal impurities have been of scientific interest since the suggestion that they could be magnetic semiconductors with potential applications in spintronics [1]. Since then, inconsistent reports on the presence of dilute magnetism have been published, with only few reports using local atomic probe methods such as Mössbauer spectroscopy.

Upon ultra-dilute ($<5\times10^{10}$ cm^{-2}) implantation in ZnO, Fe is found in the 2+ state, substituting a Zn atom [2]. Increased implantation fluences ($0.5 - 1.0\times10^{12}$ cm^{-2}) of magnetic or non-magnetic ions cause a shift of the Fermi level [2] and Fe^{3+} probe ions are now found showing slow paramagnetic spin-lattice relaxation [3] with no signature of long-range magnetic ordering [4]. While in MgO and Al_2O_3 the Fe^{3+} spin relaxation rate shows a T^2 dependence expected of a two phonon Raman process, the spin relaxation in ZnO shows an abnormal T^9 dependence [3].

The Fe^{3+} state is observed to be unstable both in time (at room temperature) and upon thermal annealing at temperatures >760 K [5]. Higher fluences ($>10^{15}$ cm^{-2}) of 3d-ions (^{57}Mn and ^{57}Co decaying to ^{57}Fe) also generate instability of the Fe^{3+} state, with the formation of amorphous zones and finally precipitation [6].

Results obtained in the intermediate fluence range in ZnO, where the probe atoms begin to interact with each other, will be discussed along with results on spin-relaxation rates in other oxides.

[1] T. Dietl et al., *Science*, **287**, 1019 (2000).
[2] R. Mantovan et al., *J. Phys.: Condens. Matter* **24**, 485801 (2012).
[3] T. Mølholt et al., *Phys. Scr.* **T148**, 014006 (2012).
[4] H. P. Gunnlaugsson et al., *Appl. Phys. Lett.*, **97**, 142501 (2010)
[5] D. Naidoo et al., *Hyp. Int.* **221**, 45-51 (2013)
[6] H. P. Gunnlaugsson et al., *Appl. Phys. Lett.* **100**, 042109 (2012)

---

e-mail address: guido.langouche@kuleuven.be

Mössbauer spectroscopy on Fe, Ru and Ir-Sn cluster compounds

Tilo Söhnel,[1,2] Morgan Allison,[1,3] Fritz E. Wagner,[4] Glen Stewart,[5] Chris Ling[3]

[1] *School of Chemical Sciences, The University of Auckland, New Zealand* ✶
[2] *Centre for Theoretical Chemistry and Physics, The New Zealand Institute for Advanced Study, Massey University, Auckland, New Zealand*
[3] *School of Chemistry, The University of Sydney, Sydney, Australia*
[4] *Physics Department E15b, Technical University, Munich, Germany*
[5] *School of Physical, Environmental and Mathematical Sciences, UNSW@ADFA, Canberra, Australia*

Mixed tin - transition metal cluster compounds form novel nano-scale clusters with a wide variety of different combinations of metals and resulting architectures which are size tunable. The central and most striking structural feature of all these stannates is the formation Sn_6-octahedra, which are filled with the different transition metals. In this presentation some Fe, Ru and Ir containing examples will be discussed in more detail.

The Fe based clusters $Fe_{4-x}Mn_xSi_2Sn_7O_{16}$ provides a novel situation in oxide compounds. It can be described as a composite of intermetallic ($FeSn_6$) clusters and (Fe/MnO_6)/(SnO_6) oxide layers within the one structure. SiO_4 tetrahedra separate these layers which leads to electronic and magnetic isolation of the repeated layers by about 7 Å resulting in a nearly perfectly 2D oxide system comparable to a one layer thick oxide “thin film”. ^{57}Fe-Mössbauer spectra seem to confirm a clear preference of Mn sitting in the oxide layers and Fe in the cluster layers (Fig. 1).

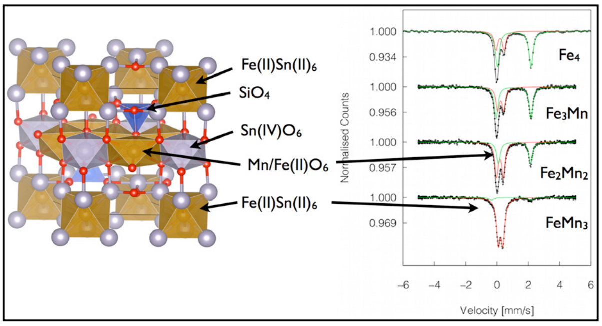

Fig. 1. Crystal structure (left) and ^{57}Fe- Mössbauer spectra of $FeFe_{3-x}Mn_xSi_2Sn_7O_{16}$

In $RuSn_6[FeO_4]O_4$ the $RuSn_6$ octahedra are isolated from each other in contrast to most of the other compounds in this group where a condensation via common corners and edges can be found. The structure of $RuSn_6[FeO_4]O_4$ is cubic and the isolated $RuSn_6$- octahedra are connected via oxygen atoms and FeO_4 tetrahedra. For $RuSn_6[FeO_4]O_4$ a tetragonal distortion which should be expected for the d^6 ion Fe^{2+} centering the FeO_4 tetrahedra could not be observed. This can be explained with a dynamic Jahn-Teller distortion. Measurements of magnetic susceptibility confirmed the spin only behaviour of Fe^{2+} from room temperature until 56 K. Below 56 K spin - orbit coupling takes place. At the same time a distortion of the local coordination of the Fe^{2+} atoms seems to occur as Mössbauer measurements show.

In $Ir_3Sn_8O_4$, the oxygen poorest of all compounds in this group of clusters, $IrSn_6$ octahedra are partly side-linked in contrast to most of the other compounds in this group. This compound shows an incommensurately modulated structure due to Ir-Ir interactions within the condensed $IrSn_6$ octahedra. ^{193}Ir- and ^{119}Sn-Mössbauer spectra seem to agree with this interpretation. This paper gives an overview about the preparation, crystallographic and Mössbauer spectroscopic characterization of this new group of cluster compounds.

Electronic address: *t.soehnel@auckland.ac.nz*

Measurement of hyperfine splitting of ^{133}Cs atoms in superfluid helium

K. Imamura,[1,2] **T. Furukawa,**[3] **X. F. Yang,**[1,4] **Y. Mitsuya,**[2] **T. Fujita,**[5] **M. Hayasaka,**[6] **T. Kobayashi,**[7] **H. Hatakeyama,**[8] **H. Ueno,**[1] **H. Odashima,**[2] **and Y. Matsuo**[9]

[1]*RIKEN Nishina Center, 2-1 Hirosawa, Wako, Saitama 351-0198, Japan*
[2] *Dept. of Physics, Meiji University, 1-1-1 Higashi-Mita, Tama-ku, Kawasaki, Kanagawa 214-8571, Japan*
[3] *Dept. of Physics, Tokyo Metropolitan University, 1-1 Minami-Osawa, Hachioji, Tokyo 192-0397, Japan*
[4] *School of Physics, Peking University, Chengfu Road, Haidian District, Beijing, 100871, China*
[5] *Dept. of Physics, Osaka University, 1-1 Machikaneyama, Toyonaka, Osaka 560-0043, Japan*
[6] *Dept. of Physics, Tokyo Gakugei University, 4-1-1Nukuikitamachi, Koganei, Tokyo 184-8501, Japan*
[7] *RIKEN, 2-1 Hirosawa, Wako, Saitama 351-0198, Japan*
[8] *Dept. of Applied Physics, Tokyo University of Agriculture and Technology, 2-24-16 Naka-cho, Koganei, Tokyo 184-8588, Japan*
[9] *Dept. of Advanced Sciences, Hosei University, 3-7-2 Kajino-cho, Koganei-shi, Tokyo, 184-8548, Japan*

We have been developing a new nuclear laser spectroscopy technique that is called OROCHI (Optical RI-atoms Observation in Condensed Helium as Ion-catcher). OROCHI utilizes superfluid helium (He II) not only as efficient stopping medium of highly energetic ions but also as a host matrix of in-situ atomic laser spectroscopy [1]. In OROCHI, highly energetic ion beam is injected into He II. The injected ions are decelerated, neutralized, and trapped as atoms. Using circularly polarized laser light, we produce atomic spin polarization of the trapped atoms and measure Zeeman / hyperfine structure (HFS) splitting using laser-radio frequency (RF)/microwave (MW) double resonance method. From the measured RF/MW resonance frequencies, we can elucidate nuclear spins and moments, respectively.

So far we have measured Zeeman splitting of the stable isotope of alkali and alkali-like atoms introduced into He II using laser ablation technique [2]. We also successfully observed Zeeman resonance using $^{84\text{-}87}$Rb beam produced by RIPS beamline at RIKEN and deduced these nuclear spin values [3-4]. Further application of OROCHI, we have to ensure that He II is suitable for measuring HFS splitting of embedded atoms that are indispensable for deducing nuclear moment value. The precision measurement of HFS splitting of atoms in He II start with ^{133}Cs atoms whose HFS splitting in vacuum was well known and have already measured in He II. The reported HFS splitting in He II is slightly different (<1%) from that in vacuum due to the effect of the surrounding helium [5]. However, the accuracy of reported values was not so high due to the uncertainty of applied magnetics field that was used to produce atomic spin polarization [5]. To know the effect of surrounding helium more precisely, we perform a series of experiments to measure HFS splitting of atoms introduced into He II. For this purpose we observe HFS resonance by sweeping MW frequencies. In particular, we scan MW frequency in discrete and synchronized steps mode. We successfully improve the measurement accuracy by an order of magnitude. In this presentation, we will report the result of our experiment in detail.

[1] T. Furukawa et al., Hyp int, **196**, 191, (2010)
[2] T. Furukawa et al., Physica E, **43**, 843, (2011)
[3] T. Furukawa et al., NIM B, **317**, 590, (2013)
[4] X. F. Yang et al., *submitted to* Phys. Rev. A, (2014)
[5] Y. Takahashi et al., Z. Phys. B, 98 391-393 (1995)

Electronic address: *kimamura@riken,jp*

First principles calculations of the Cd-doped $ZrIn_2$: a study of electronic properties and electric field gradients

L.F.D. Pereira[1], F.H.M Cavalcante[1], J.T. Cavalcante[1], E. Baggio-Saitovitch[1],
M.B. Fontes[1], H. Saitovitch[1], M. Forker[2], J. Mestnik-Filho[3], A. W. Carbonari[3]
[1]*Centro Brasileiro de Pesquisas Físicas, Rio de Janeiro, Brasil*
[2]*Institut für Strahlen und Kernphysik der Universität, Bonn, Germany*
[3]*Instituto de Pesquisas Energéticas e Nucleares, São Paulo, Brasil*

Due to their stimulating technological applications, the about 80 binary Indium Transition-Metals (In-TM) alloys are presently attracting considerable attention. The fundamental properties of these alloys as displayed by their atomic compositions, structures and charge densities, however, were extensively studied so far only for a few members of this group of alloys. The present contribution deals with $ZrIn_2$, a member of the Zirconium-Indium system ($ZrIn_2$, $ZrIn_3$, ZrIn, Zr_2In and Zr_3In), for which only few experimental and theoretical studies are available up to now. The electric field gradients (EFG) at Cd impurities on the two In sites (8*e*) of $ZrIn_2$ (space group $I4_1/amd$) have recently been determined by perturbed angular correlation (PAC) spectroscopy [1]. Here we report first principle calculations of the EFG tensor and the electronic structure of Cd-doped $ZrIn_2$. The lattice parameters that correspond to the minimum energy, the total and the partial components of the EFG tensor at Cd on the two In sites were determined and are compared to the experimental PAC results. All calculations were developed at "SsolarIII" in CBPF and at IPEN computational clusters using WIEN2k code.

[1] H. Saitovitch, P.R.J. Silva, J.Thadeu Cavalcante, M. Forker, Journal of Alloys and Compounds 505 (2010) 157-162.

Electron – nuclear spin interactions for nuclear moment studies.

Georgi Georgiev[1]

[1] *CSNSM/IN2P3/CNRS, Orsay, France*

Nuclear moments are among the most sensitive observables that can provide experimental information on the composition and purity of the nuclear wave function. They are of particular interest in regions of the nuclear chart where rapid changes in nuclear structure are expected.

The interactions between the electron and nuclear spins of free ions have been used for many years for nuclear moment studies. The experimental challenges in these measurements stem from the difficulties in the precise determination of the observed fields and the requirements for a relatively high level of statistical data. Previous measurements were mostly limited to studies of stable nuclei. With the advances of the radioactive beam facilities, providing an increasingly larger variety of radioactive species at higher intensity, nuclear moment studies based on the electron - nuclear spin interactions, can be extended to radioactive isotopes after some specific modifications.

The Time Dependent Recoil In Vacuum (TDRIV) technique on H-like ions was developed for radioactive beam geometry and tested using the 2^+ state of ^{24}Mg. The experiment, performed at the ALTO facility in Orsay, provided high-precision results that allow for a stringent test of nuclear models. The experimental details will be presented and the interpretation of the obtained g factor will be discussed in view of recent theoretical models.

The use of the Tilted Foils (TF) technique for obtaining a polarized nuclear-spin ensemble was suggested many decades ago. The extended use of this technique for nuclear moment studies has been hampered by the requirement for a specific energy regime, not easily accessible until recently at radioactive beam facilities. The possibility for post-acceleration of radioactive beams, presently available at a number of facilities, can allow for a routine application of this technique, especially in cases where other polarization methods encounter difficulties.

A combined TF-polarization plus beta-NMR setup has been installed recently at REX-ISOLDE. The results from tests using ^{8}Li beams will be presented and the new insights into the polarization mechanism and its dependencies will be presented. The perspectives for future application of this technique for nuclear moment studies will be addressed.

Electronic address: *Georgi.Georgiev@csnsm.in2p3.fr*

Ab initio calculations of electric field gradient and magnetic hyperfine field in Fe-doped SnO_2

**Qiaoli Zhang, Daqing Yuan, Ping Fan, Yi Zuo, Yongnan Zheng, Xiaoqiang Ma,
Juncheng Liang, Huanqiao Zhang and Shengyun Zhu**

China Institute of Atomic Energy, PO Box 275-50, Beijing 102413, China

Much attention has been paid to study the diluted ferromagnetic semiconductors with a Curie temperature well above room temperature, which have potential applications in spin electronics. For a better understanding of the origin of the ferromagnetism, especially in the presence of O vacancies, the microscopic electronic structure and hyperfine fields are required. These can be obtained theoretically by the *ab initio* calculations

In this paper, an *ab initio* calculations of the electric field gradients (EFGs) and magnetic hyperfine fields in the Fe doped SnO_2 were performed by the Wien2k code embodying the full-potential linearized augmented plane-wave method for two charge states of the Fe impurity that occupies a substitutional site of Sn atom, which are related to two different cases of the neutral impurity state Fe^0 and the charged acceptor state Fe^{1-} or Fe^{2-}. The Fe doped SnO_2 system can provide one or two electrons via oxygen donor vacancies. Listed in the Table 1 are the calculated electric field gradients and their asymmetry parameters and the magnetic hyperfine fields at the Fe sites.

Table 1 Calculated electric field gradients, asymmetry parameters and magnetic hyperfine fields

Supercells	V_{33}(10^{21} V/m^2)	V_{33}direction	η	magnetic hyperfine field (T)
$(SnO_2)_{15}FeO_2$	15.03	Z	0.27	22.8
$(SnO_2)_{15}FeO$ (V_{O1})	10.36	Z	0.20	-45.2
$(SnO_2)_{15}FeO$ (V_{O2})	-4.68	X	0.64	-45.1
$(SnO_2)_{15}FeO$ (V_{O3})	3.15	Y	0.05	-49.4
$(SnO_2)_{15}FeO_2$+1e	2.85	Y	0.09	-45.5
$(SnO_2)_{15}FeO_2$+2e	7.30	X	0.11	-43.9

The present results illustrate clearly that the energy level splitting of the Fe-3*d* orbit with O vacancies and without O vacancies for the $(SnO_2)_{15}FeO_2$+1e and $(SnO_2)_{15}FeO_2$+2e valences resulted in increasing the unpaired electron number and leading the Fe atoms to the high spin states, causing the giant magnetic moment. Also, our calculation yields the ferric moment of 5 μ_B per ion for $(SnO_2)_{15}FeO_2$+1e. The details will be given.

Electronic address: *zql@ciae.ac.cn*

Fluctuating Hyperfine Interactions: an Updated Computational Implementation

M. O. Zacate[1] **and W. E. Evenson**[2]

[1] *Dept. of Physics and Geology, Northern Kentucky University, Highland Heights, KY 41099, USA**
[2] *Dept. of Physics, Utah Valley University, Orem, UT 84058, USA*

The stochastic hyperfine interactions modeling library (SHIML) [1] is a set of routines written in the C programming language designed to assist in the analysis of stochastic models of hyperfine interactions. The routines read a text file description of the model, set up the Blume matrix, upon which the evolution operator of the quantum mechanical system depends, and calculate the eigenvalues and eigenvectors of the Blume matrix, from which theoretical spectra of experimental techniques can be calculated. The original version of SHIML constructs Blume matrices applicable for methods that measure hyperfine interactions with only a single nuclear spin state. In this paper, we report an extension of the library to provide support for methods such as Mössbauer spectroscopy and nuclear resonant scattering of synchrotron radiation, which are sensitive to interactions with two nuclear spin states. Examples will be presented that illustrate the use of this extension of SHIML to generate Mössbauer spectra for polycrystalline samples under a variety of fluctuating hyperfine field models.

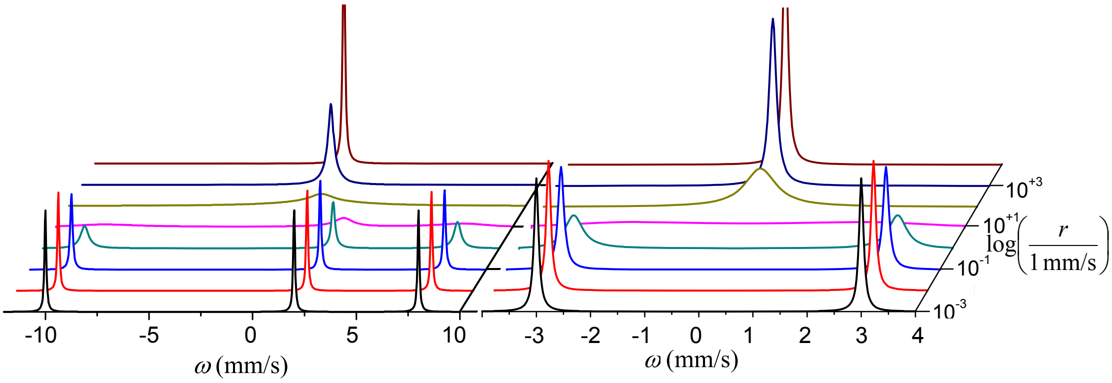

Fig. 1. Simulations for the XYZ model of an axially symmetric electric field gradient with strength 1.0 mm/s fluctuating with rate r for a Zn-like transition (5/2→1/2) on the left and for an Fe-like transition (3/2→1/2) on the right both with a 0.1 mm/s natural line width.

[1] M. O. Zacate and W. E. Evenson, *Computer Physics Communications* **182**, 1061 (2011).

---

*Electronic address: *zacatem1@nku.edu*

High-pressure studies using synchrotron-based Mössbauer spectroscopies

Gerhard Wortmann

[1] *Department of Physics, University of Paderborn, D-33095 Paderborn, Germany*

A review is given on the new Mössbauer spectroscopies using synchrotron radiation for high pressure studies. We will shortly introduce to these new methods, first nuclear forward scattering (NFS) for hyperfine spectroscopy, then nuclear inelastic scattering (NIS) for site-specific phonon spectroscopy as well as to the recently developed synchrotron Mössbauer spectroscopy (SMS), following the historical development of these new methods [1,2] and their application for high pressure studies in the Megabar range [3]. We will introduce to the use of NFS with the ^{57}Fe- and ^{151}Eu-resonances for the study of magnetism in Fe and Eu systems to pressures up to and above 1 Mbar (100 GPa). Then we will introduce to the NIS method, allowing phonon spectroscopy in the same pressure range, with the first studies of phonon spectra of metallic iron in the bcc α-phase and the high-pressure hcp ε-phase [4].
Then various NFS studies on EuX (X = O, S, Se, Te) under high pressure are presented [5-7]. These Eu(II)-chalcogenides are model systems for Heisenberg magnetism, extensively studied before with various methods with respect to magnetism and possible valence changes under high pressure. Most spectacular are recent studies on EuO up 80 GPa with the observation of a reentrant valence change back to divalency in the CsCl high-pressure phase [7]. We will also review similar high-pressure studies of Eu metal with respect to the Eu valence in the various phases [8,9]. As in the EuX systems, comparison with other synchrotron-based methods, e.g. x-ray absorption spectroscopy for valence determination, will be given [7,9]. We shortly present application of the ^{119}Sn- and ^{149}Sm-Mössbauer resonances for high-pressure studies of SnO [10] and SmS [11].
Finally we introduce to the new SMS method, allowing ^{57}Fe-Mössbauer spectroscopy in the "classical" energy mode with a $FeBO_3$ crystal filtering the resonant gamma rays from the synchrotron beam [12], similar as done in the very first ^{57}Fe-experiment [1]. Due to the extreme collimation and intensity of this gamma-ray beam, high-pressure experiments can performed in very short time (hours instead of days) and also on complex samples with different Fe sites or phases, most useful for samples from the inner of the Earth [12].

[1] E. Gerdau, R. Rüffer, et al., Phys. Rev. Lett. 54, 835 (1985).
[2] J.B. Hastings et al., Phys. Rev. Lett. 66, 770 (1991); U. van Bürck et al., Phys. Rev. B 46, 6207 (1992).
[3] R. Lübbers, G. Wortmann, H.F. Grünsteudel, Hyp. Interact. 123/124m 529 (1999).
[4] R. Lübbers et al., Science 287, 1250 (2000); H.K. Mao et al., Science 292, 914 (2001).
[5] O. Leupold, K. Rupprecht, G. Wortmann, Structural Chemistry 14, 97 (2003).
[6] K. Rupprecht at al, ESRF Highlights 2005, p.10-12.
[7] N.M. Souza-Neto et al., Phys. Rev. Lett. 109, 026403 (2012).
[8] G. Wortmann, U. Ponkratz, B. Bielemeier, and K. Rupprecht, High Press. Research 28, 545 (2008).
[9] W. Bi et al., Phys. Rev. B 85, 205134 (2012).
[10] H. Giefers et al., Phys. Rev. 74, 094303 (2006).
[11] U. Ponkratz et al., Phys. Rev. B 78, 104120 (2008).
[12] V.B. Potapkin et al., J. Synchrotron Rad. 19, 559 (2012); Nature Commun. 4 , 1427 (2013).

Electronic address: wortmann@physik.upb.de

The ^{57}Fe hyperfine interactions in the iron bearing phases in different fragments of Chelyabinsk LL5 meteorite: a comparative study using Mössbauer spectroscopy with a high velocity resolution

A.A. Maksimova[1], M.I. Oshtrakh[1,2], E.V. Petrova[1], V.I. Grokhovsky[1], V.A. Semionkin[1,2]

[1]*Department of Physical Techniques and Devices for Quality Control and*
[2]*Department of Experimental Physics, Institute of Physics and Technology,*
Ural Federal University, Ekaterinburg, 620002, Russian Federation

Chelyabinsk meteorite fell on February 15, 2013 in Chelyabinsk Region, Russian Federation. It was characterized as ordinary chondrite LL5 group, shock stage S4 and weathering W0. Various fragments of this meteorite were immediately collected by Meteoritical expedition of the Ural Federal University. It was found that these fragments were with different lithology (light, mixed light and dark, black). Four samples of these fragments with such type of lithology were chosen for comparative study of the ^{57}Fe hyperfine interactions in the iron bearing phases in these fragments: No 1 and No 1a with a light lithology, No 2 with a mixed light and dark lithology, and No 3 with a black lithology. Samples were prepared in the form of powder. Mössbauer spectra were measured using a precision Mössbauer spectrometric system with a high velocity resolution at room temperature and registered in 4096 channels. Then these spectra were converted into the 1024 channels spectra by consequent summation of four neighboring channels to increase signal-to-noise ratio for the minor spectral components.

The Mössbauer spectra of the studied fragments are similar to well-known spectra of ordinary chondrites. These spectra were fitted using magnetic sextets for the metal and troilite components, two pairs of quadrupole doublets for the M1 and M2 sites in both olivine and pyroxene and one or two single lines related to the paramagnetic γ-Fe(Ni, Co) and chromite (see Fig. 1 with the spectrum of fragment No 2). A comparison of the ^{57}Fe hyperfine parameters for the main iron bearing phases demonstrated some small variations. This fact may be a result of different origin of these fragments related to the breccia structure of Chelyabinsk LL5 meteorite as a result of several parent bodies collisions in the space.

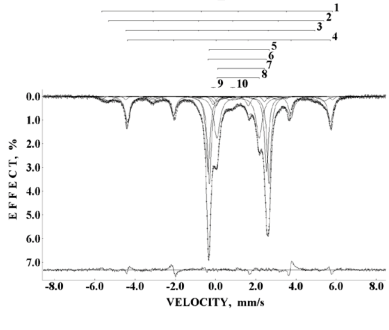

Fig. 1. Mössbauer spectrum of Chelyabinsk LL5 meteorite fragment No 2: 1–3 are the metal components, 4 is the troilite component, 5 and 6 are the olivine components related to the M1 and M2 sites, 7 and 8 are the pyroxene components related to the M1 and M2 sites, 9 is the paramagnetic metal component, 10 is the chromite component.

Electronic address: *oshtrakh@gmail.com*

^{57}Fe-Mössbauer study of LiNH$_2$-intercalated FeSe: Evidence for spin fluctuations connected with superconductivity at T_C = 43 K.

Vadim Ksenofontov,[1] Sergii Shylin[1], Sergey A. Medvedev[2], Gerhard Wortmann[3], Simon J. Clarke[4], Stefan Sedlmaier[4], Claudia Felser[2]

[1] *Institute of Inorganic and Analytical Chemistry, Johannes Gutenberg-University Mainz, D-55099 Mainz, Germany*
[2] *Max Planck Institute for Chemical Physics of Solids, D-01187 Dresden, Germany*
[3] *Department of Physics, University of Paderborn, D-33095 Paderborn, Germany*
[4] *Department of Chemistry, University of Oxford, Oxford OX1 3QR, UK*

Despite of intensive studies of Fe-based superconductors (s.c.) in the last years, the pairing mechanism is still an open question. Here we present a ^{57}Fe-Mössbauer study of LiNH$_2$-intercalated FeSe with a s.c. transition temperature, T_C = 43 K [1]. This is the highest T_C in the family of FeSe-based s.c., which possess the same structural characteristics, namely FeSe layers, here separated by the intercalated LiNH$_2$-moieties [1]. The present Mössbauer study continues previous studies, starting with the most simple system, FeSe with T_C = 8.5 K, where high pressure could dramatically enlarge T_C up to 36 K [2] and demonstrate, using ^{57}Fe-synchrotron phonon studies, that conventional electron-phonon pairing cannot explain this pressure-induced increase in T_C [2, 3]. ^{57}Fe-Mössbauer studies enabled also to observe in $Rb_{0.8}Fe_{1.6}Se_2$ with T_C = 32 K a phase separation into a magnetic phase and a non-magnetic s.c. phase, the latter with hyperfine parameters near to those of FeSe [4].

^{57}Fe-Mössbauer spectra of the present LiNH$_2$-intercalated FeSe sample exhibit at temperatures above 100 K only a quadrupole doublet with hyperfine parameters near to those of FeSe and the s.c. phase in $Rb_{0.8}Fe_{1.6}Se_2$, but with characteristic changes pointing to modifications of the electronic band structure, which could be correlated with the increase in T_C. Most important is the observation that at lower temperatures, approaching T_C, we observe beside this dominant quadrupole doublet additional magnetic subspectrum of up to 25% of the Fe sites. Detailed analysis of this magnetic subspectrum points to its dynamic character, characteristic for spin fluctuations of Fe^{2+} ions, located in the s.c. FeSe layers. We will discuss these properties also with respect to high-pressure resistivity studies of the present sample up to 6 GPa, where we observe beside a reduction of T_C down to 28 K also characteristic changes in the resistivity curves indicating corresponding changes in the fluctuation rate of these magnetic Fe ions, similar to previous observations in FeSe under pressure [5]. We compare the present results with the NMR studies [5] considering recent conclusions that also in FeAs-based s.c. systems antiferromagnetic spin fluctuations may act as “glue” for superconducting pairing. It is important especially with respect to the experimental observations and theoretical conclusions that s.c. and magnetism are closely related in the corresponding phase diagrams [6].

[1] M. Burrard-Lucas et al., *Nat. Mater.* **12**, 15 (2013).
[2] S. Medvedev et al., *Nat. Mater.* **8**, 630 (2009).
[3] V. Ksenofontov et al., *Phys. Rev. B* **81**, 184510 (2010).
[4] V. Ksenofontov et al., *Phys. Rev. B* **84**, 180508 (2011) and *Phys. Rev. B* **85**, 214519 (2012).
[5] T. Imai et al., *Phys. Rev. Lett.* **102**, 177005 (2009).
[6] D.C. Scalpino, *Rev. Mod. Phys.* ***84***, 1383 (2012).

Electronic address: *ksenofon@uni-mainz.de*

Temperature dependence of magnetic anisotropy constant in $CoFe_2O_4$ nanoparticles examined by Mössbauer spectroscopy

Sunghyun Yoon[1]

[1] *Department of Physics, Gunsan National University, Gunsan 573-701, South Korea* ✶

Magnetic anisotropy is a core factor that controls the functionality of magnetic nanoparticles. However, its significance is often overlooked that its temperature dependence is ignored in many studies, in which it is dealt with as a constant of temperature. In this study, an intuitive method for determining the temperature dependence of effective anisotropy constant in polydispersed magnetic nanoparticles using Mössbauer spectroscopy is introduced.

It is already reported that the temperature dependence of the effective magnetic anisotropy constant $K(T)$ can easily be determined if the particle size distribution $f(r)$ and the anisotropy energy barrier distribution $f_A(T)$ is known at the same time [1]. The particle size distribution $f(r)$ is obtained by fitting the first quadrant part of the hysteresis loop to the classical Langevin function weight-averaged with the log-normal distribution (Fig. 1(a)).

Mössbauer spectrum for a superparamagnetic sample generally shows a superposition of sextet and doublet corresponding to the contributions from blocked and unblocked particles, respectively. And the fraction of doublet f_D from the total absorption area at a temperature (Fig. 1(b)) reflects the fraction of iron atoms in the sample that are unblocked at that temperature within the measuring time scale τ.

The fraction of doublet at a temperature T is then the fraction of the cumulative area below some critical radius r below which the particle is superparamagnetic at that temperature in the particle size distribution $f(r)$. In this way one can get a relation between a particle radius r and the corresponding blocking temperature T_B (inset of Fig. 1(b)). Finally, one can get anisotropy constant $K(T)$ substituting r and T_B into the Neel equation, $\tau=\tau_0\exp(KV/kT)$ with $\tau=\tau_{moss}=5\times10^{-9}$ s. During a programmatic process of calculation, τ_0 was determined to be 1.4×10^{-12} s that gives the value of K at 300 K to be 2.0×10^5 J/m^3, a value reported in the literature. The resultant anisotropy constant $K(T)$ decreases with increasing temperature (Fig. 1(c)).

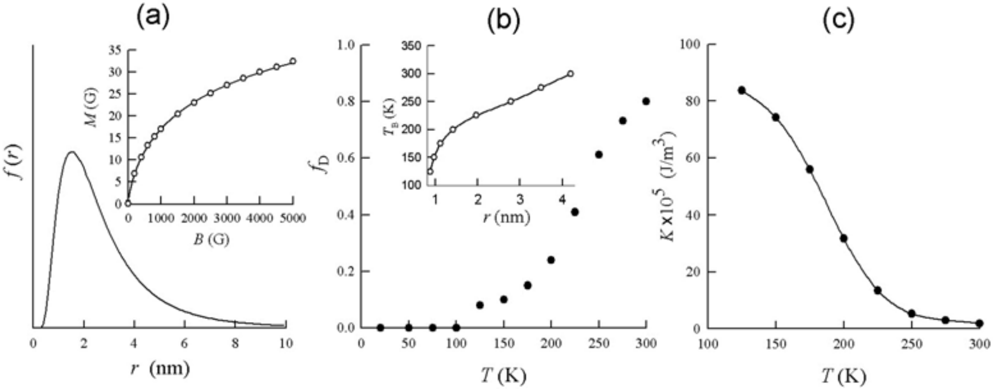

Fig. 1. (a) Particle size distribution, (b) Mössbauer doublet fraction, and (c) resultant magnetic anisotropy constant

[1] S. Yoon and K. M. Krishnan, *J. Appl. Phys*. **109**, 07B534 (2011).

Electronic addrtess: *shyoon@kunsan.ac.kr*

Phase-quantitative studies of magnetism and valence using Mössbauer spectroscopy

D.H. Ryan[1] and J.M. Cadogan[2]

*[1]Department of Physics, McGill University, Montreal, QC, H3A2T8, Canada**

[2]School of Physical, Environmental and Mathematical Sciences,
UNSW Canberra at the Australian Defence Force Academy, Canberra BC 2610, Australia

While the information provided by measurements of hyperfine interactions in solids is explicitly *local* in nature and so it cannot be used to determine long-ranged magnetic structures, it is often complementary to that derived from diffraction-based methods such as neutron diffraction, and can be essential for distinguishing candidate structures. For example, where the point symmetry permits, the ordering direction can often be established; the form of the transferred field distribution at a non-magnetic probe site can be used to distinguish between commensurate and incommensurate structures; the presence or absence of a field at a potentially magnetic site can be used to confirm that a particular species in a compound does (or does not) order. Furthermore, the local and phase quantitative nature of the information means that the *size* of the interaction can be fully separated from the *fraction* of the system that contributes. This means that, for example, a very small amount of a highly magnetic impurity cannot dominate the response. In many cases the valence of the host atom can also be determined, and again because this is local and phase quantitative, it can be used to determine directly the balance of valence states present in a mixed valence material.

I will present examples where Mössbauer spectroscopy had been used to:

- Show that two sites in a material order at distinct temperatures
- Determine the actual ordering temperature where the susceptibility response is absent
- Establish the ordering temperature of a material in the presence of a small impurity
- Observe the reorientation of magnetic order
- Distinguish the valence states in closely related materials
- Track the development of a moment as the valence evolves with composition
- Complement neutron diffraction data by distinguishing between possible magnetic structures

---

*Electronic address: `dhryan@physics.mcgill.ca`

Correlations between changes of the select Mossbauer parameters and changes in electric conductivity for the annealed fully metamict $REE_2Fe^{2+}Be_2Si_2O_{10}$

D. Malczewski[1], A. Molak[2]

[1] Faculty of Earth Sciences, University of Silesia, Bedzinska 60, 41-200 Sosnowiec, Poland
[2] Institute of Physics, University of Silesia, Uniwersytecka 4, 40-007 Katowice, Poland

Gadolinite $REE_2Fe^{2+}Be_2Si_2O_{10}$, in which REE means rare earth elements, yttrium, uranium, and thorium, belongs to the class of metamict minerals. Metamict minerals contain radioactive elements (^{238}U, ^{232}Th, ^{235}U) that degrade their crystal structures over geologic time (~10^9 years). Because of the natural occurrence of U and Th, they serve as natural analogues for radiation effects in high level nuclear waste. The electrical properties of annealed, fully metamict gadolinite $REE_2Fe^{2+}Be_2Si_2O_{10}$ are studied as a function of annealing temperature, a previously unstudied phenomenon. The electrical conductivity measured at f = 100 Hz between 110 and 750 K varies markedly, ranging from 10^{-10} to 10^{-6} Sm^{-1} for an untreated sample and 10^{-9} to 10^{-3} Sm^{-1} for a sample annealed in argon at 1373 K. Average measured activation energies for electrical conduction are 0.47 and 0.63 eV for ranges of 400 - 450 K and 500 - 600 K, respectively. The combination of polaron hopping and hydroxyl anion migration is proposed for the electrical conduction mechanism. In this study, ^{57}Fe Mössbauer spectroscopy was performed to track the transformation of the local crystal structure around the Fe positions. Good correlations can be seen between changes of the select Mössbauer parameters and the changes in electric conductivity at 300 and 500 K for the samples examined. We therefore suggest that ionic OH^- conductivity is associated with geometries (distortions, rotations) in Fe and REE polyhedra. The geometries control channel widths in the Fe/REE sheets. Electron hopping effects are most likely localized between Fe positions with a scale of Fe – Fe length. Hence, changes in the ^{57}Fe Mössbauer parameters vs. annealing temperature are not only sensitive indicators of the thermal recrystallization, but also of changes in electrical conductivity of fully metamict $REE_2Fe^{2+}Be_2Si_2O_{10}$ during annealing. Similar correlations may be expected for other metamict phases.

dariusz.malczewski@us.edu.pl

Neutrons High Pressure crystallographic structure and magnetic Study of the Fe-Cr-Hx Phase Diagram.

Amir Broide[1,2], Silvie Maskova[3], Oleg Rivin[1], Matthew S. Lucas[4], Amir Hen[2,5], Itzhak Orion[2], Shai Salhov[1], Michael Shandalov[1], Antonio F Moreira Dos Santos[6,] Jamie Molaison [6] and Itzhak Halevy[1,2]

[1] Dept. of physics, NRCN, P.O.Box 9001, Beer-Sheva, ISRAEL
[2] Nuclear engineering Department, Ben Gurion Univ., Beer-Sheva, ISRAEL
[3] Department of Condensed Matter Physics, Charles University Prague, The Czech Republic
[4] Air Force Research Laboratory, OH, USA
[5] European Commission, JRC, ITU, Karlsruhe, Germany
[6] BL3, Spallation Neutron Source, Oak Ridge National Laboratory Oak Ridge, TN

The neutron diffraction reviled the crystallographic structure, symmetry and the unit cell parameters combined with the magnetic structure. Those techniques can give an insight to the Fe-Cr phase diagram. High Pressure X-Ray diffraction in the NSLS gave the crystallographic structure, symmetry and the unit cell parameters as function of pressure. There is a known phase transition from bcc the hcp at 13GPa in the elemental iron. In the measurements made on disordered bcc solid solutions of Fe-Cr we noticed the effect of the Cr concentration on the unit cell parameter. The transition pressure in the neutron high pressure diffraction is increasing with the increase of the Cr concentration see, an example of parental sample and hydrogenated one, $Fe_{80}Cr_{20}$, is given Fig 1 & 2. Mössbauer effect of Fe-Cr at various concentrations given in Fig. 3. The SQUID measurements of Fe-Cr at various concentrations is given in Fig. 4.

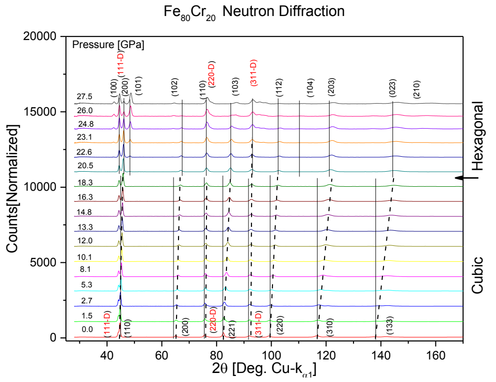
$Fe_{80}Cr_{20}$ Neutron Diffraction

Fig. 1 Neutrons Diffraction as function of pressure for $Fe_{80}Cr_{20,}$ phase transition is indicated

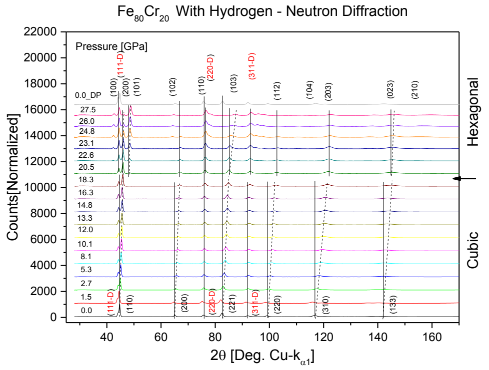
$Fe_{80}Cr_{20}$ With Hydrogen - Neutron Diffraction

Fig. 2 Neutrons Diffraction as function of pressure for $Fe_{80}Cr_{20}$ Hx, phase transition is indicated

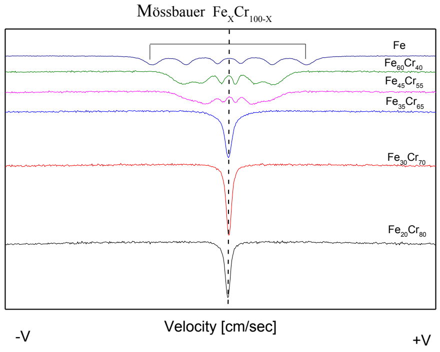
Mössbauer Fe_XCr_{100-X}

Fig. 3 Mössbauer effect for $^{57}Fe_XCr_{100-X,}$

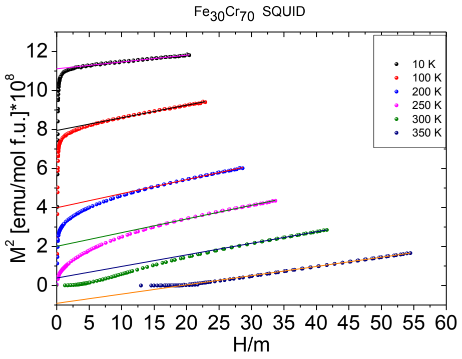
$Fe_{30}Cr_{70}$ SQUID

Fig. 4 SQUID measurement for $Fe_{70}Cr_{30,}$ as function of temperature

Halevy.itzhak.dr@gmail.com

P1

Split-vacancy palladium defect complexes in silicon and germanium

A. A. Abiona[1,*], W. Kemp[1], H Timmers[1]

[1] *School of Physical, Environmental and Mathematical Sciences,*
The University of New South Wales, Canberra, PO Box 7916, Canberra BC 2610, Australia

The defect complexes adopted by palladium atoms in germanium have been studied with time-differential γ-γ perturbed angular correlation (TDPAC) measurements that complement earlier results for silicon. The structure of these complexes and their temperature dependence is important for the palladium-induced-crystallization of germanium, which may be a lower temperature alternative to silicon in Complementary Metal-Oxide-Semiconductor (CMOS) technologies [1].

The TDPAC measurements technique used the ^{100}Pd($\rightarrow^{100}$Rh) probe that was synthesized via the heavy ion fusion evaporation reaction ^{92}Zr(^{12}C,4n)^{100}Pd and recoil-implanted into the host. Agreeing partially with the published results for silicon [2, 3], a palladium-vacancy (Pd-V) complex, aligned along <111> crystallographic direction, with a unique interaction frequency of 8.4(2) Mrad/s has been identified. This Pd-V complex has been measured to have a maximum fraction after annealing at 350 ^{0}C.

Ab initio density functional theory (DFT) calculations have been performed for palladium atoms in germanium and silicon, as well as for other relevant hosts. The DFT predictions are in excellent agreement with the experimental values for the electric field gradient observed for the palladium defect complexes in germanium and silicon. Importantly, the calculations predict a split-vacancy configuration with the Pd-atom on a bond-centred interstitial site having a nearest-neighbour semi-vacancy on both sides (V-Pd$_{BI}$-V). More specifically, single- or double-negative charge states for germanium and a single-negative charge state for the silicon, respectively, are predicted.

The good agreement between experiment and calculation gives credibility to DFT calculations for other similar host lattices, including diamond and silicon carbide [4], that will also be discussed.

References
[1] J.-H. Park *et al.*, Appl. Phys. Lett. **91**, 143107-143107-3 (2007).
[2] D.A. Brett *et al.*, Phys. Rev. B **72**, 193202 (2005).
[3] R. Dogra *et al.*, Hyperfine Interact. **177**, 33–37 (2007).
[4] A. A. Abiona, W. Kemp, H. Timmers and K. Bharuth-Ram, this conference Book of Abstracts.

Email address: *adurafimihan.abiona@gmail.com*

P2

Electronic structure and isomer shift of valence-fluctuating -YbAlB$_4$

Hisazumi Akai[1]

[1] *Institute for Solid State Physics, University of Tokyo, Kahiwa, Chiba 277-8581, Japan**

Layered Yb based heavy fermion material -YbAlB$_4$ is known to be quantum critical and superconducting at $T_C = 80$ mK without any doping [1]. So far there has been no other known pure system showing quantum criticality at ambient pressure, namely, the system is on a quantum critical point at stoichiometry and zero pressure. Furthermore the hard x-ray photoemission spectroscopy (HX-PES) proved that the valence of $+2.75$ for Yb [2], meaning that the system was in mixed valent; very rare case that valence-fluctuating system also shows a quantum criticality. It is therefore crucial to study the correlation between the valence number of Yb and the electronic structure of the system. One of the possible ways to study the valence of Yb may be a measurement of the Mössbauer isomer shift of Yb. This should be possible with the nuclear resonance forward scattering (NRSF) using synchrotron radiation. Unfortunately there has been no report of NRSF measurements on Yb systems. However, to make a theoretical prediction prior to such experiments will provide us with some pieces of information that may facilitate the effort revealing the nature of this novel quantum critical system.

In view of the above, we have studied the electronic structure of -YbAlB$_4$ on the basis of first-principles calculations, discussing its relation to the Yb valence in a quantitative way. The calculated Yb valence number at equilibrium is $+2.61$, showing a good correspondence with HX-PES. However, due to some difficulty in treating f-state in the framework of the local density approximation (LDA), on which most first-principles calculations are relying, of the density functional theory, the value of valence number remains some uncertainty. More efficient way to discuss valence of Yb may be to see the systematics of the isomer shift. Figure 1 shows one of such examples where the calculated isomer shifts are plotted as a function of arbitrary valence numbers of Yb. The detailed electronic structure of Yb f-states as well as the hybridization between those states with other bands will be discussed.

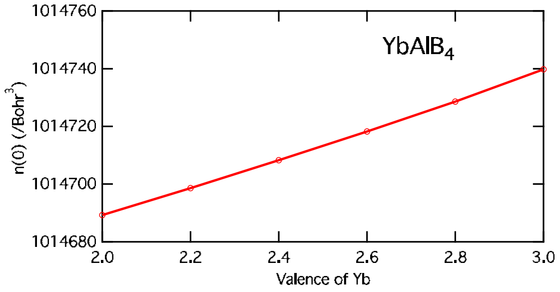

FIG. 1: Calculated isomer shift as a function of valence number of Yb in β-YbAlB$_4$

[1] S. Nakatsuji, et al., Nature Phys., **4**, 603 (2008).
[2] M. Okawa, et al., Phys. Rev. Lett., **104**, 247201 (2010).

---

*Electronic address: `akai@issp.u-tokyo.ac.jp`

Structural and optical characterization of indium-antimony complexes in ZnO

M. Deicher[1], M. Türker[1], K. Johnston[1,2], H. Wolf[1], and Th. Wichert[1]

[1] *Experimentalphysik, Universität des Saarlandes, 66123 Saarbrücken, Germany*
[2] *ISOLDE/CERN, 1211 Geneva 23, Switzerland*

ZnO with a wide band gap of 3.37 eV and a large exciton binding energy of 60 meV is considered as a promising material for optoelectronic devices. Undoped ZnO is usually n-type conductive, which is associated with the presence of native point or impurity atoms like hydrogen. Despite of lots of research, achieving reliable p-type doping of ZnO with group V elements (N, P, As, Sb) acting as acceptors located on O lattice sites is one of the main obstacles to realize optoelectronic devices based on ZnO.

Since the ionic radii of the group V elements, especially As^{3-} and Sb^{3-} far exceed that of O^{2-}, these elements more likely occupy Zn sites and act as donors. Indeed, using the emission channeling technique it was shown that the majority of implanted Sb ions occupy Zn sites in ZnO [1] and the experimentally observed p-type conductivity is probably due to the formation of Sb-defect complexes acting as acceptors.

A way out of this challenge might be the theoretically proposed codoping [2] or cluster doping [3] of acceptors and donors. The concept is to dope simultaneously donors and acceptors, whereby a formation of donor-acceptor complexes should enhance the solubility of the acceptor and its incorporation onto the desired lattice site.

In the present work In as donor and Sb as a potential acceptor are used for codoping ZnO by ion implantation. For this purpose, radioactive ^{111}In donors has been used as probe atoms sensing the neighborhood of the donors via hyperfine interaction detected by perturbed $\gamma\gamma$ angular correlation spectroscopy (PAC). After doping ZnO with ^{111}In and stable Sb by implantation, two additional electric field gradients (EFG) are observed after annealing at 1000 K indicating the formation of In-defect complexes. Due to the wurtzite structure of ZnO, even for identical defect complexes two different EFG are expected to occur. Photoluminescence (PL) spectra for indium and antimony codoped ZnO and ZnO that was exclusively doped with Sb have been recorded in the temperature range 4 K to 100 K for additional characterization of the codoping process. These results will be compared with the results of PL measurements where Sb-related optical states have been identified by the production of ^{121}Sb via the radioactive decay chain of implanted ^{121}Ag [4].

This work has been supported by the Bundesministerium für Bildung und Forschung (BMBF) under Contract No. 05K10TS2.

[1] U. Wahl, J.G. Correia, T. Mendonça, and S. Decoster, *Appl. Phys. Lett.* **94**, 261901 (2009).
[2] T. Yamamoto and H. Katayama-Yoshida, *Physica B* **302-303**, 155 (2001).
[3] L.G. Wang and A. Zunger, *Phys. Rev. Lett.* **90**, 256401 (2003).
[4] J. Cullen, D. Byrne, K. Johnston, E. McGlynn, and M.O. Henry, *Appl. Phys. Lett.* **102**, 192110 (2013).

Electronic address: *manfred.deciher@tech-phys.uni-sb.de*

Dynamical property of Li in Li-ion conductions studied by ^{8}Li β-NMR

S. Yamaoka[1], **M. Mihara**[1], **K. Matsuta**[1], **M. Fukuda**[1], **T. Minamisono**[1], **M. Yaguchi**[1], **J. Ono**[1], **Y. Kamisho**[1], **R. Kanbe**[1], **S. Shinozaki**[1], **M. Tanaka**[1], **K. Mukai**[2], **J. Sugiyama**[2]

[1]*Dept. Physics, Osaka University, 1-1 Matikaneyama, Toyonaka, Osaka 560-0043 Japan**
[2] *Toyota Central R&D Labs., Inc. / 41-1 Yokomichi, Nagakute, Aichi 480-1192 Japan*

In order to investigate the behavior of Li in Li-ion conductor materials, we have performed the β-NMR of short-lived β-ray emitter ^{8}Li ($I^\pi = 2^+$, $T_{1/2} = 0.83$ s). When a spin polarized nucleus is injected into a Li-ion conductor material, the spin polarization will relax if the injected ^{8}Li migrates between lattice sites due to fluctuation of internal field. In the present study, spin-lattice relaxation time T_1 or spin-spin relaxation time T_2 of ^{8}Li in various Li-ion conductive materials $LiCoO_2$, $Li_7La_3Zr_2O_{12}$(LLZ), Si and so on were measured by means of the β-NMR technique. Spin polarized ^{8}Li nuclei were produced through the ^{7}Li(d,p)^{8}Li reaction and implanted into the samples after selecting a recoil angle.

Fig. 1 shows typical results of the time variation of ^{8}Li polarization in various materials at room temperature from which T_1 was obtained. We have measured temperature dependence of T_1 for $LiCoO_2$ and LLZ and T_2 for Si. The dynamical property of ^{8}Li in these materials will be discussed.

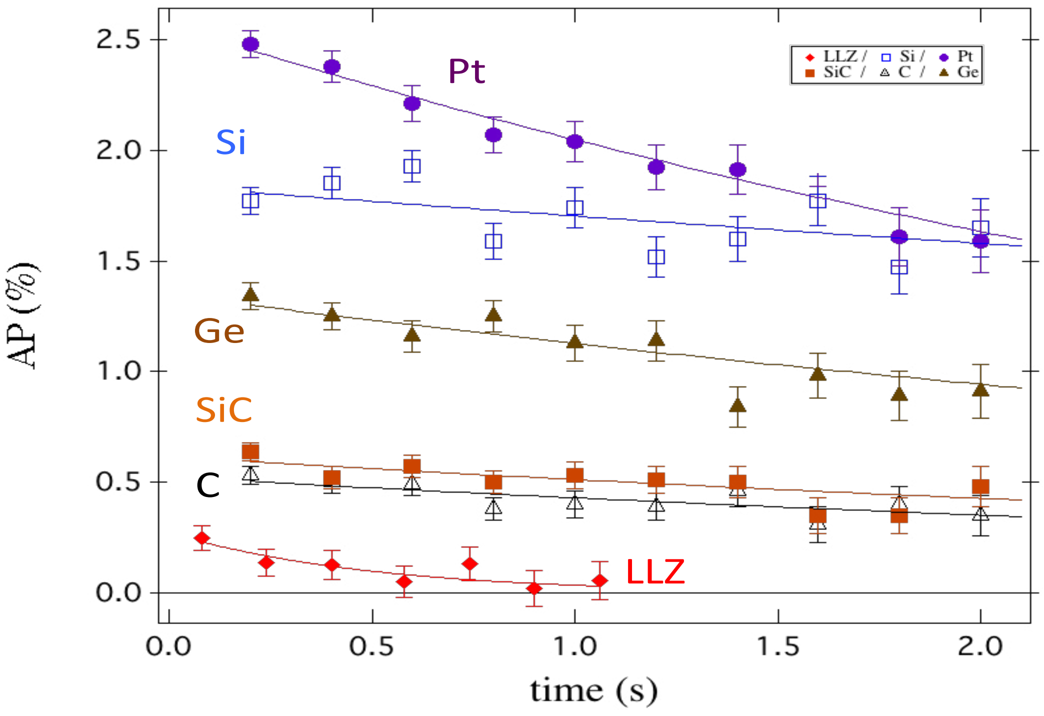

Fig. 1. Time variation of ^{8}Li polarization in various materials at room temperature.

Electronic address: *yamaoka@vg.phys.sci.osaka-u.ac.jp*

Orientation of a defect induced electric field gradient in ZnO

P. Kessler[1], K. Lorenz[2], G. Correira[2], K. Johnston[3], R. Vianden[1]

[1]Helmholtz – Institut für Strahlen- und Kernphysik, 53115 Bonn, Germany
[2]Instituto Tecnólogico e Nuclear, P-2686-953 Sacavém, Portugal
[3]Technische Physik, Universität des Saarlandes, 66041 Saarbrücken, Germany

To produce ferromagnetic ordering in ZnO, so called dilute magnetic semiconductors (DMS), one possible way or model are magnetic polarons, suggested by Coey et al. [1]. These consist in the case of ZnO of an oxygen vacancy (O_N) and a transition metal ion. Those two form a so called bound magnetic polaron that might be able to produce ferromagnetism in ZnO. The O_N could be produced with implantation or even during the implantation of the transition metals so the implantation damage could be used to form these polarons. Since the O-atoms penetrate deeper into the crystal than the Zn-atoms, because of the different masses (Zn: 65 u and O: 16 u), a Zn-rich crystal environment can be produced near the transition metals and the O_N could be trapped at those impurities and form polarons.

This problem can be addressed by means of the perturbed angular correlation (PAC) method, which is particularly sensitive to electric field gradients (EFG) produced by point defects. It can be especially useful to answer the question if O_N are formed and if they can be trapped by impurities during annealing. PAC uses radioactive isotopes as probe atoms to which vacancies can be bound and which would result in a very strong signal. This was already done with the PAC probe ^{111}In, where additional Zn was implanted to produce a Zn-rich region and indeed it was found that possibly O_N were bound to the In [2]. In this work this was studied further. The implantation conditions were varied and the probe ^{117}Cd was also used. After the implantation of the probe atoms subsequently isochronous annealing steps at different temperatures were applied. It was observed that at a temperature of 900 K defects similar to the ones found by Forkel et al, [2] are present. PAC measurements for different orientations of the ZnO crystal allowed to determine the orientation of the defect induced EFG. At annealing temperature of 1300 K these implantation related defects could be fully annealed. This leads to the conclusion, that oxygen vacancies are formed during implantation that get mobile at 900 K and are trapped by In and Cd and most likely by other impurities. So introducing transition metals via ion implantation could be a valid method to produce magnetic polarons and thus DMS.

[1] J. M. D. Coey, *Nature Materials* **4**, 173 (2005)
[2] D. Forkel, H. Föttinger, M. Iwatschenko-Borho, F. Meyer, W. Witthuhn and H. Wolf, *Mat. Res. Soc. Symp. Proc.* **46**, 481 (1985)

Electronic address: *kessler@hiskp.uni-bonn.de*

Spin crossover complexes - Muon spin relaxation and Mössbauer studies

Yann Garcia,[1] **Stewart J. Campbell**[2]**, James S. Lord**[2]**, Philipp Gütlich**[4]

[1] *Institute of Condensed Matter and Nanosciences, Université Catholique de Louvain, Place L. Pasteur 1, 1348 Louvain-la-Neuve, Belgium.*
[2]*School of Physical, Environmental and Mathematical Sciences, The University of New South Wales Canberra, The Australian Defence Force Academy, ACT 2600, Australia.*
[3]*ISIS, Rutherford Appleton Laboratory, Chilton, Didcot OX11 OQX, UK.*
[4]*Institut für Anorganische Chemie und Analytische Chemie, Universität Mainz, Staudingerweg 9, 55099 Mainz, Germany.*

Iron(II) spin crossover (SCO) complexes continue to attract a great deal of interest with focus centred on gaining a full understanding of their magnetic, optical, structural and vibrational properties as well as developing smart applications in nanotechnologies [1]. Although SCO materials have been investigated extensively by ^{57}Fe Mössbauer spectroscopy [2], the use of muon spin relaxation (μSR) has only developed over the last decade [3-8]. μSR provides information about magnetic fluctuations in a time window around 10^{-9} s to 10^{-5} s [9], thus complementing the information available from ^{57}Fe Mössbauer spectroscopy [10].

We have investigated a series of well characterised model iron(II) complexes by temperature dependent ^{57}Fe Mössbauer spectroscopy and μSR techniques at ISIS, UK. The thermally induced SCO in these materials could be monitored by following the initial asymmetry parameter, a_0, in zero-field. We established that the behaviour of a_0 correlates well with the shape of the SCO curve derived from magnetic susceptibility measurements, whether smooth, abrupt, hysteretic, or stepwise. The sensitivity of this method combined with ^{57}Fe Mössbauer spectroscopy proves useful for detecting the SCO of just a few spins [8]. In addition, the longitudinal field dependence of a_0 not only provides information on the nature of the muonic species - diamagnetic muons, diamagnetic like muonium, paramagnetic muonium and radicals - but also on their interactions and respective localization in the crystal lattice. Useful insights to the electronic structure and dynamic phenomena of these model SCO complexes can be derived [7]. Recent developments of a new class of SCO switches showing fluorescence [11] or alcohol sensing abilities [12], in the crystalline state, will also be covered.

---

[1] P. Gütlich, A. B. Gaspar, Y. Garcia, *Beilstein J. Org. Chem.* **9**, 342 (2013).

[2] P. Gütlich, Y. Garcia - Chemical applications of Mössbauer spectroscopy, in Mössbauer spectroscopy - Tutorials book (Eds Y. Yoshida, G. Langouche), Springer, chapter **2**, 23 (2013).

[3] S. J. Blundell, F. L. Pratt, C. A. Steer, I. M. Marshall, J. -F. Létard, *J. Phys. Chem. Solids* **65**, 25 (2004).

[4] (a) S. J. Campbell, V. Ksenofontov, Y. Garcia, J. S. Lord, Y. Boland, P. Gütlich, *J. Phys. Chem. B* **107**, 14289 (2003). (b) Y. Garcia, V. Ksenofontov, S. J. Campbell, J. S. Lord, Y. Boland, P. Gütlich, *J. Phys. Chem. B* **108**, 17838 (2004). (c) Y. Garcia, S. J. Campbell, J. S. Lord, Y. Boland, V. Ksenofontov, P. Gütlich, *J. Phys. Chem. B* **111**, 111111 (2007).

[7] Y. Garcia, S. J. Campbell, J. S. Lord, P. Gütlich, *Inorg. Chim. Acta* **361**, 3577 (2008).

[8] Y. Garcia, S. J. Campbell, J. S. Lord, J. Linares, M. M. Dîrtu, A. Vendrell Pérez, Y. Boland, V. Ksenofontov, P. Gütlich, *Hyperfine Interact.* doi 10.1007/s10751-013-0909-3 (2014).

[9] S. F. J. Cox, *J. Phys. C: Solid State Phys.* **20**, 3187 (1987) 3187.

[10] L. Asch, J. Chappert, G. M. Kalvius, *Hyperfine Interact.* **42**, 1137 (1988).

[11] Y. Garcia, F. Robert, A. D. Naik, G. Zhou, B. Tinant, K. Robeyns, S. Michotte, L. Piraux, *J. Am. Chem. Soc.* **133**, 15850 (2011).

[12] A. D. Naik, K. Robeyns, C. Meunier, A. Léonard, A. Rotaru, B. Tinant, Y. Filinchuk, B. L. Su, Y. Garcia, *Inorg. Chem.* **53**, 1263 (2014).

Electronic address: yann.garcia@uclouvain.be

Probing the influence of spatial confinement on magnetic and superconducting properties by nuclear resonant scattering

K. Houben[1], S. Couet[2], M. Bisht[2], C. Petermann[2], M. Trekels[2], D. G. Merkel[3], A. Chumakov[3], R. Rüffer[3], M. Hu[4], J. Zhao[4], E. E. Alp[4], A. Vantomme[2], M. J. Van Bael[1], K. Temst[2]

[1]*Laboratory of Solid-State Physics and Magnetism, KU Leuven, Belgium*
[2]*Instituut voor Kern- en Stralingsfysica, KU Leuven, Belgium*
[3]*European Synchrotron Radiation Facility (ESRF), BP 220, F-38043 Grenoble Cedex, France*
[4]*Advanced Photon Source (APS), Argonne National Laboratory, Argonne, Illinois, 60439, USA*

In this talk we present recent experimental results that underline the unique contribution of the isotope-selective technique of nuclear resonant scattering to elucidate the magnetic and vibrational properties of confined correlated electron systems. The first example is related to the magnetic properties of synthetic multiferroic structures, while the second example relates the vibrational properties of Sn nanostructures to their superconducting behavior.

In the relatively new class of artificial composite multiferroics, a ferromagnet (FM) and a ferroelectric (FE) are coupled through an interface with the aim to control the magnetic properties using electric fields. This magneto-electric coupling is strongly influenced by the structure and chemistry of such an interface. Isotope sensitive techniques offer the unique possibility to selectively investigate the *interface chemistry and magnetism in Fe/FE systems in an electric field* (FE = $BaTiO_3$ or $LiNbO_3$). NRS experiments revealed that strong oxidation of a very thin layer of Fe at the interface is triggered in large enough electric fields. This creates a magnetically dead interface layer and an irreversible decrease of the magneto-electric coupling. Material parameters such as the work function difference and the dielectric constant of the FE are crucial for this field-induced interface oxidation [1].

The interaction of phonons with electrons is of crucial importance in conventional superconductivity. When reducing the system dimensions down to the nanometer scale, deviations in the phonon density of states (PDOS) with respect to the corresponding bulk PDOS are observed. These deviations are the result of phonon confinement effects and/or surface/interface phonon modes. An increase in T_C has been observed in nanoscale Sn structures. Phonon softening, an increase of low-energetic phonon modes, is believed to be the reason for the increase in T_C. So far, very little is known about the phonon behavior in tin nanostructures because of the difficulty of experimentally probing atomic vibrations at this scale. We have studied the phonon density of states of α-Sn layers, β-Sn islands and cluster-assembled β-Sn films at low temperatures (± 25 K) at the ID-18 beamline at the ESRF and at the 03-ID beamline at the APS. The superconducting behavior of the β-Sn islands and cluster-assembled films has been characterized by SQUID magnetometry. The link between superconductivity, in particular the increase of T_C in Sn nanostructures, and the confinement effects in the PDOS is being investigated.

[1] S. Couet, M. Bisht, M. Trekels, M. Menghini, C. Petermann, M.J. Van Bael, J.P. Locquet, R. Rüffer, A. Vantomme, K. Temst, Adv. Funct. Mater. **24**, 71 (2014)

Electronic address: *kristiaan.temst@fys.kuleuven.be*

Nuclear resonance scattering above 30 keV

R. P. Hermann[1]

[1] *Jülich Centre for Neutron Science JCNS, Peter Grünberg Institute PGI,*
Leo Brandt Str.1, Forschungszentrum Jülich GmbH, D-52425 Jülich, Germany

Measurements of the partial density of phonon states with inelastic nuclear resonance scattering approach their 20th anniversary[1]. Monochromatization in the meV range is required in order to properly resolve the phonon spectrum. Obtaining such resolution becomes very challenging for nuclear resonances above 30 keV[2], as an energy resolution $\Delta E/E$ better than 3.10^{-8} is required. With the use of a single crystal sapphire backscattering monochromator we have been successful in carrying out measurements with the antimony-121 37.2 keV[3], tellurium-125 35.4 keV[4] and xenon-129 39.9 keV[5] nuclear resonances. Phonon properties were obtained in thermoelectric bulk antimonides and tellurides[6,7] as well as in similar compounds with confined geometry such as nanowires[8] or nanopowder[9].

The possibilities for future extensions for nuclear resonance scattering above 40 keV will be discussed, notably by considering which further isotopes might be accessible for phonon spectroscopy, which are currently suitable for hyperfine interaction investigations, *e.g.* ^{73}Ge at 67 keV[10], which resonances close to 90 keV hold hope for future investigations, and which diffulties are encountered for extreme conditions investigations.

The Helmholtz Gemeinschaft Deutscher Forschungszentren is acknowledged for funding VH NG-407 “Lattice dynamics in emerging functional materials” and HRJRG-402 “Sapphire Ultra Optics for Synchrotron Radiation”. The ESRF and APS are acknowledged for provision of synchrotron radiation at ID18 and ID22N, and at 6IDD respectively; the DFG for funding SPP1386 'Nanostructured thermoelectrics'; the for funding project 'NanoKoCh' number 03X3540B. I am greatly indebted to I. Sergeev, A. Chumakov, R. Rüffer, H.-C. Wille, A. Saïd, Yu. Shvyd'ko, J. Perßon, B. Klobes, A. Möchel, D. Bessas, P. Bauer Pereira, T. Claudio Weber, R. Simon, P. Alexeev, A. Jafari, M. Sougrati, A. Mahmoud, L. Stievano, and V. Asadchikov for the fruitful collaborations.

---

[1] Seto M. et al., Phys. Rev. Lett. **74**, 3828 (1995); Sturhahn W. et al., Phys. Rev. Lett. **74**, 3832 (1995); Chumakov A. et al., Europhys. Lett. **30**, 427 (1995).
[2] Sergueev I. et al., J. Synchr. Rad. **18**, 802 (2011).
[3] Wille H.-C. et al., Phys. Rev. B **76**, 140301(R) (2007).
[4] Wille H.-C. et al., Europhys. Lett. **91**, 62001 (2010); Klobes B. et al., Hyp. Inter. **226**, 713-719 (2014).
[5] Klobes B. et al., EPL **103**, 36001 (2013).
[6] Diakhate M. S., Phys. Rev. B **84**, 125210 (2011).
[7] Bessas D. et al., Phys. Rev B **86**, 224301 (2012).
[8] Bessas D., et al., Nanoscale **5**,10629-10635 (2013).
[9] Claudio T., et al., Phys. Stat. Sol. B **251**, 919-923 (2014).
[10] Simon R. E., et al., EPL **104**, 17006 (2013).

Electronic addrtess: *r.hermann@fz-juelich.de*

$FeSb_2$ – a still puzzling material

Michael Reissner,[1] Klaudia Hradil[2], Walter Steiner[1], Andreas Leithe-Jasper[3],Björn Petersen[4]

[1] *Institute of Solid State Physics, Vienna University of Technology, A-1040 Wien, Austria* ✷
[2] *X-Ray Center, Vienna University of Technology, A-1040 Wien, Austria*
[3] *Max-Planck-Institut für Chemische Physik fester Stoffe, D-01187 Dresden, Germany*
[4] *Forschungs-Neutronenquelle Heinz Maier-Leibnitz (FRM II), D-85748 Garching, Germany*

$FeSb_2$ is investigated since several decades, because of its interesting magnetic and electronic properties. Especially in the last ten years new interest arose, because new amazing properties were discovered, which made it to a promising candidate for application like thermoelectric and high speed electronics. Usually $FeSb_2$ is described as a nearly ferromagnetic small gap semiconductor [1] with a semiconductor – metal transition above 80 K [2]. It crystallizes in the marcasite structure type, where Fe occupies only one crystallographic site, which is surrounded by distorted Sb octahedra [3]. This is in agreement with Mössbauer spectra, which can be fitted by only one sub-spectrum, corresponding to a high spin ferric ground state [6]. Problems with interpretation appear, if Mössbauer spectra are taken in external magnetic fields. In that case measured spectra are extremely complex [4]. An interpretation in terms of only one sub-spectrum can only explain approximately 60 to 70% of the spectrum. For the rest up to at least five more sub-spectra are necessary. One obstacle lies in the fact that tiny differences in preparation conditions changes the magnetic behaviour, which makes it quite complicate to compare results on different samples and to figure out the common physics in this material. Whereas some groups find a diamagnetic signal at low temperatures others report only positive susceptibility values under same measuring conditions. Often also upturns in the lowest temperatures are found, indicating of secondary phases. A comparison of results obtained with different methods on different samples is therefore a challenge. In this work, we report about a reinvestigation of $FeSb_2$ by dc magnetic, high-field ^{57}Fe Mössbauer, X-ray and neutron diffraction measurements. All measurements were performed on the same sample. During sample preparation a single crystal formed together with $FeSb_2$ powder. Dc magnetic measurements were performed on the single crystal in all three crystallographic directions. In contrast to our previous work no upturn was present at lowest temperatures. Diamagnetism was found only for B parallel to the b-axis. Neither from X-ray nor from neutron diffraction data traces of secondary phases could be proved. Nevertheless, the in-field Mössbauer spectra show the same complex structure as reported before. Whereas the neutron diffraction data give no hint for a distortion of the structure, which could explain the splitting of the one crystallographic site into several sites with different surrounding, hints for such distortion comes from analysis of the radial-density function obtained from high energy X-ray investigations, pointing out a partial shift of the iron atom from the center of the octahedral along the apical axis.

[1] A.V.Lukoyanov et al., *Eur. Phys .J. B* **53**, 205 (2006).
[2] C.Petrovic et al., *Phys. Rev.B* **67**, 155205 (2003).
[3] J.Steger, E.Kostiner, *J. Solid State Chem.* **5**, 131 (1972).
[4] A.Farhan et al., *J.Phys.:Conf. Ser.* **217,** 012142 (2010).

Electronic address: *reissner@tuwien.ac.at*

Hyperfine fields and magnetic anisotropy in $Nd_2Fe_{14}B$ and $Sm_2Fe_{17}N_3$

Hisazumi Akai[1]

[1]*Institute for Solid State Physics, University of Tokyo, Kahiwa, Chiba 277-8581, Japan**

In order to meet the ever increasing demand for better permanent magnets, to design novel magnetic materials that have both the high saturation magnetization and strong magnetic anisotropy enough to be served as ingredients of permanent magnets is necessary. Although both the quantities are the bulk properties of materials, to analyze and design magnetic materials, it is desirable to experimentally decompose them into each contribution of different sites in the unit cell of the crystal of complicated structure with several species of atoms. One of the suitable ways to perform this procedure is to see the NMR/NQR data of the system [1][2].

Most high performance permanent magnets now used are Fe-based rare-earth magnets. It is known that the high saturation magnetization of those materials originates from Fe and the strong magnetic anisotropy stems from f-state of rare-earth elements such as Nd and Sm. Therefore both the Fe and rare-earth HFI/NQI's provide us with important pieces of information: Fe NMR enable us to detect site dependence of the local magnetic moment and magnetic anisotropy (Fe sites also contribute to the magnetic anisotropy) while rare-earth NQR directly give the information of electric field gradients (EFG) that are related to the shape of the f-electron cloud as well as the EFG produced by ligands. The coupling of the former with the latter, combined with the spin-orbit coupling, is the main origin of the magnetic anisotropy of Fe-based rare-earth magnets.

In this study we focus on the hyperfine fields and magnetic anisotropy of typical materials used as permanent magnets, $Nd_2Fe_{14}B$ and $Sm_2Fe_{17}N_3$ from theoretical points of view. The detailed electronic structure together with the hyperfine interactions are discussed on the basis of the first-principles calculation. In particular, the relations between the observed hyperfine fields and the magnetic anisotropy are studies in detail. The effects of doping of those materials by other elements such as Dy and the effects of N adding in $Sm_2Fe_{17}N_3$ are discussed.

[1] R.L. Streever, Phys. Lett., **65A**, 360 (1978).

[2] Cz. Kapusta, H. Figiel, G. Stoch, J.S. Lord, and P.C. Riedy, IEEE Trans. Magn., **29**, 2893 (1993).

---

*Electronic address: `akai@issp.u-tokyo.ac.jp`

Lattice location and magnetism of isolated Fe impurities in narrow band semiconductor InSb.

S.K. Mohanta and S.N. Mishra

Tata Institute of Fundamental Research, Homi Bhabha Road, Mumbai-400005, India

Magnetic behavior of dilute transition metal (TM) impurities dissolved in semiconductor hosts – also known as –dilute magnetic semiconductors (DMS) is a frontier area of research as they hold promise of future applications in spin selective electron transport – "Spintronics". The existence of stable local moments on the TM atoms is a key problem in this area. Here, we report the lattice location and magnetism of isolated Fe impurities implanted in the narrow band semiconductor, InSb. The results obtained from measurements of local susceptibility and spin relaxation rate for ^{54}Fe nuclei, using the time differential perturbed angular distribution (TDPAD) technique, reveal two distinct occupation sites for the implanted Fe atoms (see Fig. 1), with majority (75%) of them replacing In and a minority fraction (25%) entering the Sb position. The magnetic response of the Fe, displayed in Fig. 2, shows Curie-Weiss type local susceptibility and a Korringa like spin relaxation rate, reflecting the existence of stable localized moments on the Fe atoms. The experimental results are supported by detailed *ab-initio* electronic structure calculations performed within the frame work of density functional theory.

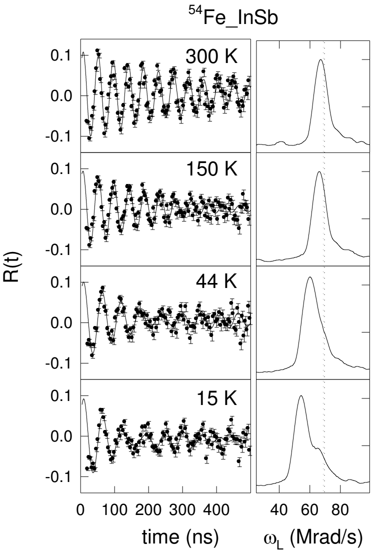

Figure 1: Spin rotation spectra of ^{54}Fe in InSb

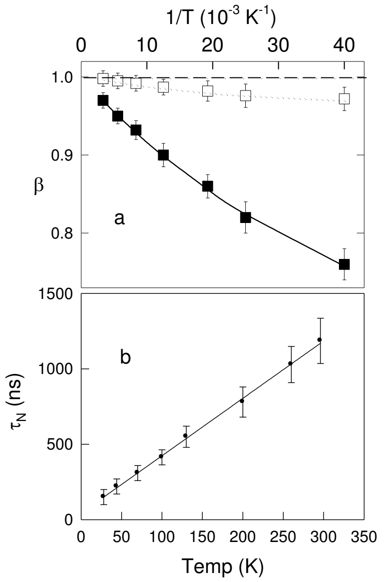

Figure 2: (a) Local susceptibility β, and (b) Spin relaxation time τ_N of ^{54}Fe in InSb

---

Electronic address: mishra @*tifr.res.in*

Magnetic interactions in NiO at ultra-high pressure.

V. Potapkin[1], **L. Dubrovinsky**[2], **I. Sergueev**[3], **D. Bessas**[4], **I. Kantor**[4], **R. P. Hermann**[1,5]

[1] *Jülich Centre for Neutron Science JCNS and Peter Günrberg Institut PGI, JARA-FIT, Forschungszentrum Jülich GmbH, D-52425, Jülich, Germany**
[2] *Bayerisches Geoinstitut, Universität Bayreuth, D-95440, Bayreuth, Germany*
[3] *Deutsches Elektronen-Synchrotron - D-22607 Hamburg, Germany*
[4] *European Synchrotron radiation Facility, BP220, F-38043, Grenoble, France*
[5] *Faculté des Sciences, Université de Liège - B-4000 Liège, Belgium, EU*

For the field of strongly correlated electronic systems, one of the most important compounds is nickel monoxide (NiO): it is one of the first compounds, that was studied in order to understand behavior of strongly correlated electronic systems, moreover, it was treated by N.F. Mott and co-authors as prototype Mott insulator[1]. Using NiO as example they explained that wide d-d energy gap U occurs in transition metal oxides due to strong Coulomb repulsion of *d*-electrons on transition metal side. Through existence of metallic high-pressure phase of NiO was predicted immediately[1], up till recently the exact pressure of insulator to metal transition was not known. Numerous preformed theoretical studies gave contradictory predictions regarding the pressure range of insulator to metal transition (IMT) in nickel monoxide, from 230 GPa[2] to above 1 TPa[3]. The main difficulty for experimental studies proved to be the predicted transition pressure (above 200 GPa). In that pressure range limited number of experimental methods can be applied. Recently the long-sought insulator-metal transition in nickel oxide has been reported to be found at ~240 GPa [4], the authors performed resistivity measurements under pressure. It is know, that in Mott insulators IMT happens due increasing broadening of *d*-electrons bands with eventual delocalization of *d*-electrons [5]. As the *d*-electrons are the source of magnetism in such compounds, the IMT in them accompanied by magnetic ordering collapse through the same mechanism[2]. Thus, without magnetic ordering investigation the real nature of observed transition cannot be determined. Here we present a study of hyperfine splinting in NiO up to ~280 GPa by recently developed ^{61}Ni Nuclear Forward Scattering (NFS) [6] - the time domain analog of ^{61}Ni Mössbauer spectroscopy. Before, we had already successfully applied the technique for investigation of the magnetic properties of Ni metal up to 260 GPa [7]. Currently, ^{61}Ni NFS is the only technique suitable for studding antiferromagnetic magnetic ordering in NiO under high pressure. In the studied pressure range the hyperfine splitting. *i.e.* magnetic ordering In NiO do not collapse, moreover three fold increase of hyperfine splitting value was observed, from 8.5 at ambient pressure to ~ 24 Tesla at 280 GPa. This indicates that up to ~280 GPa there is no magnetic collapse in NiO, *i.e.* no IMT.

[1] S. N F Mott, *Metal-Insulator Transitions, 2nd Edition* (Taylor & Francis, 1990).
[2] R. E. Cohen, Science **275**, 654 (1997).
[3] X.-B. Feng and N. Harrison, Phys. Rev. B **69**, 035114 (2004).
[4] A. Gavriliuk, I. A. Trojan, and V. V. Struzhkin, Physical Review Letters **109**, 086402 (2012).
[5] I. G. Austin and N. F. Mott, Science **168**, 71 (1970).
[6] I. Sergueev, A. I. Chumakov, T. Beaume-Dang, R. Rüffer, C. Strohm, and U. van Bürck, Physical Review Letters **99**, 097601 (2007).
[7] I. Sergueev, L. S. Dubrovinsky, M. Ekholm, O. Y. Vekilova, A. I. Chumakov, M. Zając, V. B. Potapkin, I. Kantor, S. Bornemann, H. Ebert, S. I. Simak, I. A. Abrikosov, and R. Rüffer, Physical Review Letters **111**, 157601 (2013).

Electronic address: *v.potapkin@fz-juelich.de*

New Table of Recommended Nuclear Electric Quadrupole Moments

Blank line (12 points)

N. J. Stone[1]

Blank line (12 points)

[1] *Dept. of Physics and Astronomy, University of Tennessee, Knoxville TN 37996 USA*

Blank line (12 points)

A new Table of Recommended Nuclear Electric Quadrupole Moments has been prepared for the Nuclear Data Section of the IAEA, Vienna [1]. The main feature of the new Table is the adoption, wherever possible, of the best available calculation of the electric field gradient (efg), required to extract the moment from the measured quantity in most measurement methods. All original results have been normalized to take account of differences between the efg used in the original publication and the adopted value. Many adopted efgs are from modern calculations of multi-electron states in atoms, ions and molecules. Others derive from analysis of muonic atoms. The choice has followed that of Pyykko [2] in the majority of cases. The normalisation process has led to considerable changes in the recommended moments for several elements. The most notable changes concern the moments of F, Ca, Ge, Se, and Sn isotopes where individual adjustments, both positive and negative, have reached 25%. For the majority of elements current efg calculations have errors estimated below 5% with the best close to 1%. However some 17 elements: He, Si, P, Ar, Ag, Cd, Te, Ce, Tm, W, Pt, Tl, Po, At, Cm, Bk and Cf remain, in the sequence to einsteinium at $Z = 99$, for which no basic reference standard efg has been adopted and the best available calculation or estimate has considerably larger uncertainty.

For many elements where several methods of measurement have been employed in the study of different isotopes and states, adoption of efg in a single system is not sufficient to cover all measurements. Subsidiary adopted efgs are specified and referenced.

The aim of the new table is to provide a standard reference in which the value given for each moment is the best available and for which full provenance is given. It is the intention that the table should be brought up to date at intervals as improved efg calculations and new experimental results become available.

[1] N.J.Stone, *INDC(NDS)-0650* (2014) *IAEA Nuclear Data Section, Vienna*
[2] P.Pyykko, *Molecular Physics* **106** 1965 (2008) and private communication (2011).

Electronic address: *n.stone@physics.ox.ac.uk*

Development of ^{129}Xe comagnetometer for precise measurement of neutron electric dipole moment

M. Mihara,[1] Y. Masuda,[2] K. Matsuta,[1] S.C. Jeong,[2] S. Kawasaki,[2] Y. Watanabe,[2] K. Hatanaka,[3] and R. Matsumiya[3]

*[1]Dept. Physics, Osaka Univ., 1-1 Machikaneyama, Toyonaka, Osaka 560-0043, Japan**
[2]IPNS, KEK, 1-1 Ohho, Tsukuba, Ibaraki 305-0801, Japan
[3]RCNP, Osaka University, 10-1 Mihogaoka, Ibaraki, Osaka 567-0047, Japan

The neutron electric dipole moment (nEDM) has been providing strict constraints on theories underlying the CP violation that predict larger nEDM than the standard model. In order to exceed the present upper limit on the nEDM of $\mid d_n \mid< 3 \times 10^{-26} e$ cm measured at Grenoble [1], several groups are now developing new methods of nEDM measurements to reduce systematic errors as well as new ultracold neutron (UCN) sources to achieve higher statistics. The systematic error at the Grenoble experiment was dominated by the the geometric phase effect (GPE) for the ^{199}Hg comagnetometer. We have proposed a ^{129}Xe comagnetometer which can possibly reduce the GPE to 4 $\times 10^{-28} e$ cm because of a buffer gas effect. [2]
We are now developing a ^{129}Xe comagnetometer shown in Fig. 1. Spin polarized ^{129}Xe nuclei are used to monitor the static magnetic field in a nEDM cell where both spin polarized UCN and ^{129}Xe are confined. Highly spin polarized ^{129}Xe produced by means of the spin exchange optical pumping technique is accumulated in a cold trap, and then is introduced into the nEDM cell. The spin precession of ^{129}Xe nuclei will be observed using two-photon excitation of Xe atoms. Details of our plan and the progress will be presented.

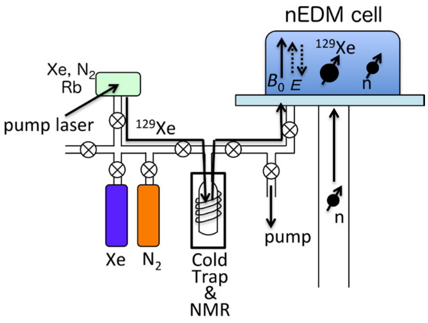

FIG. 1: Schematic design of ^{129}Xe comagnetometer.

---

[1] C.A. Barker et al., Phys. Rev. Lett. **97**, 131801 (2006).
[2] Y. Masuda et al., Phys. Lett. A **376**, 1347 (2012), Physics Procedia **51**, 89 (2014).

---

*Electronic address: `mihara@vg.phys.sci.osaka-u.ac.jp`

EDM measurement in ^{129}Xe atom using dual active feedback nuclear spin maser

T. Sato[1], **Y. Ichikawa**[2], **Y. Ohtomo**[1], **Y. Sakamoto**[1], **S. Kojima**[1], **C. Funayama**[1], **T. Suzuki**[1], **M. Chikamori**[1], **E. Hikota**[1], **M. Tsuchiya**[1], **T. Furukawa**[3], **A. Yoshimi**[4], **C.P. Bidinosti**[5], **T. Ino**[6], **H. Ueno**[2], **Y. Matsuo**[7], **T. Fukuyama**[8], **K. Asahi**[1]

[1] *Dept. Physics, Tokyo Inst. of Technology, 2-12-1 Oh-okayama, Meguro, Tokyo 152-8551, Japan**
[2] *RIKEN Nishina Center, 2-1 Hirosawa, Wako, Saitama 351-0198, Japan*
[3] *Dept. Physics, Tokyo Metropolitan Univ., 1-1 Minami-Ohsawa, Hachioji, Tokyo 192-0397, Japan*
[4] *Research Core for Extreme Quantum World, Okayama Univ., 3-1-1 Tsushimanaka, Kita, Okayama 700-8530, Japan*
[5] *Dept. Physics, Univ. of Winnipeg, 515 Portage Avenue, Winnipeg, Manitoba, Canada*
[6] *Inst. of Material Structure Science, KEK, 1-1 Oho, Tsukuba, Ibaraki 305-0801, Japan*
[7] *Dept. Advanced Sciences, Hosei Univ., 3-7-2 Kajino-cho, Koganei, Tokyo 184-8584, Japan*
[8] *RCNP, Osaka Univ., 10-1 Mihogaoka, Ibaraki, Osaka 567-0047, Japan*

The origin of the matter-dominated universe is one of the open questions in the Standard Model of elementary particles. Experimental search for a permanent electric dipole moment (EDM), which violates T and hence CP-symmetry, are expected to shed light on this question. Our present objective is to perform an EDM measurement of the diamagnetic atom ^{129}Xe, at the level of $|d| = 10^{-28}$ $e$cm, which is a more than one order of magnitude improvement from the present upper limit $|d| < 4.1\times10^{-27}$ $e$cm for ^{129}Xe [1]. In this experiment, a scheme of active feedback nuclear spin masers [2,3], which enable the Larmor spin precession to be sustained semi-permanently, is employed to achieve a precision measurement of the spin precession of ^{129}Xe.

Co-magnetometry using ^{3}He spin maser was employed to cancel out ^{129}Xe frequency drifts originating from fluctuations in the external magnetic field. At present, the frequency precisions of the masers are mainly limited by frequency drifts due to contact interaction between a ^{3}He/^{129}Xe atom and a polarized Rb atom, an agent which must be present to facilitate the optical pumping of the noble gases [4]. To eliminate this effect, a double-cell geometry was employed [5]. In this configuration, the maser cell is divided into two parts, one for optical pumping and the other for spin detection and masing. In addition, linearly polarized laser light is introduced to the detection part of the cell in order to destroy the longitudinal polarization of Rb atoms, thereby reducing maser frequency drifts caused by the contact interactions.

These developments will enable us to reach a maser frequency precision of 1 nHz, which is required for the EDM detection at a level of 10^{-28} $e$cm. In this presentation, the present status of the experiment and analysis of the ^{3}He and ^{129}Xe maser signals will be reported.

[1] M.A. Rosenberry et al., *Phys. Rev. Lett.* **86**, 22 (2001).
[2] A. Yoshimi et al., *Phys. Lett. A* **304**, 13 (2002).
[3] A. Yoshimi et al., *Phys. Lett. A* **376**, 1924 (2012).
[4] Y. Ichikawa et al., *EPJ Web of Conf.* **66**, 05007 (2014).
[5] E. Hikota et al., *EPJ Web of Conf.* **66**, 05005 (2014).

---

*Electronic address: *sato@yap.nucl.ap.titech.ac.jp*

P66

Development of high-homogeneity magnetic field coil for ^{129}Xe EDM experiment

Y. Sakamoto,[1] C. P. Bidinosti[2], Y. Ichikawa[3], T. Sato[1], Y. Ohtomo[1], S. Kojima[1], C. Funayama[1], T. Suzuki[1], M. Tsuchiya[1], T. Furukawa[4], A. Yoshimi[5], T. Ino[6], H. Ueno[3], Y. Matsuo[7], T. Fukuyama[8], K. Asahi[1]

[1] *Dept. Physics, Tokyo Inst. of Technology, 2-12-1 Oh-okayama, Meguro, Tokyo 152-8551, Japan*[*]
[2]*Dept. Physics, Univ. of Winnipeg, 515 Portage Avenue, Winnipeg, Manitoba, Canada*
[3] *RIKEN Nishina Center, 2-1 Hirosawa, Wako, Saitama 351-0198, Japan*
[4] *Dept. Physics, Tokyo Metropolitan Univ., 1-1 Minami-Ohsawa, Hachioji, Tokyo 192-0397, Japan*
[5] *Research Core for Extreme Quantum World, Okayama Univ., 3-1-1 Tsushimanaka, Kita, Okayama700-8530, Japan*
[6]*Institute of Material Structure Science, KEK, 1-1 Oho, Tsukuba, Ibaraki 305-0801, Japan*
[7] *Dept. Advanced Sciences, Hosei Univ., 3-7-2 Kajino-cho, Koganei, Tokyo 184-8584, Japan*
[8] *RCNP, Osaka Univ., 10-1 Mihogaoka, Ibaraki, Osaka 567-0047, Japan*

A permanent electric dipole moment (EDM) is an excellent indicator of physics beyond the Standard Model (SM). The typical magnitude of EDMs predicted by models beyond the SM are by many orders larger than what is expected from SM physics. An EDM can be detected as a difference between the spin precession frequencies measured with an electric field applied parallel and antiparallel to a magnetic field.

In our setup, ^{129}Xe and ^{3}He gas are enclosed in a glass cell, and there precession frequencies are measured by means of the spin maser technique. The He gas acts as a comagnetometer. One of the essential parameters in this measurement is the amplitude of the spin maser signal. The factors determining the amplitude of the signal are the spin polarization and the ratio of the transverse relaxation time T_2 to the longitudinal relaxation time T_1. In particular, ^{3}He spin which exhibits a long T_1 but attains only a low polarization in our Xe-He coexisting cell, is also largely affected by T_2. The major cause of transverse relaxation is the inhomogeneity of the magnetic field.

In our previous setup [1], typical T_2 values obtained for ^{3}He in a 20-mm–diameter cell were in the range of 1,000 s. In the present work we aimed to realize a T_2 of several thousands of seconds, by improving the field homogeneity. The setup consists of (from outer to inner) a triple layer μ-metal magnetic shield, an inner ferrite magnetic shield, and a central coil to generate a static homogeneous magnetic field. The intended use of the ferrite shield is to eliminate thermal noises by virtue of its high permeability and resistivity, however we found it to be too strongly magnetized and it was not employed in the present tests.

The magnetic shield was demagnetized by standard method, and a residual magnetic field as low as 30 μG was realized at the center of the shield. The coil to generate the static field was designed such that the field gradient is kept below 6.0 μG/cm, in order to achieve the target T_2. The setup includes a current stabilization system with a feedback mechanism. As a result of the developments discussed above, T_2 for ^{3}He was measured via free induction decay experiments to be ~11,000 s, an improvement of more than ten times from the previous setup.

[1] A. Yoshimi, T. Inoue et al., *Phys. Lett. A* **376**, 1924 (2012)

---

[*]Electronic address: *y.sakamoto@yap.nucl.ap.titech.ac.jp*

P52

Structural, Magnetic and Optical Studies of Ni-Nanostructures Embedded in Al_2O_3 matrix

R. Dogra[1*], **A.Kumar**[1], **P. Thakur**[2], **A.Sharma**[3], **S. Chopra**[4], **K. D. Devi**[4], **Ravi Kumar**[1]

[1] *Beant College of Engineering and Technology, Gurdaspur-143521, India*
[2] *Diamond Light Source, Didcot, Oxfordshire,UK*
[3] *Beamline Research Division, Pohang Accelerator Laboratory, Pohang 790-784, South Korea*
[4] *Inter University Accelerator Center, Aruna Asaf Ali Marg, New Delhi-110067, India*

The work reports the formation and characterization of Ni nanostructures embedded in Al_2O_3 (sapphire) matrix. Single crystals of sapphire were implanted with 80 keV negative Ni ions at a fluence of 1×10^{16}, 5×10^{16}, 7×10^{16} ions cm^{-2} with current density of 15 $\mu A/cm^2$ and post annealed in air at 600 °C for 4 hrs. X-ray diffraction, AFM/MFM and UV-Visible absorption, investigations confirmed the formation of embedded nickel nanostructures. XRD spectrum for Ni-implanted Al_2O_3 sample clearly indicates the presence of Ni(111) metallic phase along with the NiO_x phase at fluence of 7×10^6 ions/cm^2. AFM image indicates the rms surface roughness around 12.5 nm in the Ni implanted sample and ~1.7 nm for smooth surface of Al_2O_3. The magnetic phase contrast observed in MFM measurements reveals the formation of magnetic domain due to Ni nanostructure formation. Three absorption bands at 3.69, 4.38 and 5.15 eV have been observed with the UV-VIS studies of Ni-Al_2O_3 composite matrix. These absorption bands can be designated as broad band of Ni nanoparticles.

*Electronic Address: drdogra@yahoo.com

g-factor Measurements of High Spin States in ^{108}Cd

Ping Fan[1], Daqing Yuan[1], Yongnan Zheng[1], Yi Zuo[1], Qiaoli Zhang[1], Xiaoqiang Ma Xiaoguang Wu[1], Guangsheng Li[1], Lihua Zhu[2], Qiwen Fan[1], Juncheng Liang[1], Xizhen Zhang[1],Shengyun Zhu[1]

1.China Institute of Atomic Energy, P. O. BOX 275-50, Beijing, 102413, China.
2. School of Physics and Nuclear Energy Engineering, Beihang University, Beijing 100191, China

The magnitude and sign of g-factors can be affected dramatically by the quasi-particle alignment, since the g-factors of the protons and neutrons in high-*j* orbit are rather different. Therefore, measurements of g-factors can provide direct information on the quasi-particle alignment. The present work was motivated to measure g-factors of the rotational states of the ground state band (GSB) in ^{108}Cd and to study the quasi-particle alignment that is attractive and significant in nuclear structure studies at high spins.

High spin states of ^{108}Cd was populated by the fusion-evaporation reaction ^{76}Ge(^{37}Cl,1p4n)^{108}Cd at beam energy of 135MeV from the HI-13 tandem accelerator at China Institute of Atomic Energy, and the g-factors were determined by the TMF-IMPAD method. In the experiment, the emitted γ rays were detected by four BGO Compton suppressed HPGe detectors placed in the beam-detector plane at $\pm 55^{o}$ and $\pm 125^{o}$ with respect to the beam direction. The coincidence data were recorded in a multi-parameter event-by-event mode with a VME data acquisition system. The precession angle and the g-factors of each state are obtained from the γ ray counts of each transition and the transient magnetic field calculated with the empirical formula.

The g factors of the ground state band of 10^+, 12^+, 14^+, 16^+ states in ^{108}Cd were measured. The obtained values of g factors are -0.25, -0.20, -0.11 and -0.089, respectively, which demonstrates the alignment of $g_{7/2}$ neutron.

Electronic address：fanping@ciae.ac.cn

Measurement of Lifetime and Quadupole moments in neutron rich ^{131,132}I

T. Bhattacharjee[1], **D. Banerjee**[2], **A. Saha**[1], **P. Das**[1] **and S. K. Das**[2]

[1] *Variable Energy Cyclotron Centre, 1/AF Saltlake, Kolkata – 700 064, India* ✶
[2] *Accelerator Chemistry Section, Radio Chemistry Division (BARC),VECC, 1/AF Saltlake, Kolkata – 700 064, India*

The neutron rich iodine nuclei are of contemporary physics interest as these are close to double shell closure of ^{132}Sn. The systematic of the quadrupole moments in some of the odd-A iodine nuclei [1] revealed some anomaly regarding the quadrupole moments of the $\pi g_{7/2}$ and $\pi d_{5/2}$ orbitals at neutron shell closure of N=82, which is a topic of current research interest around ^{132}Sn [2,3]. The complete spectroscopy of the low lying states of these nuclei, including the measurement of level lifetimes and transition moments, is thus required in order to address the said anomaly.

In the present work, the lifetimes and quadrupole frequencies have been measured for several low lying states of ^{131,132}I. The states have been populated from the decay of ^{131m,132}Te nuclei produced via ^{nat}U(α,f) reaction followed by radio-chemical separation. A detection setup consisting of three planar LaBr$_3$(Ce) detectors was used for the present work. The level lifetimes ~ ns have been measured by de-convolution method (for 149.7 and 1797 keV states of ^{131}I) and those ~ ps have been measured by using Mirror Symmetric Centroid Difference (MSCD) Technique [4] (for 1899 keV state of ^{131}I and 162 keV level of ^{132}I). The Time Differential Perturbed Angular Correlation (TDPAC) Technique has been used for the measurement of quadrupole frequencies by doping ^{131,132}Te into natural Te metal matrix. The doping was performed during the reduction of externally added Te(VI) salt to Te(0) metal. Figure 1 depicts the results for level lifetime measured with MSCD method. The preliminary values of quadrupole frequencies for 49 keV state of ^{132}I and 1797 keV state of ^{131}I have been shown in Figure 2. The quadrupole moments can subsequently be calculated with a prior knowledge of electric field gradient for which the theoretical calculation is in progress using Wien2K code.

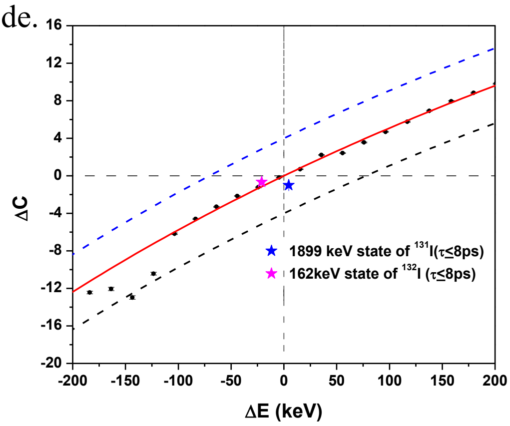

Figure 1: MSCD results obtained in the present work

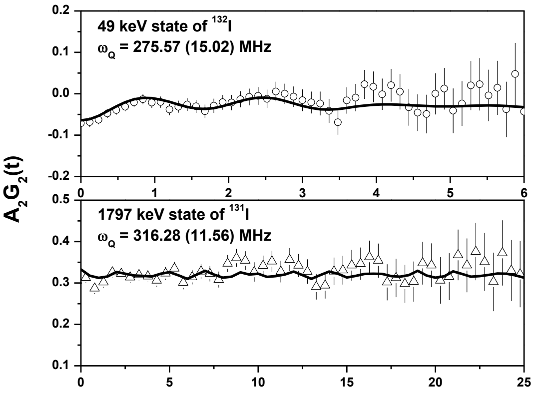

Figure 2:TDPAC spectra obtained in the present work

[1 D. W. Hafemeister, G. Dzpasquali and D H. Dzwaardf, Phys. Rev.**135**, B1089 (1964).
[2] J. Shergur et al., Phys. Rev **C65**, 034313 (2002).
[3] L. Coraggio et al., Phys. Rev **C72**, 057302 (2005).
[4] T. Bhattacharjee et al., Phys. Rev**. C88**, 014313 (2013).

Electronic address: btumpa@vecc.gov.in

Correlations between ^{14}N NQR frequencies and ^{14}N local environment in molecular crystals

^{14}N Nuclear Quadrupole Resonance (^{14}N-NQR) recieved increased attention recently due to its potential for pharmaceutical analysis.[1] From the spectroscopic point of view, ^{14}N-NQR is very selective and can also provide quantitative information in carefully designed experiments. The most often proposed use of ^{14}N-NQR in pharmaceutical analysis is related to detection and quantization of polymorphs, though several other uses are also attractive. One of the biggest obstacles for a wider ^{14}N-NQR addoption is a very slow process of searching for the resonance frequencies. Current methods excite only a fraction of the whole spectrum, so that frequent changes of the setup involving mechanical adjustmenets of a variable capacitor are required. Alternative methods for a faster search are being developed, but so far have other disadvantages.

In order to speed up the current searching process, we decided to restrict the searching region with an approximate forecast of the ^{14}N-NQR frequency, which is based on the fact, that the ^{14}N-NQR frequency reflects the detailed arrangment of charges around the ^{14}N nucleus. The idea is to find the most likely frequency by comparing the molecular structure of the sample under investigation and a database of approximately 1000 molecules with known ^{14}N-NQR frequencies. The approach used was first to select a smaller substructure around the ^{14}N in the molecule of interest, e.g. first neighbors, and find all the frequencies in the database which correspond to nitrogen within a similar substructre. The substructure is then being progressively increased and the frequencies corresponding to the largest substructure found, assigned to the most likely frequency. An example for frequencies corresponding to different aliphatic nitrogens is shown in Fig. 1.

Our approach is an alternative to typical methods for NQR frequency calculations, which use DFT theory and precise crystal structure to find the ^{14}N-NQR frequency. Although such calculations often give good estimates, much better than the proposed approach, they are typically complicated and require some manual fine tuning.

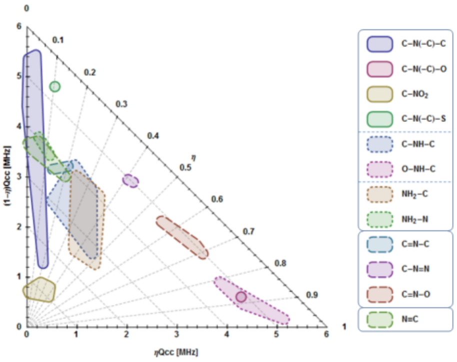

Fig. 1. ^{14}N quadrupole coupling constant C_Q and assymetry parameter η for aliphatic nitrogen in various functional groups.

---

[1] E. Balchin et al., *Anal. Chem.* **77**, 3925 (2005).

P40

Chemical and magnetic ordering in $Fe_{0.5}Ni_{0.5}PS_3$

D.J.Goossens,[1] G.A.Stewart,[2] W.T.Lee,[3] and A.J.Studer[3]

[1]*Research School of Chemistry, The Australian National University, Canberra, ACT 0200, Australia**
[2]*School of Physical, Environmental and Mathematical Sciences,*
The University of New South Wales, Canberra, ACT 2600, Australia
[3]*Australian Nuclear Science and Technology Organisation, Lucas Heights, NSW 2234, Australia*

The MPS$_3$ family of layered magnetic materials ($M = \mathrm{Fe}^{2+}, \mathrm{Ni}^{2+}, \mathrm{Mn}^{2+}$, etc) shows many unusual properties. We have recently observed time-dependent magnetisation and two magnetic phase transitions in $Fe_{0.5}Ni_{0.5}PS_3$ [1] and here we use neutron diffraction and Mössbauer spectroscopy to explore the magnetic and structural ordering. Neutron diffraction shows that the staggered magnetisation lies closest to the Brillouin curve for $J = 1$, which is the spin for quenched Ni^{2+}. In agreement with neutron diffraction, Mössbauer shows a magnetic ordering temperature of $\sim$ 120K. It does not show any evidence of a second, low temperature (re)ordering, suggesting that the low temperature transition seen previously [1] is a result of the time dependence of the magnetisation and is not apparent when the sample is given time to relax between measurements. The presence of three magnetic Fe-site environments when four chemical environments (Fe_3, Fe_2Ni, $FeNi_2$ and Ni_3) are possible may indicate that the mixture is not random, but shows some local ordering; the neutron results show evidence for a similar conclusion.

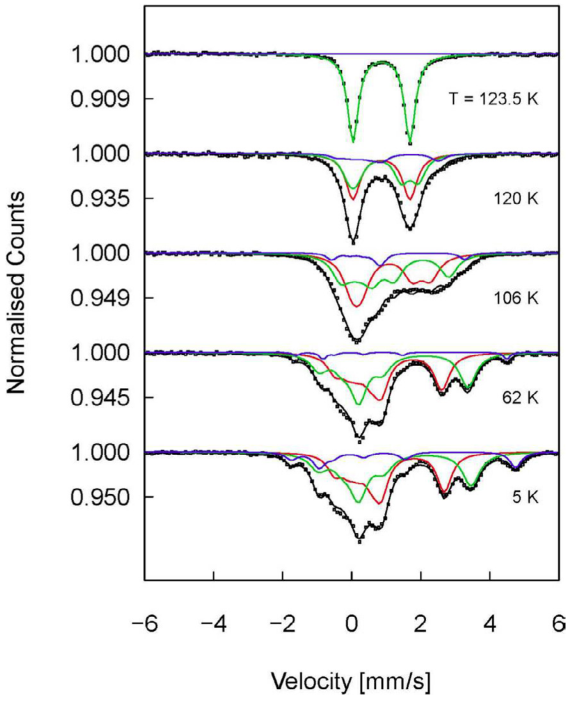

FIG. 1: A sample of the ^{57}Fe-Mössbauer spectra recorded for $Fe_{0.5}Ni_{0.5}PS_3$ as a function of temperature. In each case, the fitted theory (black line) is a sum of three magnetically-split sextets (coloured lines) which are associated with three distinct magnetic Fe-site environments.

[1] D.J. Goossens et al., J. Magn. Magn. Mater. **334**, 82 (2013)

---

*Electronic address: `darren.goossens@anu.edu.au`

P48

Damage accumulation in Au^{2+} irradiated SiC/SiC composites

N. Chaâbane[1], **M. Le Flem**[2], **Th. Vandenberghe**[2], **S. Urvoy**[2], **C. Sandt**[3], **Y. Serruys**[4]

[1] *CEA, INSTN/UEINE, F-91191 Gif-sur-Yvette, France* ✷
[2] *CEA, DEN/DMN/SRMA, F-91191 Gif-sur-Yvette, France*
[3] *Synchrotron SOLEIL, L'Orme des Merisiers, Saint-Aubin, 91192 Gif-sur-Yvette Cedex, France*
[4] *CEA, Laboratoire JANNUS, F-91191 Gif-sur-Yvette, France*

Silicon carbide fiber-reinforced silicon carbide matrix composites (SiC/SiC) are attractive for advanced energy system applications, including nuclear fission and fusion. The irradiation may affect the microstructural stability of SiC/SiC composites. In this study, SiC/SiC composites with Tyranno S (TS), Tyranno SA3 (TSA3) and Hi-Nicalon type S (HNS) were irradiated with 12 MeV Au ions at room temperature and 800 °C up to 0.05 and 1 displacement per atom (dpa) doses. Damaged materials were investigated by Raman spectroscopy and AFM analyses on the irradiated surface and by transmission electron microscopy along the beam penetration. Damages were mainly located at amorphous zones in the matrix, as well as in all the fibers themselves, detected after 1 dpa irradiation at room temperature. TS fiber shrinkage is suggested and consistent with AFM analyses of the composite surface highlighting a 350 nm step height among SiC matrix and TS fibers. On the opposite, the advanced SiC fiber (TSA3 and HNS) did not shrink and showed a superior dimensional stability. The formation of the amorphous layer was confirmed by Raman spectroscopy results. However, the amorphization occurrence and the different behaviors of the TS fibers (shrinkage) and the matrix (swelling), were both limited at higher irradiation temperature (800 °C): irradiation defect annealing resulted in the occurrence of a slightly disordered material evidenced by Raman, and in less discrepancies in volume changes of matrix and fibers. These microstructural features were confirmed by cross-sectional microstructural observation performed using transmission electron microscopy.

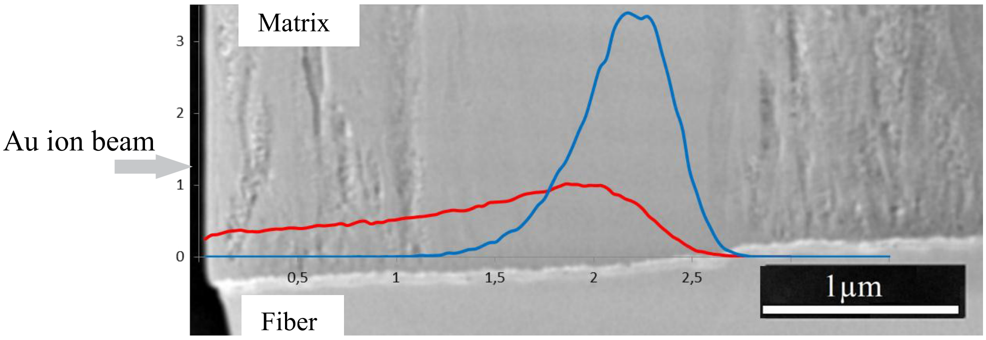

Fig. 1. Cross sectional TEM image of TS fibers (fabricated by FIB) and depth distribution of Au ions (arbitrary units, blue line) and dpa profile (for a 3.75×10^{16} m^{-2} fluence, red line).

Electronic address: *nihed.chaabane@cea.fr*

μSR HOWTO

Jess H. Brewer[1]

[1]*Dept. of Physics & Astronomy / Univ. of British Columbia / Vancouver, BC / V6T 1Z1 Canada**

Over the past half century, muon spin rotation/relaxation/resonance (μSR) has become an indispensible tool for molecular and materials science. The history of μSR has been covered elsewhere. My goal in this talk will be to describe the various techniques of μSR (some of which are depicted below) and explain what they are (and are *not*) good for.

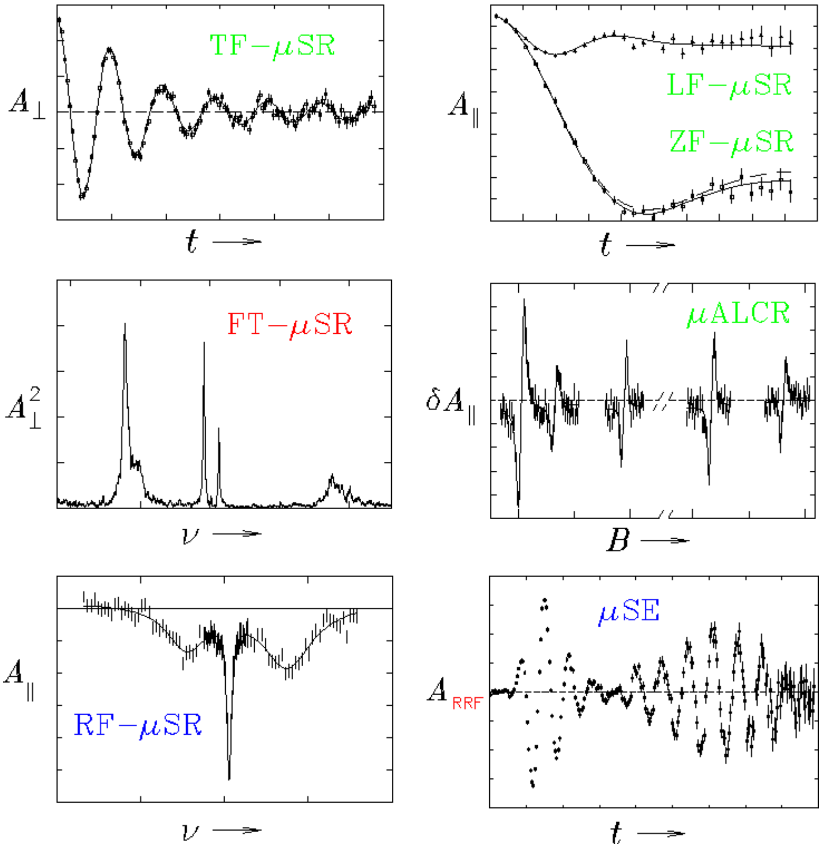

FIG. 1: Selected acronyms for standard μSR techniques: Transverse Field (TF) μSR (muon spin *rotation/-relaxation*); Longitudinal field (LF) and Zero Field (ZF) muon spin *relaxation*; Fourier Transform (FT) μSR *spectroscopy*; Muon Avoided Level Crossing Resonant *relaxation*; Radio Frequency (RF) muon spin *resonance*; and RF-driven TF Muon Spin Echos.

Each of these methods has been adapted for many different uses, some more effective than others. I will present a more comprehensive chrestomathy for newcomers to μSR, complete with recommendations and warnings.

Many excellent reviews and books [1–3] are now available for those wishing to acquire a more comprehensive knowledge of the history, methods, applications, successes and future potential of μSR. This presentation will only attempt to achieve a broad overview of the field.

[1] A. Schenck, "*Muon Spin Rotation Spectroscopy: Principles and Applications in Solid State Physics*" (Hilger, Bristol, 1986) and references therein.
[2] J.H. Brewer, Encyclopedia of Applied Physics **11**, 23-53 (VCH Publishers, Inc., 1994).
[3] Alain Yaouanc and Pierre Dalmas de R'eotier, International Series of Monographs on Physics **147**, 1-504 (Oxford University Press, 2010) and references therein.

---

*Electronic address: `jess@phas.ubc.ca`

Collinear Laser Spectroscopy and β NMR at NSCL/MSU

Kei Minamisono[1, 2] **for BECOLA collaboration**[#]

[1] *National Superconducting Cyclotron Lab., Michigan State University, East Lansing, MI 48824, USA*
[2] *Department of Physics and Astronomy, Michigan State University, East Lansing MI 48824, USA*

Collinear laser spectroscopy (CLS) and β-ray detecting nuclear magnetic resonance (β NMR) have been extensively used [1] to determine nuclear ground and isomeric state properties, such as mean squared charge radii and electromagnetic moments to study evolution of nuclear structure at/across shell closures. Long chains of isotopes of a selection of elements have been systematically investigated at ISOL-type facilities, taking advantage of the small emittances and high intensities of low-energy beams (~60 keV) of nuclides produced via the ISOL technique. This production method, however, suffers from a serious limitation: long release times from the targets can lead to large decay losses for short-lived nuclides. In-flight production and separation available at NSCL, on the other hand, can provide high-energy beams (> 50 MeV/nucleon) of isotopes of all elements lighter than uranium. The conversion of the fast beams into high-quality, low energy beams via thermalization in a gas [2] for low-energy precision measurements has already been exploited at NSCL [3]. The limited rate, however, of the produced low-energy radioactive beams requires highly sensitive detection methods e.g. the bunched-beam CLS [4] and β NMR.

The BEam COoler and LAser spectroscopy (BECOLA) facility [5] at National Superconducting Cyclotron Laboratory (NSCL) at Michigan State University is a collinear laser spectroscopy facility, which was recently commissioned online. BECOLA is used to perform both laser hyperfine structure measurements (bunched-beam CLS) and atomic/nuclear spin manipulation using optical pumping and nuclear-magnetic resonance techniques (β NMR) for rare isotopes at low counting rates. Charge radii and ground-state nuclear moments of light transition metals will be initially targeted, which are difficult to produce at other facilities. BECOLA was designed to accept low-energy beams (<60*q* keV with *q* being the charge state of the beam) from the NSCL gas stopping stations and also from the future Facility for Rare Isotope Beams (FRIB) without any modification to the system. A beam cooler and buncher trapped and released the ions as beam bunches towards the CLS beam line. The ion beam was collinearly-overlapped with laser light and resonant-photon detection or optical pumping to produce polarization for β NMR were performed.

Recent results of collinear laser spectroscopy on bunched potassium isotopes as well as future prospects of BECOLA facility will be discussed.

[1] K. Blaum et al., *Physica Spectra* **T152**, 014017 (2013).
[2] L. Weissman et al., *Nucl. Instrum. Methods Phys Res.* **A540**, 245 (2005).
[3] G. Bollen et al., *Phys Rev. Lett.*, **96**, 152501 (2006).
[4] A. Nieminen et al., *Phys. Rev. Lett.* **88**, 094801 (2002).
[5] K. Minamisono et al., *Nucl. Instrum. Methods Phys. Res.* **A709**, 85 (2013).

Electronic addrtess: minamiso@nscl.msu.edu

[#] *Michigan State University, TRIUMF, TU Darmstadt, ORNL*

The Australian Synchrotron: Shining a Light on Australian Research

Michael James,[1]

[1] *Australian Synchroton, 800 Blackburn Rd, Clayton VIC 3168, Australia* ✷

Together, the Australian Synchrotron in Melbourne [1] and the 20 MW OPAL research reactor in Sydney represent Australia's largest ever investment in scientific infrastructure. In isolation, each facility has hit its stride; with first generation beamlines completed and vibrant international user programs in place. Collectively, the use of neutrons and synchrotron light has aided the untangling of many complex scientific problems.

The Australian Synchrotron has nine beamlines in routine scientific operation, with our 10th – the Imaging and Medical beamline – running user experiments while continuing to be commissioned. With its primary focus as a user facility, the Australian Synchrotron has hosted more than 20,000 user visits, and has enabled the publication of more than 1500 peer-reviewed scientific journal articles.

In this talk I will give a brief overview of the Australian Synchrotron; highlighting the different instrument capabilities, before presenting a wide-ranging set of industrially relevant and recently published high-impact scientific studies that have used synchrotron radiation.

A diverse range of systems will be covered including areas of health, pharmaceuticals and medical research; new electronic materials; nanotechnology; environmental science; food and nutrition; cultural heritage; earth sciences; advanced materials and new energy technologies.

Fig. 1. The Main Building of the Australian Synchrotron, hosting the accelerator and beamlines.

---

[1] N. Mills et al., *Synchrotron Radiation News* **26**, 16 (2013).

Electronic address: *michael.james@synchrotron.org.au*

Atomic Level Observation of Ag-ion Hopping Motion in AgI Nanoparticles

W. Sato,[1,2,3] R. Mizuuchi[2], N. Irioka[3], S. Komatsuda[2], S. Kawata[4], A. Taoka[1,2], Y. Ohkubo[5]

[1] *Institute of Science and Engineering, Kanazawa University, Kanazawa, Ishikawa 920-1192, Japan*✳
[2] *Graduate School of Natural Science and Technology, Kanazawa University, Kanazawa, Ishikawa 920-1192, Japan*
[3] *School of Chemistry, Kanazawa University, Kanazawa, Ishikawa 920-1192, Japan*
[4] *Department of Chemistry, Faculty of Science, Fukuoka University, Fukuoka, Fukuoka 814-0180, Japan*
[5] *Research Reactor Institute, Kyoto University, Kumatori, Osaka 590-0494, Japan*

Silver iodide (AgI) offers superionic conductivity, and applications of this solid-state conductivity are desired in a wide field of industry. This conducting phenomenon, however, emerges only in its high-temperature α phase ($\geq$ 420 K) because of temperature-dependent crystal structures, which is indeed a barrier to the practical applications of this compound. Recently, an epoch-making technique overcame this situation: AgI powder coated by a poly-N-vinyl-2-pyrrolidone (PVP) can partially preserve the conducting α phase even at room temperature, recording the conductivity of $1.5 \times 10^{-2}\ \Omega^{-1}\mathrm{cm}^{-1}$ [1]. For a detailed understanding of ionic conductivity of this compound, in the present work, local dynamics of Ag^{+} ions was investigated by means of the time-differential perturbed angular correlation (TDPAC) technique using the probe of ^{111}Ag(→^{111}Cd) nuclei.

The probe was separated by an anion-exchange chromatography from Pd matrix irradiated with thermal neutrons in Kyoto University Reactor. The isolated ^{111}Ag was then incorporated in AgI powder when it was synthesized by precipitation with PVP powder. TDPAC measurements of the ^{111}Ag(→^{111}Cd) probe were performed at various temperatures to observe temperature dependence of the spectra.

The TDPAC spectra observed for the PVP-coated AgI nanoparticles at 453 K and 333 K are shown in Fig. 1. The directional anisotropy of the spectra shows exponential relaxation reflecting dynamic perturbation arising from fast fluctuation of the extranuclear charge distribution, namely, hopping motion of Ag^{+} ions. It is considered that PVP-coating has made it possible for the α phase to survive even at 333 K, realizing superionic conductivity. In the present session, successful atomic-level observation of room-temperature dynamic motion of Ag^{+} ions is reported, and the activation energy of the local dynamics obtained from the temperature dependence of the relaxation constants is also presented [2].

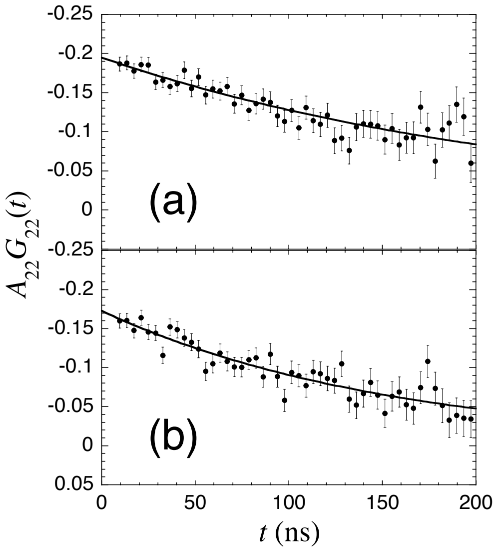

Fig. 1. TDPAC spectra of ^{111}Cd(←^{111}Ag) in PVP-coated AgI (a) at 453 K and (b) at 333 K.

[1] R. Makiura et al., *Nature Mater.* **8**, 476 (2009).
[2] W. Sato et al., Submitted for publication.

Electronic address: *wsato@se.kanazawa-u.ac.jp*

Carbon Nanotubes Filled or Decorated for Advanced Applications: Properties Insight through Hyperfine Interactions of ^{57}Fe and ^{119}Sn Nuclei

A. P. Douvalis[1], **A. Rossos, D. Gournis**[2], **T. Bakas**[1]

[1] *Physics Department, University of Ioannina, 45110 Ioannina, Greece* ✶
[2] *Department of Materials Science and Engineering, University of Ioannina, 45110 Ioannina, Greece*

Research and technological interest on Carbon Nanotubes (CNTs) has increased substantially since their discovery. CNTs themselves possess very important properties like thermal and electrical conductivity, high surface to volume area and excellent mechanical properties. Further, surface functionalization led to the formation of CNTs hybrid nanostructures decorated with a large variety of radicals, molecules or particles. In addition CNTs encapsulation of metallic nanowires [1] has developed further their potential of use in advanced applications, including energy storage and conversion, biomedicine, catalysis, cancer therapy and magnetic information data storage [2].

In this work we present studies of the structural, electronic and magnetic properties of metallic Sn and relative alloy nanowires encapsulated, as well as Fe-related magnetic metallic alloy and oxide nanoparticles decorating CNTs hybrid samples. The results suggest that different preparation routes can provide samples with a variety of different morphologies, structural and magnetic properties.

In particular, through the study of the hyperfine interactions of ^{57}Fe and ^{119}Sn nuclei, using the unique and powerful atomic-level investigation tool of Mössbauer Spectroscopy (Fig. 1), the properties of the Fe- and Sn-related nano-phases developed in the samples and their interactions are revealed. Guided by the knowledge gained through these insights, we can suggest the design and development of new hybrid materials that provide paths for exploiting the properties of these novel hybrid nanostructures, which successfully incorporate and may enhance the properties of their counter-components.

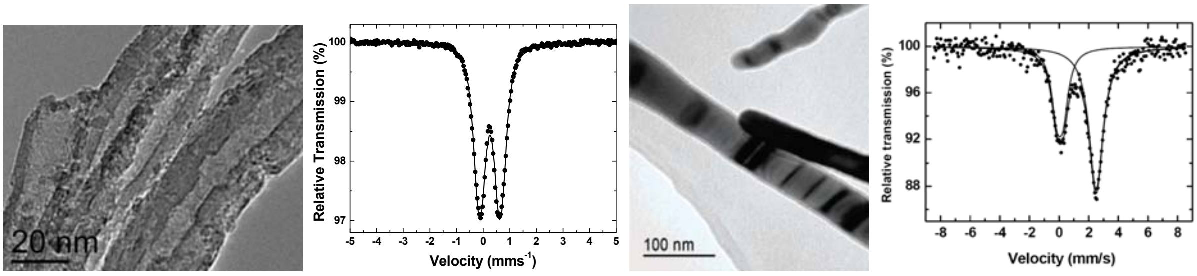

(a) (b) (c) (d)

Fig. 1. Transmission electron microscopy images of γ-Fe_2O_3 nanoparticles decorating (a) and Sn nanowires encapsulated (c) CNTs hybrid samples and their corresponding ^{57}Fe (b) and ^{119}Sn (d) Mössbauer spectra.

Acknowledgments: This research has been co-financed by the European Union (European Social Fund – ESF) and Greek national funds through the Operational Program "Education and Lifelong Learning" of the National Strategic Reference Framework (NSRF) – Research Funding Program: THALES. Investing in knowledge society through the European Social Fund (no. 377285).

[1] L. Jankovic et al., *Nano Letters* **6**, 1131 (2006).
[2] T. Tsoufis et al., *J. Nanoparticle Research* **15**, 1924 (2013).

✶ Electronic address: *adouval@uoi.gr*

Application of the MIMOS II spectrometer in to study ductile Heusler alloys

T. Gasi,[1] V. Ksenofontov,[1] C. Felser[2] and G. Klingelhöfer[1]

[1] *Institute of Inorganic and Analytical Chemistry, Johannes Gutenberg-University Mainz, D-55099 Mainz, Germany*
[2] *Max Planck Institute for Chemical Physics of Solids, D-01187 Dresden, Germany*

Heusler compounds are intermetallic compounds having the general formula X_2YZ, where X and Y are transition elements and Z a main group element. This remarkable class of materials has found a major role for technological applications especially those with half metallic properties or those for spin transfer torque (STT) applications. One of the drawbacks of Heusler compounds is the antisite disordering effect, which strongly influences the magnetic and structural properties of these compounds. It is worthwhile to notice that the XRD technique is not able to distinguish between the types of antisite disorder, because the scattering factor of the 3d elements is very similar, that is why we use the advantage of the Mössbauer spectroscopy as a powerful local technique to monitor this effect.

The new Heusler phases Fe_2YZ (Fe_2CuGa, Fe_2CoGe) have been successfully synthesized and investigated in detail [4]. They all show a cubic Heusler structure, however, the Mössbauer studies confirm the antisite disordering. Fe_2CuGa and Fe_2CoGe compounds are ductile and therefore it is impossible to grind them to proceed transmission measurements. Hence, they were analyzed in Mössbauer gamma- and x-ray backscattering mode. Also there is a possibility of structural changes of such samples, especially if they obey a shape memory effect, due to a mechanical treatment. Results of measurements of bulk samples Fe_2CuGa and Fe_2CoGe in gamma- and x-ray backscattering mode using the miniaturized MIMOS II spectrometer [1,2,3] are presented in Fig. 1. In these experiments we have demonstrated that Mössbauer measurements in backscattering mode are indispensable in case when preparation of powdered samples or thin foils can modify their structure and properties.

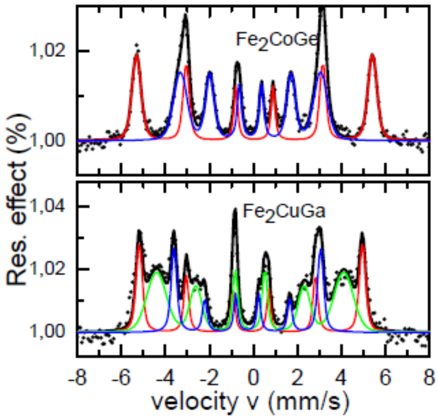

Fig. 1. ^{57}Fe gamma- backscattering spectra obtained with the Mössbauer spectrometer MIMOS II

[1] G. Klingelhöfer et al., *Journal of Geophysical Research - Planets,* **108, No.E12,** 8067 (2003).
[2] G. Klingelhöfer et al., *Science*, **Vol. 306,** 1740 (2004).
[3] C. Schröder et al., *Planetary and Space Science.* **52**, 997 (2004).
[4] T. Gasi et al., *Phys. Rev.* B **87**, 064411 (2013).

Electronic address: *klingel@uni-mainz.de*

^{14}N NQR and Relaxation in Ammonium Nitrate

David Stephenson

Chemistry Dept., University of the West Indies, St. Augustine, Trinidad and Tobago.

The potential for misuse of ammonium nitrate fertilizer as an improvised explosive has prompted investigations into the possible detection of this compound using NQR. So far a complete NQR spectrum has not been presented and consequently neither has complete relaxation analysis been carried out.

The two high frequency lines in ammonium nitrate are well known [1] (the ν_+ and ν_- lines of the nitro group). Using the technique of double contact cross relaxation it is possible to record all six possible ^{14}N lines in the title compound with good signal to noise ratio (see figure 1). The technique also allows determination of all three relaxation transition probabilities [2] for both the ammonium nitrogen and the nitro nitrogen.

The spectrum was recorded on a double resonance spectrometer using mechanical sample transport. Following transfer to low field the first cross relaxation contact was established using a solenoid driven by a digital power supply. A typical contact time used was 10 ms it was kept short to eliminate double (and triple) proton flips which considerably complicate an already congested spectrum. There was then a waiting time during which the proton magnetization was removed by pulsing the cross relaxation solenoid (using a low current) at a rate of 2 kHz. The solenoid was again switch on for 10 ms before the sample returned to high field and the recovered proton magnetization measured. Using this technique not only can low frequencies be easily recorded, but by varying the waiting time a complete relaxation profile for both the ammonium nitrogen and the nitro nitrogen can be obtained (see table 1).

	NH_4	NO_3
W_+ (s^{-1})	0.0124	0.0301
W_- (s^{-1})	0.0174	0.0139
W_0 (s^{-1})	0.0225	0.0333
T_{1a} (s)	23.0	16.9
T_{1b} (s)	16.4	10.5

Table 1. The relaxation transition probabilities between the ^{14}N levels (W_+ corresponds to the ν_+ transition etc.). The estimated error in the W values is ±10%. T_{1a} and T_{1b} are the two exponential time constants the relaxation of the ^{14}N will follow. (Note: T_1 has been defined as $1/(2W)$)

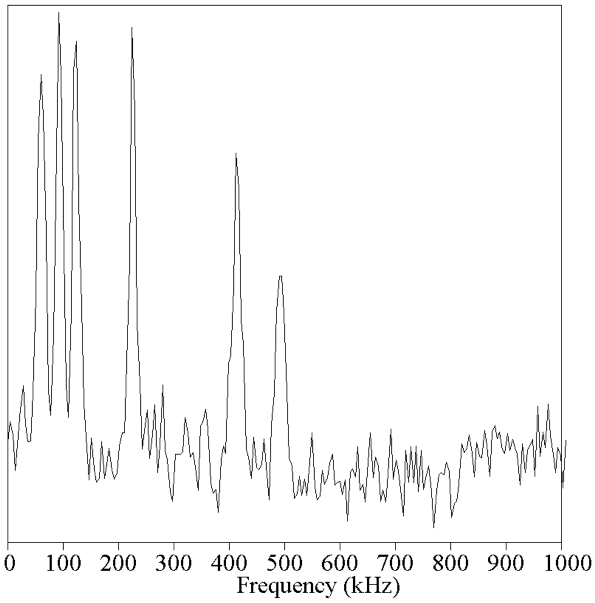

Figure 1. The double contact cross relaxation spectrum of ammonium nitrate. The y-axis is recovered magnetization in arbitrary units. The peaks show up as an enhancement of the recovered signal.

[1] J. Seliger, V. Zagar, R. Blinc., J. Magn. Reson. A, **106**, 214 (1994).
[2] D. Stephenson, Z. Naturforsch., **55a**, 79 (2000).

Electronic address: david.stephenson@sta.uwi.edu

Experimental search for the electron electric dipole moment with laser cooled francium atoms

T. Inoue,[1,2,*] S. Ando,[2] T. Aoki,[2] H. Arikawa,[2] S. Ezure,[2] K. Harada,[2]
T. Hayamizu,[2] T. Ishikawa,[2] M. Itoh,[2] K. Kato,[2] H. Kawamura,[1,2] A. Uchiyama,[2]
T. Aoki,[3] T. Furukawa,[4] A. Hatakeyama,[5] K. Hatanaka,[6] K. Imai,[7] T. Murakami,[8]
H.S. Nataraj,[9] T. Sato,[10] Y. Shimizu,[11] T. Wakasa,[12] H.P. Yoshida,[6] and Y. Sakemi[2]

[1] *Frontier Research Institute of Interdisciplinary Sciences, Tohoku University,*
6-3 Aoba, Aramaki, Aoba-ku, Sendai, Miyagi, 980-8578, Japan
[2] *Cyclotron and Radioisotope Center, Tohoku University, Miyagi, Japan*
[3] *Graduate School of Arts and Sciences, University of Tokyo, Tokyo, Japan*
[4] *Department of Physics, Tokyo Metropolitan University, Tokyo, Japan*
[5] *Department of Applied Physics, Tokyo University of Agriculture and Technology, Tokyo, Japan*
[6] *Research Center for Nuclear Physics, Osaka University, Osaka, Japan*
[7] *Advanced Science Research Center, Japan Atomic Energy Agency, Ibaraki, Japan*
[8] *Department of Physics, Kyoto University, Kyoto, Japan*
[9] *Indian Institute of Technology Roorkee, Uttarakhand, India*
[10] *Department of Physics, Tokyo Institute of Technology, Tokyo, Japan*
[11] *Department of Physics, Tohoku University, Miyagi, Japan*
[12] *Department of Physics, Kyushu University, Fukuoka, Japan*

A search for a permanent electric dipole moment (EDM) of an elementary particle, an atom or a molecule constitutes a stringent test beyond the standard model (SM) of particle physics. Actually, the latest experimental upper limits of the EDMs of the electron [1] and the neutron [2] enters the region predicted by some theoretical models beyond the SM.

We are constructing a laser cooled francium (Fr) factory at Cyclotron and Radioisotope Center, Tohoku University to search for the electron EDM. Fr has the largest enhancement factor of the electron EDM in alkali atoms through the relativistic effect. Although Fr has no stable isotope, some isotopes of Fr, such as ^{210}Fr, have the long life time enough to perform the EDM experiment. The laser cooled and trapped atom would have a long coherence time and some systematic effects due to the velocity of the atom and the field inhomogeneity can be suppressed in comparison with experiments using atomic or molecular beam. Thus, the laser cooled Fr is selected to improve the systematic error. In our experiment, Fr is produced through the nuclear fusion reaction by using the gold target and the oxygen beam accelerated by the AVF cyclotron. After that, Fr is transported as an ion by using electrostatic fields about 10 m from the reaction point in order to avoid noises and damages from radiation. Then, the Fr ion is neutralized to be applied the laser cooling and trapping technique. In this presentation, we will report the present status of the laser cooled Fr factory and the EDM measurement system such as a magnetometer and an electric field application system which are recently being constructed.

[1] The ACME Collaboration et al., Science **343**, 269 (2014).
[2] C.A. Baker et al., Phys. Rev. Lett. **97**, 131801 (2006).

---

[*] Electronic address: `inoue_t@cyric.tohoku.ac.jp`

Teaching hyperfine interactions in the 21st century

Stefaan Cottenier[1, 2]

[1]*Center for Molecular Modeling, Ghent University,*
Technologiepark 903, BE-9052 Zwijnaarde, Belgium
[2]*Department for Materials Science and Engineering, Ghent University,*
*Technologiepark 903, BE-9052 Zwijnaarde, Belgium**

The long term health of a research community depends on how efficiently that community attracts 'new blood': young researchers with new inspiration, who choose to devote their career to the field. The first place where we can capture the attention of these new generations, is the classroom. Indeed, many of us, present here at this conference, have been dragged into the field by an inspiring master course. Unfortunately, teaching is a topic where the hyperfine community faces an uphill battle. At many universities, courses about hyperfine interactions and nuclear methods either do not exist, or they are a small part of a larger course. At those places where a dedicated hyperfine course is offered, it is typically a niche topic that attracts rarely more than 5 or 10 students. With everyone's time being under pressure, this amount of students does not justify or motivate spending a lot of time to improve existing hyperfine courses.

Wouldn't the following be an ideal situation? Imagine you could offer to your students a course that teaches them the conceptual foundations of hyperfine interactions and of experimental methods based thereupon. A course that is engaging, and that stimulates your students (including the 'average' ones) to think deeply about these topics. A course that brings your students in contact with the modern research literature on nuclear methods. And in contact with their peers all over the world studying the same topic. A course that is sufficiently flexible to integrate it with a specialized course about the details of one specific nuclear method you might be offering. A course that smoothly adapts itself to the teaching schedule of your university. Etc.

The good news is: such a course exists. In this contribution I will describe our experience at Ghent University with the preliminary version of a course on nuclear methods that tries to realize all of the above. Expect words as flipped classroom, time- and place-independent learning, MOOC, etc. I will sketch my vision on how this material can be further developed into a course that reflects the community consensus about the basics of our field. Eventually, I will show how you can contribute to the development of this course, and how you can use this newly developed material in your own lectures.

I believe this can catalyze a community effort by which we will be able to teach hyperfine interactions and nuclear methods to far more students than we do now, in a much more engaging way, and with a fraction of the effort it would take you to develop all of this yourself. The future will show whether this will indeed lead to a surge in the number of young people interested in working in this field.

---

*Electronic address: `stefaan.cottenier@ugent.be`

P4

Damage annealing in Fe/Mn implanted ZnO

Krish Bharuth-Ram

We have performed ^{57}Fe emission Mössbauer Spectroscopy (eMS) studies upon implantation of low fluence ($<10^{13}$ cm^{-2}) of ^{57}Mn ($T_{½}$ = 1.5 min) into ZnO single crystals. At temperatures above room temperature, components assigned to damage fractions (i.e. Fe in local amorphous surroundings due to the implantation damage) have not been observed, reflecting the radiation hardness of ZnO [1].

Higher fluence (10^{15} cm^{-2}) co-implantation of ^{57}Co and ^{57}Fe gives rise to components which are assigned to Fe in damage environments [2], showing a transition from essentially damage free environment to the initial formation of local amorphous regions.

In this contribution we present eMS results from low fluence ($<10^{13}$ cm^{-2}) and low temperature (300K – 120 K) implantations of ^{57}Mn into ZnO. The spectra show the presence of Fe in damage sites, identical to those observed with ^{57}Co/^{57}Fe implantations. Starting with a negligible contribution to the spectra collected at room temperature, the relative spectral area of the damage components increases as the implantation/measurement temperature is lowered.

The results will be discussed in terms of damage accumulation in ZnO and in comparison to data obtained on substitutional and interstitial Fe fractions in eMS measurements performed at higher temperatures.

[1] H. P. Gunnlaugsson et al., *Appl. Phys. Lett.*, **97**, 142501 (2010)
[2] H. P. Gunnlaugsson et al., *Appl. Phys. Lett.* **100**, 042109 (2012)

Electronic address: Krish Bharuth-Ram (kbr@tlabs.ac.za)

P5

First principles calculations of hyperfine interactions in Fe-doped ZnO and other oxides

A. Mokhles Gerami[1,2] K. Johnston[1], H. P. Gunnlaugsson[3], K. Bharuth-Ram[4], G. Langouche[5], M. Vaez-Zadeh[2]

[1] *PH Department, ISOLDE/CERN, 1211 Geneva 23, Switzerland*
[2] *Dept. of physics, K.N.Toosi University of Technology, P.O.Box 15875-4416, Tehran, Iran*
[3] *Department of Physics and Astronomy, Aarhus University, DK-8000 Aarhus C, Denmark*
[4] *School of Physics, Durban University of Technology, Durban 4000, South Africa*
[5] *Department of Physics and Astronomy, University of Leuven, Leuven, Belgium*

Building on a considerable body of experimental work which has used Mossbauer spectroscopy to investigate the nature of Fe in semiconductors such as ZnO [1, 2], we have performed first principle calculations to further examine the nature of Fe^{2+} and Fe^{3+} in ZnO.

Using WIEN2K, experimental parameters including the Isomer shift (IS) and Quadrupole splitting (QS) were calculated using density function theory (DFT) in two different approximations: Pedrew-Burke-Ernzerhof (PBE) and the PBE+U with a Hubbard-like coulomb term. This latter term is of considerable importance and has often been neglected in similar studies [3]. When properly accounted for – including Fe and Zn d-bands *and* oxygen p-bands – in 32 atom supercells with one Fe atom we find that our calculations show good agreement with experimental results. Furthermore, the effect of applying an external magnetic field of 0.6 T on the hyperfine parameters is discussed, where again close agreement to experiment is obtained.

Finally, a discussion on extending these calculations to other materials such as MgO and TiO_2 will be given. Here less experimental work has been performed and first principle results can considerably aid the experimental picture.

References

[1] H. P. Gunnlaugsson *et al.*, *Appl. Phys. Lett.*, **97**, 142501 (2010)
[2] H. P. Gunnlaugsson *et al.*, *Appl. Phys. Lett.* **100**, 042109 (2012)
[3] Y. Abreua *et al* Solid State Communications **185** 25 (2014)

P6

First principles calculations of hyperfine interactions in ZnO and other oxides

Krish Bharuth-Ram

Building on a considerable body of experimental work which has used Mossbauer spectroscopy to investigate the nature of Fe in semiconductors such as ZnO [1, 2], we have performed first principle calculations to further examine the nature of Fe^{2+} and Fe^{3+} in ZnO.

Using WIEN2K, experimental parameters including the Isomer shift (IS) and Quadrupole splitting (QS) were calculated using density function theory (DFT) in two different approximations: Pedrew-Burke-Ernzerhof (PBE) and the PBE+U with a Hubbard-like coulomb term. This latter term is of considerable importance and has often been neglected in similar studies [3]. When properly accounted for – including Fe and Zn d-bands *and* oxygen p-bands – in 32 atom supercells with one Fe atom we find that our calculations show good agreement with experimental results. Furthermore, the effect of applying an external magnetic field of 0.6 T on the hyperfine parameters is discussed, where again close agreement to experiment is obtained.

Finally, a discussion on extending these calculations to other materials such as MgO and TiO_2 will be given. Here less experimental work has been performed and first principle results can considerably aid the experimental picture.

References

[1] H. P. Gunnlaugsson *et al.*, *Appl. Phys. Lett.*, **97**, 142501 (2010)
[2] H. P. Gunnlaugsson *et al.*, *Appl. Phys. Lett.* **100**, 042109 (2012)
[3] Y. Abreua *et al* Solid State Communications **185** 25 (2014)

P7

Static quadrupolar effects in disordered MAX phases

C Brüsewitz,[1,*] U Vetter,[1] H Hofsäss,[1] and M W Barsoum[2]

[1]*II. Physikalisches Institut, Universität Göttingen,*
Friedrich-Hund-Platz 1, 37077 Göttingen, Germany
[2]*Department of Materials Science and Engineering,*
Drexel University, Philadelphia, PA 19104, USA

MAX phases are a class of machinable, ternary carbides and nitrides with remarkable damage tolerance and stability. The perturbed angular correlation (PAC) method promises new insights into their unusual properties due to the local sensitivity of the method. Recently, the A-site specific electric field gradients (EFG) at implanted ^{111}In-^{111}Cd probe atoms have been studied in many MAX phases with perturbed angular correlation spectroscopy (PAC) [1]. Based on those results, further investigations were carried out on disordered phenomena in MAX phases.

The first part of this work is dedicated to the effect of MAX phase solid solutions on the EFG. A fifty-fifty exchange of the M-, A-, or X-element in Ti_2AlC was realized by the synthesis of TiVAlC, $Ti_2(Al,In)_{0.5}C$, and $Ti_2Al(C,N)_{0.5}$. Distinct EFGs were observed instead of a superposition of the EFGs found in pure MAX phases. The fully annealed PAC spectra of the specific solid solutions showed different broadening of the EFG tensor components. This specific broadening can not only be explained by differences of the pure EFGs, but also has to be due to different bondings between the probe atom and the corresponding exchanged atoms. Contrary to Vegard's law, a linear interpolation of the solid solutions' characteristic EFGs was not given.

The second part deals with the effect of uniaxial compression on polycrystalline materials' EFGs in general and the MAX phases' EFGs in particular [2]. Only weak stress dependencies of V_{zz} were observed for the MAX phases, in contrast to strong stress dependencies of e.g. titanium or zinc. In all systems, a reversible broadening of the EFG tensor components was visible under load. It is not yet clear whether this broadening is caused solely by elastic deformation or, in case of the MAX phases, as well by reversible dislocation nucleation or the incipient kink band mechanism which is supposed to be responsible for the remarkable mechanical properties [3]. An irreversible broadening of the EFG tensor components was visible with the onset of permanent deformation, presumably due to an increase in defect densities.

The third part addresses the concept of gradient elastic constants. Gradient elastic constants connect the EFG tensor with a stress or strain tensor [4] and are required for a quantitative description of the former mentioned experimental results. The structure of the gradient elastic tensor was explicitly determined for the appropriate crystal symmetry 6/mmm, the number of independent constants was found to be four. A method was developed in order to determine those constants with the help of DFT calculations implemented in WIEN2k.

This work was financially supported by the DFG under contract no. HO 1125/19-2.

[1] D. Jürgens. PhD thesis, Universität Göttingen, 2014.
[2] C. Brüsewitz, U. Vetter, H. Hofsäss, M. W. Barsoum. *J. Phys. Condens. Matter*, accepted, 2014.
[3] M. W. Barsoum. Wiley-VCH, 2013.
[4] R. G. Shulman, B. J. Wyluda, and P. W. Anderson. *Phys. Rev.*, 107(4):953–958, 1957.

---

[*] cbruese@gwdg.de

P8

Hyperfine field at Mn in the intermetallic compound $LaMnSi_2$ measured by PAC using ^{111}Cd nuclear probe

Cláudio Domienikan[1], Brianna Bosch-Santos[1], Gabriel Adolfo Cabrera Pasca[1], Rajendra N. Saxena[1], Artur W. Carbonari[1]

[1]Instituto de Pesquisas Energéticas e Nucleares, Av. Prof. Lineu Prestes, 2242 – Cidade Universitária – CEP 05508-000 São Paulo, Brazil

Magnetic hyperfine field has been measured in the orthorhombic intermetallic compound $LaMnSi_2$ with PAC spectroscopy using radioactive ^{111}In-^{111}Cd nuclear probe. The sample of $LaMnSi_2$ was prepared by melting pure metallic components in stoichiometric proportion in an arc furnace under argon atmosphere. After melting the sample was sealed in a quartz tube under helium atmosphere, annealed at 1323 K for 60h and then quenched in to water. X-ray analysis showed that the sample has the single phase with the expected crystal structure for $LaMnSi_2$. ^{111}In was introduced in the sample by thermal diffusion at 1323 K for 60h. PAC measurements were carried out with a six BaF_2 detector spectrometer at several temperatures between 50 K and 410 K. The results were analyzed using a model for combined electric quadrupole and magnetic dipole interactions. Comparison of the results with previous studies of PAC in similar compounds shows that ^{111}Cd probes occupy Mn sites. Results show well-defined quadrupole and magnetic interactions at all temperatures. The magnetic hyperfine field (B_{hf}) measured at 50 K is 7.5(1) T. The temperature dependence of B_{hf} follows the normal behavior for host magnetization. The ferromagnetic transition temperature (T_c) was determined to be 402(1) K.

Electronic addrtess:rnsaxena@ipen.br

P9

Hyperfine Interactions in rutile and anatase structures of TiO_2 thin films

Juliana Marques Ramos[1,2], Artur Wilson Carbonari[1], Thiago Martucci[1], Reiner Vianden[2]

[1]*Instituto de Pesquisas Energéticas e Nucleares, University of São Paulo, Av. Prof. Lineu Prestes, 2242 – Cidade Universitária – CEP 05508-000 São Paulo, Brazil*
[2]*Helmholtz-Institut für Strahlen- und Kernphysik, University of Bonn, Nussallee 14-16, 53115 Bonn, Germany*

Thin films of TiO_2 were investigated by perturbed γ-γ angular correlation (PAC) spectroscopy using ^{181}Ta as probe nuclei in order to study the behavior of the hyperfine parameters as a function of temperature for both the anatase and rutile phases. Because this oxide is a candidate for diluted magnetic semiconductor (DMS), the possible occurrence of room temperature ferromagnetism was also investigated. In order to investigate if the presence of oxygen vacancies could induces ferromagnetism, we carried out measurements as implanted and after annealing in vacuum. The structure, composition and surface morphology of the samples were investigated by x-ray diffraction, x-ray fluorescence, scanning electron microscopy, respectively. The magnetic properties of the samples were characterized by magnetization measurements..

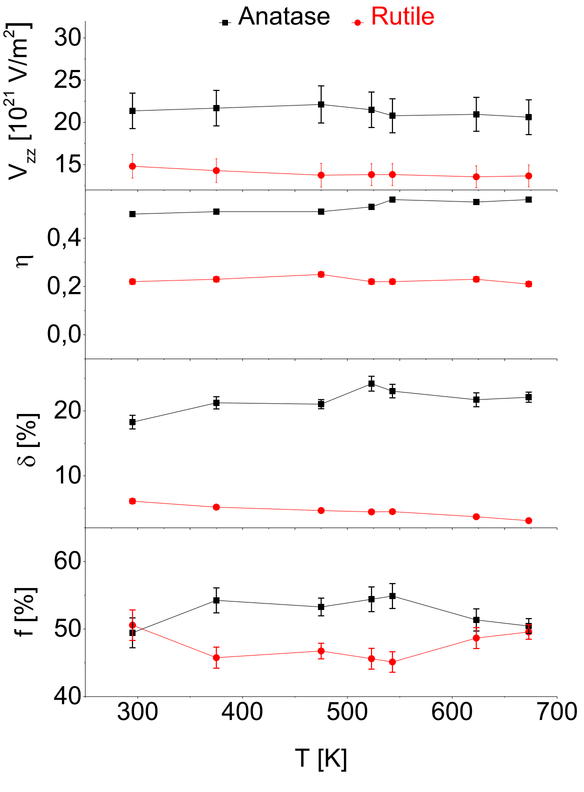

Fig. 1. Hyperfine parameters of TiO_2 measured using ^{181}Hf(^{181}Ta) as probe nuclei.

Magnetization results show no ferromagnetic behavior. The x-ray fluorescence results show no impurities, and the scanning electron microscopy results show that the particles are smaller than 10 nm. PAC results indicate the presence of two electric quadrupole interactions which were assigned to rutile and anatase phases [1]. One of them, with well-defined electric quadrupole frequency ($\delta < 5\%$) and asymmetry parameter $\eta \sim 0.2$, corresponding to an electric field gradient around 1.4×10^{22} V/m^2 was assigned to the rutile phase. The other interaction, with wide distributed electric quadrupole frequency ($\delta \sim 20\%$), with axial asymmetry ($\eta \sim 0.5$) corresponding to an electric field gradient around 2.1×10^{22} V/m^2 was assigned to the anatase structure. We conclude that, the absence of the ferromagnetism is because the absence of a magnetic transition metal dopant, which is responsible for the magnetic interaction, in accordance with the work of Dietl *et al* [2].

[1] D. D. Banerjee. et al., *Journal of Physics and Chemistry of Solids* **983-987**, 71 (2010).
[2] T. Dietl. et al., *Science* **1019-1022**, 287 (2000).

Electronic address of the first author: *emrjmr@gmail.com*

P10

Study of the instability of compound La-doped Fe_3O_4 by Perturbed Gamma-Gamma Angular Correlations

I. T. Matos[1], B. Bosch-Santos[1], G. A. Cabrera-Pasca[1], P. B. A. Fechine[2], A. W. Carbonari[1]

[1] *Instituto de Pesquisas Energéticas e Nucleares, IPEN-CNEN/SP, University of São Paulo, USP, Av. Prof. Lineu Prestes, 2242, São Paulo, SP, 05508-000, Brazil.*
[2] *Departamento de Química Analítica e Físico-Química, Universidade Federal do Ceará, UFC, Campus do Pici, CP 12100, Fortaleza, CE 60451-970, Brazil*

The integration of nanotechnology with molecular biology offers great advantages in biomedical applications. Some of these applications include "drug delivery", imaging, labeling and tracking cells using Fe3O4 nanoparticles. Doping with rare-earth element can enhance the properties of the particles for these applications, especially for imaging. In this work, doping of ferrite Fe_3O_4 nanoparticles, which present a cubic inverse spinel structure, with low concentrations (1% a 5%) of La were investigated by perturbed γ-γ angular correlation (PAC) spectroscopy using ^{111}In(^{111}Cd) as probe nuclei. The aim of the present experiments was to investigate the behavior of temperature dependence of the magnetic hyperfine field. It was, however, observed that samples oxidize at 200°C and undergo a structural change to Fe_2O_3 at above 600ºC. The structure of samples was characterized by X-ray diffraction (XRD) and the results show that all samples crystallize in the expected structure.

P11

The effect of substitution of Ge for Si on the magnetic properties of $LaMn_2Si_2$ investigated by PAC spectroscopy with ^{111}Cd probe nuclei

B. Bosch-Santos, A. W. Carbonari, G. A. Cabrera-Pasca, R. N. Saxena

Instituto de Pesquisas Energéticas e Nucleares, IPEN, University of São Paulo, USP,
Av. Prof. Lineu Prestes, 2242, São Paulo, SP, 05508-000, Brazil

The effect of Ge substitution for Si in $LaMn_2Si_2$ compound on the magnetic hyperfine field (B_{hf}) properties has been investigate by perturbed γ-γ angular correlation (PAC) spectroscopy using ^{111}Cd as probe nuclei at Mn sites. The magnetic properties of $LaMn_2X_2$ (X = Si, Ge) compounds are associated with the magnetic ordering of Mn ions, which form a magnetic subsystem ordering at relatively high temperatures. The ferromagnetic transition when Ge gradually substitutes Si with concentrations of 10%, 20%, 40%, 80% and 100% will be discussed in this work. Samples of $LaMn_2Si_2(Ge_2)$ (La = 99.9%, Mn = 99.999%, Si = 99.999%, and Ge = 99.9999% purity) were prepared by arc-melting the constituent elements in stoichiometric proportions. The compounds were characterized by X-ray diffraction and the results analyzed with Rietveld method. Results show that all samples crystallize in the expected tetragonal structure with single phase containing Si and Ge ions on the same crystallographic site. Carrier-free ^{111}In (^{111}Cd) probe nuclei were added to the compounds having by thermal diffusion. PAC measurements were carried out in the temperature range of 10 K to 325 K. PAC results show that the dependence of B_{hf} with temperature follows the expected behaviour for the host magnetization, and can be fitted by Brillouin function for $J_{Mn} = 5/2$. Results also show a transition from antiferromagntic ordering with T_N= 480 K and T_N= 415 K followed by a ferromagnetic ordering with T_C= 308.5 K and T_C= 323.6 K, respectively for $LaMn_2Si_2$ and $LaMn_2Ge_2$. However, when Ge concentration increases T_N decreases while the Curie temperature increases.

P12

Ab initio high-throughput study of extrinsic point defects in Si and Ge

Michael Sluydts,[1] Jan Vanhellemont,[2] Veronique Van Speybroeck,[1] and Stefaan Cottenier[1,3]

[1]*Center for Molecular Modeling, Ghent University,*
Technologiepark 903, BE-9052 Zwijnaarde, Belgium
[2]*Department of Solid State Sciences, Ghent University,*
Krijgslaan 281 S1, BE-9000 Gent, Belgium
[3]*Department for Materials Science and Engineering, Ghent University,*
*Technologiepark 903, BE-9052 Zwijnaarde, Belgium**

Much of initial semiconductor research was performed on Ge. End of the 1960's, interest largely shifted to Si, due to its advantages for CMOS technology. Approaching the nanoscale, Si CMOS is now reaching its physical limits. Previously problematic properties of Ge, such as the difficulty to grow stable thermal oxides are no longer relevant and the advantage of the much higher carrier mobility can be exploited.

To further explore its use, one needs a body of knowledge on Ge properties that is comparable to the one we have for Si. Given the decades of intense experimental efforts that were dedicated to Si, this is not trivial. High-throughput Density-Functional Theory calculations are one way to speed up the generation of essential knowledge on Ge properties.

The present high-throughput study focuses on one specific property: the embedding enthalpy of extrinsic point defects. This has been examined for both Si and Ge, allowing us to verify our computational method through comparison with reliable experimental data for Si, while filling in missing data for both materials. All elements from the first six periods of the periodic table (excluding lanthanides) were put at six different positions in the Si or Ge lattice. The lattice around the introduced impurity was allowed to relax. The embedding enthalpy for each impurity at each site has subsequently been determined. This approach has provided a substantial set of data for further analysis. Calculated results will be compared with available experimental data – many of those being obtained by nuclear methods (quadrupole interactions from Mössbauer, TDPAC, NMR or EPR, lattice locations studies by (emission) channeling, . . .). Trends through the periodic table and the degree of transferability of knowledge for Si to the corresponding situation for Ge, will be discussed.

---

*Electronic address: `stefaan.cottenier@ugent.be`

P13

Effect of temperature on the phase transformation of iron phosphate in the production of methyl methacrylate

Blank line (12 points)

Avinash Harilal[1], Venkata D. B. C. Dasireddy[1], K. Bharuth-Ram[1,2] and H. B. Friedrich[1]

Blank line (12 points)

[1]School of Chemistry and Physics, University of KwaZulu-Natal, Durban, South Africa.
[2]Durban University of Technology, Durban 4000, South Africa

Blank line (12 points)

Methyl methacrylate (MAA) is an alpha beta unsaturated compound and exhibits reactivity typical of this class of compounds, namely the vinyl function and the carboxylic acid or ester group [1]. There exists a small number of reports of the gas phase oxidative dehydrogenation reactions to produce MAA [1-3]. Iron phosphate catalysts are widely used for these types of reactions. The change in the phase of the iron phosphates during the reactions influences the yield towards the MAA [2]. In the present work, we present results of our investigation of the transformation of iron phosphate phase in a synthesized iron phosphate catalyst, and comparative investigations on a commercial grade iron phosphate catalyst and as well as an iron oxide catalyst.

Iron phosphate catalyst was prepared using ammonia gel method illustrated in [1-2]. Commercial iron phosphate catalyst was impregnated on colloidal silica using wet-impregnation. The prepared catalysts were characterized by room temperature X-ray diffraction (XRD) and *in situ* XRD. Mössbauer spectroscopy (MS) was used to determine the phase of the iron in the catalysts before and after the reaction conditions, and to determine the phase transformation under oxidation and reduction conditions.

The Mössbauer spectra of the commercial catalyst was fitted with two paramagnetic doublets with parameters characteristic of Fe^{3+} species corresponding to $FePO_4$ [2-3], the broad line widths reflecting a distribution of quadrupole splittings. The large quadrupole splitting observed is probably an indication that the environment around the Fe^{3+} ion is distorted [2, 4]. The Mössbauer spectrum of the synthesized iron phosphate catalyst was similar to that of the commercial catalyst and showed the presence of the ferric ion only. The spectral parameters confirm the occurrence of the $FePO_4$ tridymite-like phase which has 100 % Fe^{3+} species and is in agreement with the experimental route used [2-3]. The isomer shift and quadrupolar splitting values obtained for the $FePO_4$ catalysts showed the existence of both the tridymite-like as well as the quartz type $FePO_4$ phase. Both $FePO_4$ phases transform with temperature under the reduction and oxidation atmospheres to alpha $FePO_4$ phase which was evidenced in both MS and XRD studies.

---

[1] M. Ai, *Catalysis Today* **52**, 65 (1999).
[2] F.B. Khan, et al., *Hyperfine Interactions* **197**, 317 (2010).
[3] J.-M. Millet, et al., *Topics in Catalysis* **15**, 139 (2001).
[4] P. Bonnet, et al., *Journal of Catalysis* **158**, 128 (1996).

Electronic address: *Dasireddy@ukzn.ac.za,harilal.avinash@sasol.com*

P14

Theoretical and experimental estimation of hyperfine quadrupole splitting in intermetallic compound $Zr(Cr_x, Fe_{1-x})_2$

Bateev A.B. Filippov V.P. and Eydlina M.A.

National Research Nuclear University MEPhI (Moscow Engineering Physics Institute)

Zirconium alloys are used in nuclear reactors as fuel claddings, grids and other structural components. Iron and chromium are added to improve mainly corrosion and radiation properties of structural elements. Solubility of iron in alpha zirconium is not greater than 0.02 mas.%. The rest of iron in zirconium alloy forms with zirconium intermetallic compounds the type of which depends on the doping elements. In binary alloys with Fe (24 mas.%) the compounds Zr_2Fe and Zr_3Fe are formed. But in alloys containing iron and chrome the compounds of type $Zr(Fe_{1-x}, Cr_x)_2$ are formed with structures indicated as C14 and C15 [1,2].

In the present work an attempt is made to compare the theoretical and experimental estimation of values of the quadrupole splitting for structure C14. The calculation was carried out using the classic formula of electric field potential generated by a point charge on the nucleus of iron-57. The nearest iron and zirconium atoms were considered as the point charges. In crystal lattice of intermetallic compound the chromium atoms can replace iron atoms. As the iron and chromium atoms have approximately equal charges and sizes their influence were considered in calculations as the same. The calculation was carried out for two nonequivalent positions of iron atoms corresponding to the so-called 2*a* and 6*h* sites. It is obtained that the values of the quadrupole splitting for these positions may change from 0.23 mm/s. to 0.34 mm/s. Atoms in the 2*a* states have an environment in the form of two inverted tetrahedra, atoms in 6*h* states have less symmetrical environment. The ratio of the areas of states 2*a* and 6*h* approximately corresponds to 1:3, and the ratio of quadrupole splittings ~1.5.

The comparison of calculated data with experimental data was carried out for alloy (Zr-1.2%Sn-1.0%Fe-0.5%Cr) (mas.%). Mossbauer spectrum of this alloy shows widening lines of quadrupole splitting. Fitting of the spectrum allows to identify three system lines of quadrupole splitting. The lines with parameters of the quadrupole splitting $\Delta E=0.8\pm0.1$ mm/s and isomer shift $\delta=0.32\pm0.1$ mm/s belong to the intermetallic compound Zr_3Fe [2]. Another two systems of lines of quadrupole splitting with spectra parameters $\Delta E_1=0.29\pm0.04$ mm/s, $\delta_1=0.19\pm0.02$ mm/s and $\Delta E_2=0.21\pm0.02$ mm/s, $\delta_2=0.23\pm0.02$ mm/s belong to intermetallic compound $Zr(Fe, Cr)_2$ in the states C14 and C15, respectively. Comparison of theoretical and experimental data can give the basis to assume that described values of quadrupole splitting in the literature can have some bugs to iron atoms in the structure of the C14.

[1] V.P. Filippov, A.B. Bateev,·Yu.A. Lauer, N.I. Kargin, *Hyperfine Interaction* **45-55**, 217(2013).

[2] D. Pecheur, V.P. Fiippov, A.B. Bateev, Yu.Yu. Ivanov, *Zirconium in the Nuclear Industry*: *Thirteenth International Symposium*. ASTM STP 1423, Gerry D. Moan ad Peter Ruling, Eds., ASTM International, West Conshohocken, **135-153**, PA 2002.

P17

High Pressure crystallographic structure and Mössbauer Study of the Fe-Cr-Hx Phase Diagram.

Amir Broide[1,2], Silvie Maskova[3], Matthew S. Lucas[4], Itzhak Orion[2], Amir Hen[2,5], Shai Salhov[1], Michael Shandalov[1], Zhiqiang Chen[6] and Itzhak Halevy[1,2]

[1] Dept. of physics, NRCN, P.O.Box 9001, Beer-Sheva, ISRAEL
[2] Nuclear engineering Department, Ben Gurion Univ., Beer-Sheva, ISRAEL
[3] Department of Condensed Matter Physics, Faculty of Mathematics and Physics, Charles University
Ke Karlovu 5, 12116 Prague 2, The Czech Republic
[4] Air Force Research Laboratory, OH, USA
[5] European Commission**,** Joint Research Center, Institute for Transuranium Elements
Fundamental Actinides Research, Postfach 2340, D-76125 Karlsruhe, Germany
[6] NSLS, Brookhaven National Laboratory, NY 11973, USA

The crystallographic structure, symmetry and the unit cell parameters combined with the magnetic structure gives an insight to the Fe-Cr phase diagram. High Pressure X-Ray diffraction in the NSLS gave the crystallographic structure, symmetry and the unit cell parameters as function of pressure. There is a known phase transition from bcc the hcp at 13GPa in the elemental iron. In the measurements made on disordered bcc solid solutions of Fe-Cr we noticed the effect of the Cr concentration on the unit cell parameter. The transition pressure is increasing with the increase of the Cr concentration see Fig 1 & 2. Mössbauer effect of Fe-Cr at various concentrations given in Fig. 3. Recently the Fe-Cr system was hydrogenated and compered to the parental system.

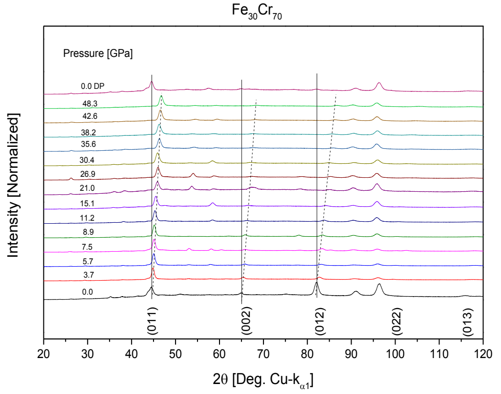

Fig. 1 X-ray diffraction as function of pressure for $Fe_{30}Cr_{70}$, no phase transition is indicated.

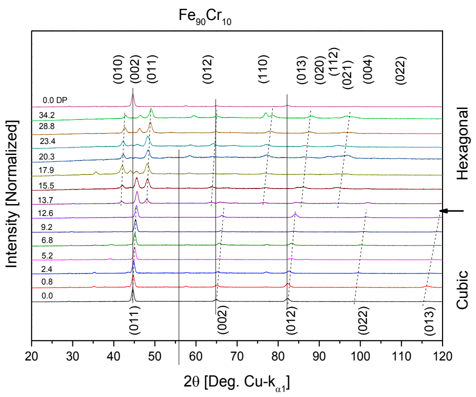

Fig. 2 X-ray diffraction as function of pressure for $Fe_{90}Cr_{10}$ phase transition is indicated at 13.7GPa

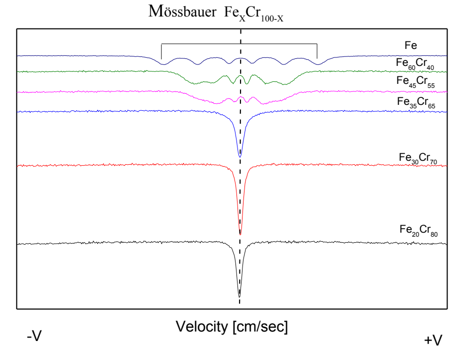

Fig. 3 Mössbauer effect of Fe-Cr at various concentrations.

Halevy.itzhak.dr@gmail.com

References

1. Matthew S. Lucas, M. Kresch, R. Stevens, and B. Fultz Phonon partial densities of states and entropies of Fe and Cr in bcc Fe-Cr from inelastic neutron scattering PHYSICAL REVIEW B 77, 184303 _2008

2. Matthew S. Lucas, A. Papandrew, and B. Fultz Partial phonon densities of states of ^{57}Fe in Fe-Cr: Analysis by a local-order cluster expansion PHYSICAL REVIEW B 75, 054307 ,2007

P18

Microwave absorption and ^{57}Fe Mössbauer properties of Ni-Ti and Co-Zr doped barium hexaferrite

S J Harker,[1,2] G A Stewart,[2] A Amiet,[3] and W D Hutchison[2]

[1]*Defence Science and Technology Organisation,*
Russell Offices, Canberra ACT 2600, Australia
[2]*School of Physical, Environmental and Mathematical Sciences,*
The University of New South Wales, Canberra, ACT BC 2610, Australia[*]
[3]*Maritime Division, Defence Science and Technology*
Organisation, Fisherman's Bend Vic 3207, Australia

Fine particle doped barium hexaferrite, $Ba(A_xFe_{12-x})O_{19}$, where A is the dopant or dopant combination, is one of several candidates for high density magnetic recording and radar absorption applications. For the latter application the doping is used to lower the ferromagnetic resonance (FMR) frequency of barium hexaferrite into the desired radar frequency. ^{57}Fe Mössbauer spectroscopy can be used to derive information about the preferred site occupation of the dopants when combined with other techniques [1, 2].

Here, complementary microwave network analysis and magnetic data are presented for doped barium hexaferrite with A = Co^{2+}/Zr^{4+} $(0 \leq x \leq 2.5)$ and Ni^{2+}/Ti^{4+} $(0 \leq x \leq 3)$. The dopant site occupations have been investigated using ^{57}Fe Mössbauer spectroscopy in combination with a consideration of dopant-site matching and the measured influence on cell volume obtained from x-ray powder diffraction.

[1] A. González-Angeles, G. Mendoza-Suárez, A. Grusková, J. Sláma, J. Lipka, and M. Papánová, Materials Letters **59**, 1815 (2005).
[2] P. Quiroz, B. Halbedel, A. Bustamante, and J. C. González, Hyperfine Interact. **202**, 97 (2011).

---

[*] Electronic address: `stephen.harker@defence.gov.au`

P19

Electrical Conductivity, DSC, XRD, and ^{7}Li NMR Studies of n-$C_mH_{(2m+1)}OSO_3M$ (m = 12, 14, 16, 18, 20; M = Li, Na, K)

Yoshiaki Morimoto,[1] Satoru Hirakawa,[2] and Hisashi Honda[1,2]

[1]*International College of Arts and Sciences, Yokohama City University, Kanazawa-ku, Yokohama, 236-0027, Japan*

[2]*Graduate School of Nanobioscience, Yokohama City University, Kanazawa-ku, Yokohama, 236-0027, Japan*

Electrical conductivity (σ), differential scanning calorimetry (DSC) thermograms, X-ray diffraction (XRD) analysis, and ^{7}Li NMR spectroscopy characterization of n-$C_mH_{(2m+1)}OSO_3M$ solids (m = 12, 14, 16, 18,20; M = Li, Na, K) (abbreviated to CmM) were performed as a function of temperature. Samples of CmM were prepared by n-$C_mH_{(2m+1)}OSO_3H$ and MOH. DSC thermograms of these compounds revealed that these salts had several solid-solid phase transitions with large entropy changes, in addition, some crystals showed small entropy changes at melting points. These properties are similar to those detected in rotator crystals. ^{7}Li (I = 3/2) NMR spectra of these compounds recorded at various temperatures suggested that the Li^+ ions are localized in the crystal (Fig. 1). In contrast, electrical conductivity measurements indicated that there are ion transfers in CmM crystals (Fig. 2). Since self-diffusion of Li^+ ions are rarely reported in Li salts, this study gives valuable data for Li ion conductors.

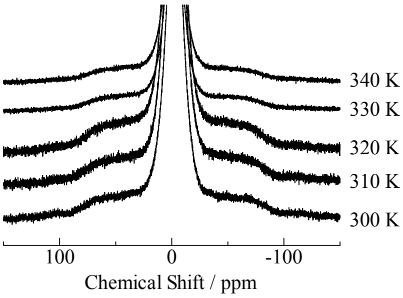

Fig. 1 ^{7}Li NMR spectra of C18Li. The spectra were recorded at 233.23 MHz.

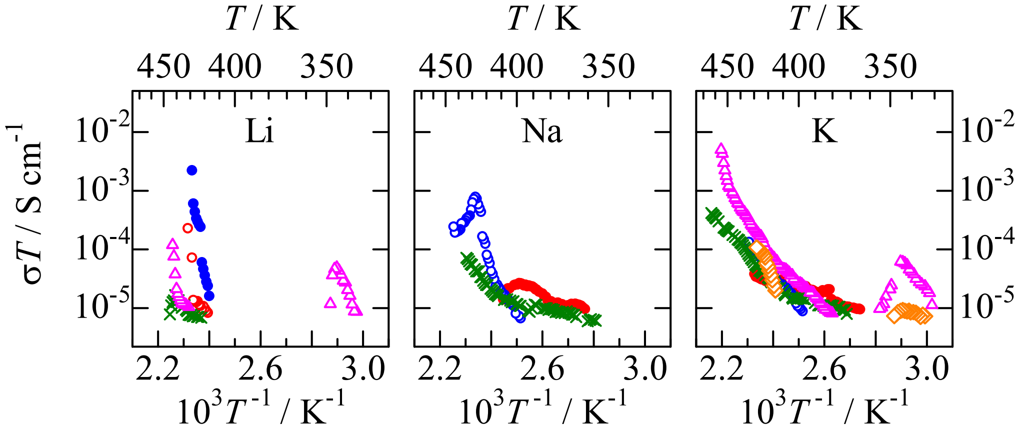

Fig. 2 Electrical Conductivity (σ) of C8Li (○), C14Li (●). C18Li (×), C20Li (△), C12Na (●), C14Na (○), C16Na (×), C12K (●), C14K (○), C16K (×), C18K (△), C20K(◇) as a function of temperature.

E-mail: hhonda@yokohama-cu.ac.jp

P20

Evolution with applied field of the magnetic structure of TbNiAl$_4$

W.D. Hutchison[1*], **R. White**[1], **D.J. Goossens**[2], **A.J. Studer**[3] **and K. Nishimura**[4]

[1] *School of Physical, Environmental and Mathematical Sciences, The University of New South Wales, Canberra ACT 2600, Australia.*
[2] *Research School of Chemistry, Australian National University, Canberra ACT 0200, Australia.*
[3] *Bragg Institute, Australian Nuclear Science and Technology Organisation, Lucas Heights NSW 2234, Australia.*
[4] *Graduate School of Science and Engineering, University of Toyama, Toyama 930-8555, Japan.*

The family of metamagnetic compounds RNiAl$_4$, orthorhombic structure (space group #63, Cmcm) with R = rare earth, exhibit a range of interesting magnetic behaviours. There are multiple magnetic phases, and crystal field driven anisotropy, with these behaviours varying somewhat for different rare earth ions (R) (see [1] and references therein]. TbNiAl$_4$ is both an illustrative and experimentally accessible example. It has two phase transitions (three phases) as a function of temperature in low applied magnetic field. The Neél temperatures in zero applied field are T_N ~34.0 K and $T_{N'}$ ~28.0 K, corresponding to transitions from paramagnet to incommensurate antiferromagnet (AF), and then to *a* axis aligned linear AF phases, respectively [1]. As a function of applied field it undergoes a series of magnetic phase transitions [2] (see Figure 1). Neutron diffraction studies using single crystals in applied magnetic fields, up to 11.5 T, were used to obtain the intermediate and high field spin arrangement [3]. We find that not only does the applied field drive the system from commensurate to incommensurate ordering, but that the phase transition shows hysteresis such that a mixed phase state can be observed. This mixed state simultaneously showing commensurate and incommensurate antiferromagnetic ordering, along with ferromagnetism. However, comparisons of these results with a microscopic study of the variation of the Tb hyperfine field with applied field, via low temperature nuclear orientation, poses some additional questions about how the intermediate and mixed phases evolve [4]. This issue is examined in detail in this paper.

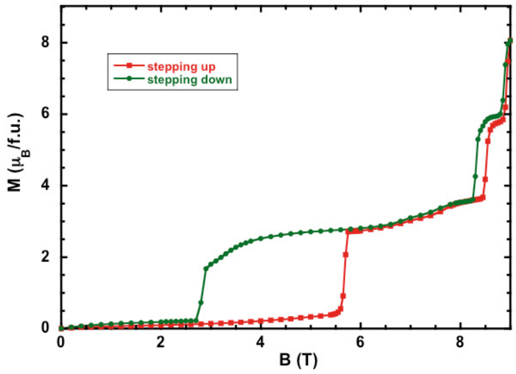

Figure 1. Magnetisation data for a TbNiAl$_4$ single crystal at 2.0 K with the applied magnetic field along the *a* axis.

[1] W.D. Hutchison, D.J. Goossens, K. Nishimura, K. Mori, Y. Isikawa and A.J. Studer, *J. Magn. Magn. Mater.* **301**, pp. 352-358, 2006.

[2] T. Mizushima, Y. Isikawa, A. Mitsuda, K. Kobayasi, F. Ishikawa, T. Goto and S. Kawano, *J. Magn. Magn. Mater.* **272-276**, e475-e476, 2004.

[3] W.D. Hutchison, D.J. Goossens, R.E. Whitfield, A.J. Studer, K. Nishimura and T. Mizushima, *Phys. Rev. B* **86**, 014412:1-5, 2012.

[4] W.D. Hutchison, *Hyperfine Interactions* **220,** 11–20 (2013).

---

[*] Electronic address: *w.hutchison@adfa.edu.au*

P23

β-NMR Study of Boron in Diamond

T. Izumikawa[1], M. Mihara[2], K. Matsuta[2], M. Fukuda[2],
T. Ohtsubo[3], S. Ohya[3], T. Minamisono[2]

[1] *Radioisotope Center, Niigata University, Niigata 951-8510, Japan*
[2] *Department of Physics, Niigata University, Niigata 950-2181, Japan*
[3] *Department of Physics, Osaka University, Toyonaka, Osaka 560-0043, Japan*

The highly boron-doped diamond is of great interest because of its high or super electrical conductivity. In order to investigate the crystallographic properties of it, we performed the β-NMR experiment on ^{12}B nuclei implanted in single crystal diamond.

The β-emitter ^{12}B were produced ^{11}B (d, p) ^{12}B reaction using a 1.5 MeV deuteron beam, and the polarized nuclei were obtained by selecting the recoil angle. The recoil ^{12}B were implanted in the single-crystal synthetic diamond (Type Ib). The <110> axes of the crystals were placed approximately parallel to the external magnetic field of 6.0 kOe. After the production and recoil implantation for 25 ms, the rf oscillating magnetic field was applied for 12 ms. The polarization change due to the rf was determined by the β-ray counting asymmetries.

The maintained polarization of ^{12}B was measured by use of widely modulated rf around the Larmor frequency (νL ± 200 kHz) as a function of temperature from 160 K to 320 K. The obtained polarization was almost constant of about 0.9% in the temperature range. The initial polarization for this system was obtained as about 8.1% from the β-NMR on ^{12}B implanted in Pt. Therefore about 10% of implanted ^{12}B maintained its polarization in this range of frequency. Conversely, about 90% of implanted ^{12}B was undetected in the present experiment. The missing ^{12}B may be affected by the strong hyperfine interaction that shift the resonance frequency far away from the Larmor frequency or destroy the polarization in an instant.

The polarization changes using narrower modulated rf of ±25 kHz and ±10 kHz were also measured. The poralization changes by the narrower rf were almost the same with the case of widely modulated rf.

Electronic address: *izumika@med.niigata-u.ac.jp*

P24

The effect of single and double quenching heat treatments on the mechanical properties of low alloy steel

Kyeongpil Kim[1], Byung Jun Kim[1*], Sanghui Lee[1], Jae-ho Jang[1], Dae-Geun Nam[1], Gi-Chan Sung[2]

[1] *Korea Institute of Industrial Technology, 618-230 Busan, South Korea*
[2] *Sehwa M&P Co., LTD, 680-090 Ulsan, Korea*
**Corresponding author: jun7741@kitech.re.kr*

For spent fuel storage, low alloy steel is widely used for shielding materials for dry storage cask of spent fuel because of their excellent mechanical properties, weldability and low price [1]. However, they may suffer embrittlement by high levels of radiation and heat for a long period. Therefore, it is important to improve mechanical properties of low alloy steel for the integrity of structure materials. Recently, it showed that a double quenching tempering (DQT) heat treatment process resulted in a significant improvement of strength and toughness by austenite grain refinement. In this study, the microstructure and mechanical properties of DQT heat treated specimens were investigated to improve the mechanical properties of low alloy steels comparing the conventional single quenching and tempering (CQT) heat treated specimen. The grain size of DQT process has a fine average grain size comparing the CQT process. A fine grained structure with DQT specimen affects the mechanical properties such as the reduction of hardness and increase of elongation. The DBTT after DQT process is shifted to lower temperatures in Fig.1. The reason for the reduction of DBTT and USE after the DQT process is related to the changes of microstructure which are transformed from bainite to pearlite phase and the reduction of grain size with decreasing the temperature of heat treatment.

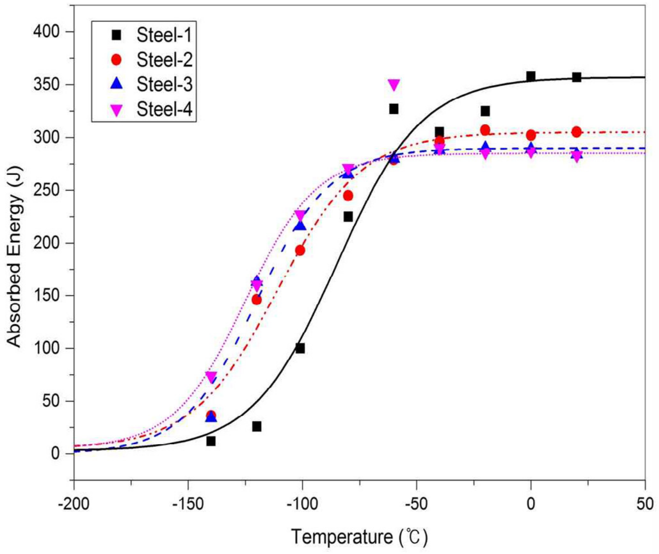

Fig. 1. The energy absorbed vs temperature curves for four steels.

[1] Anil Kumar Shinha, Chengjian Wu, and Guoquan Liu, Steel Heat Treatment: Metallugy and Thechnologies, Second Edition, CRC Press Traylor & Francis Group, p18-32, 2007.

Electronic address: *Presenting. jun7741@kitech.re.kr*

P25

Atmosphere Dependence of Local Structures Formed by Al and In Impurities in Zinc Oxide

S. Komatsuda[1], **W. Sato**[1,2], **Y. Ohkubo**[3]

[1] *Graduate School of Natural Science and Technology, Kanazawa University, Kakumamachi, Kanazawa, Ishikawa 920-1192, Japan* ✳
[2] *Institute of Science and Engineering, Kanazawa University, Kakumamachi, Kanazawa, Ishikawa 920-1192, Japan*
[3] *Research Reactor Institute, Kyoto University, Kumatori, Osaka 590-0494, Japan*

Impurity-induced properties emerging in ZnO has been attracting increasing attention toward its application to functional materials in a wide field of industry. It is known that the physical properties, induced by doped impurities and/or oxygen vacancies, are very sensitive to changes in local structures formed by doped impurities as well as in their concentrations and compositions. From this point of view, we investigated the factors determining the local structures and their stability for the samples synthesized on different conditions by means of the time-differential perturbed angular correlation (TDPAC) method, employing the ^{111}Cd(← ^{111}In) probe. In one of our previous studies[1], we observed contrastive atmosphere dependence of the stability of aggregations of ^{111}In and Al impurities doped in 100 ppm Al-doped ZnO: (i) Al and In impurities associate with each other by their thermal diffusion in air, and (ii) the ^{111}In probe can be detrapped from the Al aggregations in high-temperature vacuum, resulting in substitution at defect-free Zn sites. In the present work, in order to extend quantitative discussion on the kinetics of the dissociation process of Al and In ions, we investigated the annealing-time and annealing-temperature dependences of the detrapping process during heat treatment in vacuum.

Figure 1(a) shows a TDPAC spectrum obtained for a typical sample of 100 ppm Al-doped ZnO heat-treated at 1373 K in air. Figures 1(b) and 1(c) are those obtained for samples synthesized by two step heat treatments: firstly in air at 1373 K and secondly in vacuum at 1148 K (a) for 15 min and (b) for 12 h. Figure 1(a) shows that ^{111}In ions are trapped in the field of Al forming local associations in ZnO matrix[2]. For the spectra in Fig. 1(b) and 1(c), a different component corresponding to the probe at the defect-free Zn site has become visible for the sample annealed in vacuum for 15 min, and it becomes predominant after the annealing for 12 h. In the present paper, these observations are quantitatively discussed based on the rate constant and the activation energy for the dissociation reaction of Al and ^{111}In.

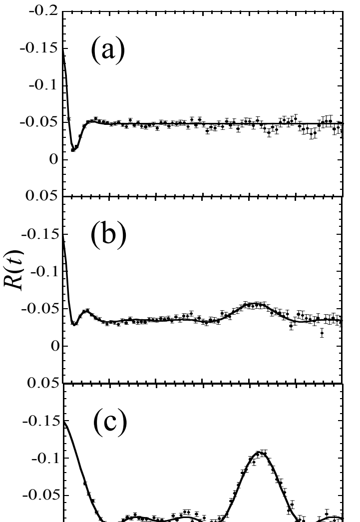

Fig. 1. (a) TDPAC spectrum of ^{111}Cd(←^{111}In) in 100 ppm Al-doped ZnO annealed in air at 1373 K. TDPAC spectra of ^{111}Cd(←^{111}In) in 100 ppm Al-doped ZnO annealed in vacuum at 1148 K (b) for 15 min and (c) for 12 h after the measurement of the spectrum (a).

[1] S. Komatsuda, W. Sato, and Y. Ohkubo, J. Radioanal. Nucl. Chem. Accepted for publication.
[2] S. Komatsuda, W. Sato, S. Kawata, and Y. Ohkubo, J. Phys. Soc. Jpn. **80**, (2011) 095001.

Electronic address: *sayaka@stu.kanazawa-u.ac.jp*

P26

INVESTIGATION OF HYPERFINE INTERACTIONS IN INDIUN (III) COMPLEXING IN AQUEOUS SOLUTION

Andre L. Lapolli[1], Artur W. Carbonari[1]

[1]*Instituto de Pesquisas Energéticas e Nucleares, IPEN-CNEN/SP, Universidade de São Paulo,*
05508-000 São Paulo, SP, Brazil

Perturbed $\gamma\gamma$ angular correlation (PAC) spectroscopy has been used to study by ^{111}In complexing in aqueous solutions have been pH=4 to pH=14. This chemical environment it is expected the formation of species such as $[In(H_2O)_6]^{3+}$ in a very low pH and $[In(OH)_6]^{3-}$ to very high pH [1]. This work aims to obtain detailed information on the chemical behavior of the probe nucleus ^{111}In as the advancement of studies with biomolecules is intended to know in detail the chemical reactions in biological systems without interference of this nucleus. Samples were made by appropriate addition of NaOH solution and HCl solution. The pH measurements were performed at approximately 25 º C with accuracy in high precision pH meter 0.01. The radioactive probe ^{111}In-^{111}Cd was inserted into the samples (10μL of $InCl_3$ pH neutron in 100 μL of the solution). Samples were measured at 295 K and 77 K temperature in the standard 6-BaF_2 detectors PAC spectrometer. The interpretation of the results was based on the measurements of dynamic interaction (295 K) characterized by rotational frequency (λ) from which valuable information on species formed in the environment. PAC measurements at 77 K showed interaction frequency (ν_Q), asymmetry parameter (η) and the distribution of the quadrupole frequency (δ).The results at both 77 K and 295 K are varied for different pHs but are not in agreement with the work of Demille[2].

[1] J. Celeda and D.G. Turck, *J. Inort. Nucl. Chem* **36**, 373 (1974).
[2] G.R Demille, et al., *Chemical Physics Letters* **44**, 164 (1976).

P27

Calculation of the Charge State Distribution of ^{111}Cd Following Electron Capture

B. Q. Lee,[1] A. E. Stuchbery,[1] T. Kibédi,[1] and F. G. Kondev[2]

[1]*Department of Nuclear Physics, The Australian National University, ACT 0200, Australia*
[2]*Argonne National Laboratory, Argonne, Illinois 60439, USA*

^{111}In is the most commonly used probe in Perturbed Angular Correlation (PAC) spectroscopy. ^{111}In decays to ^{111}Cd by electron capture (EC) decay; the decay leaves an initial vacancy in the atomic shell of ^{111}Cd. The initial vacancy will then propagate towards the outer-shells rapidly ($\sim 10^{-12}$s) by means of radiative transitions and Auger processes in the so-called "Auger cascade" relaxation scheme. In each Auger process, an atomic electron will be emitted, thus increasing the ionization number of the atom by one. The number of vacancies in the atom can be multiplied, through Auger processes, leaving the atom in a highly ionized state (^{111}Cd^{x+}). If these vacancies created live long enough, especially in insulators doped with ^{111}In, they can modify the local charge distribution around the probe after the emission of the first γ-ray, producing dynamic processes that can be observed by PAC; in the case of ^{111}Cd probe, dynamic hyperfine interactions can happen in a time window of approximately 10-400 ns [1]. This is the so-called "*electron-capture after-effects*" (ECAE).

Calculation of charge state distribution of ^{111}Cd following EC decay is important in the study of the *after-effects* in PAC spectroscopy. A pilot computational model of Auger cascade, based on a Monte Carlo method, using up-to-date nuclear input data and atomic transition probabilities from the evaluated atomic data library (EADL) [2], has been developed. Details of the model have been published elsewhere [3, 4]. The charge state distribution of the residual ^{131}Xe atoms following the decay of $^{131\text{m}}$Xe have been calculated and compared with available experimental data in vapor phase [4]. Reasonably good agreement with experimental results have been achieved. The calculated charge state distribution of the residual ^{111}Cd atoms in the EC decay of ^{111}In will be presented.

---

[1] L. A. Errico, *et al*, Hyperfine Interactions **120/121** (1999) 457.
[2] S. T. Perkins, UCRL-50400 **30**.
[3] B. Q. Lee, *et al*, Comp. and Math. Meth. in Med., Article ID 651475 (2012)
[4] B. Q. Lee. *et al*, EPJ Web of Conf. **63** (2013) 01002.

P29

Production of Spin Polarized Li Isotope Beam through Heavy Ion reactions

J.Ohno[1], **M.Mihara**[1], **Y.Kamisho**[1], **M.Fukuda**[1], **K.Matsuta**[1], **T.Minamisono**[1], **Y.Morita**[1], **M.Yaguchi**[1], **K.Iwamonto**[1], **M.Wakabayashi**[1], **R.Kanbe**[1], **M.Tanaka**[1], **S.Shinozaki**[1], **S.Yamaoka**[1], **K.Watanabe**[1], **S.Iwakiri**[1], **R.Yanagihara**[1], **D.Nishimura**[2], **T.Izumikawa**[3], **T.Ohtsubo**[4], **S.Suzuki**, **M.Nagashima**[4], **T.Sakai**[4], **K.Abe**[4], **Y.Nakamura**[4], **D.Murooka**[4], **A.Ozawa**[5], **D.Nagae**[5], **Y.Ishibashi**[5], **Y.Abe**[5], **T.Niwa**[5], **T.Nagatomo**[6], **A.Kitagawa**[7], **S.Sato**[7], **M.Torikoshi**[7], **S.Momota**[8], **K.Kubo**[9], **J.Sugiyama**[10], **H.Shirai**[11], **and N.Yoshida**[11]

*[1]Dept. Physics, Osaka University, 1-1 Matikaneyama-machi Toyonaka-shi Osaka-fu, 560-0043, Japan** *[2]Dept. Physics, Tokyo University of Science, [3]Radioisotope Center,Niigata University, [4]Dept. Physics, Niigata University, [5]Dept.Physics, University of Tsukuba, [6]RIKEN Nishina Center, [7]National Institute of Radiological Science, [8]Kochi University of Technology, [9]International Christian University, [10]Toyota Central Research and Development Laboratories Inc., [11]Dept. Physics, Tokyo Institute of Technology*

Spin polarized radioactive nuclear beams are useful for materials science as β-NMR probes which exhibit extremely high sensitivity to the NMR detection. So far, short-lived β-NMR probe nucleus ^{8}Li (I^{π} = 2^{+}, $T_{1/2}$ = 838 ms) has been used strongly for the materials science. In the present study, we have performed the production test of polarized ^{8}Li and another candidate of ^{9}Li (I^{π} = $3/2^{-}$, $T_{1/2}$ = 178 ms) which has shorter lifetime than ^{8}Li through the heavy ion reactions of ^{10}B, ^{11}B, and ^{12}C.

The experiment was performed at Heavy Ion Medical Accelerator in Chiba (HIMAC) in National Institute of Radiological Science (NIRS).Polarized ^{8,9}Li nuclei were produced by using ^{10,11}B or ^{12}C primary beams at an energy of 70 *A* MeV with a Be target. The result of polatization and yield of ^{8}Li and ^{9}Li are shown in FIG. 1. Polarization was observed for ^{8}Li at high momentum side with other than a ^{10}B beam. The result of ^{9}Li suggests the possibility that large polarization is generated with a ^{10}B beam which picks up a neutron in the reaction process.

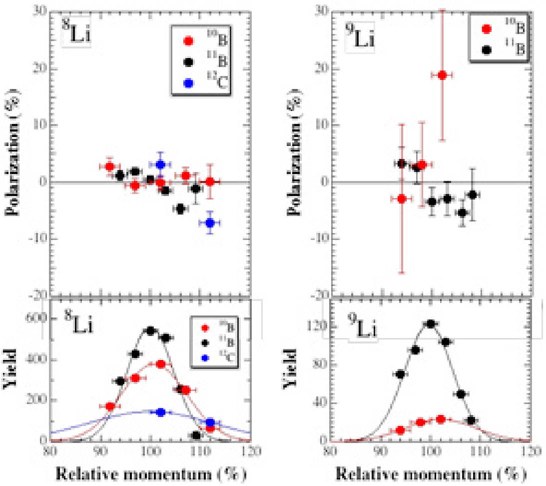

FIG. 1: Polarization and yield of ^{8,9}Li produced through the projectile fragmentation of ^{10,11}B and ^{12}C on a Be target at 70 *A* MeV.

---

*Electronic address: oono@vg.phys.sci.osaka-u.ac.jp

P30

Observation of 4d local moment on Rh impurity in the quantum critical alloy $Nb_{1+y}Fe_{2-y}$.

S.K. Mohanta, S.M. Davane and S.N. Mishra

Tata Institute of Fundamenta Research, Homi Bhabha Road, Mumbai-400005, India

Quantum critical behavior in magnetic systems is a topic of current interest. The intermetallic alloy system Nb1+yFe2-y has been shown to exhibit quantum criticality for y = 0.02 [1, 2]. We have performed microscopic investigations for the Fe rich alloy $Nb_{0.95}Fe_{2.05}$ by measuring the local susceptibility of ^{100}Rh using the time differential perturbed angular correlation spectroscopy. The parent ^{100}Pd nuclei have been produced and recoil implanted in the $Nb_{0.95}Fe_{2.05}$ host via the nuclear reaction $^{11}B(^{93}Nb, 4n)^{100}Pd$ at laboratory energy Elab = 58 MeV. With this reaction the activity obtained with 150 nA beam current and an irradiation time of 16 hrs was found to be reasonably good for subsequent PAC measurements. Fig. 1 shows the g-ray energy spectrum recorded by a HpGe detector, 24 hrs after irradiation. It can be seen that the 75-84 keV g-lines of ^{100}Rh produced during the electron capture decay of ^{100}Pd are clearly resolved with very little contamination from other reaction products. Fig. 2 displays typical PAC spectra in external applied field, B_{ext} ~ 0.7 T recorded at select temperatures. The local susceptibility $\beta(T)-1 = h\omega_L(T)/(g_N\mu_N B_{ext})$ is shown in Fig. 3. Above 70 K, $\beta(T)$ shows a Curie-Weiss behavior: $\beta-1 = C/(T+T_{sf})$ yielding C = -24 K and T_{sf} = 8 K which, indicates the presence of a stable magnetic moment on Rh. Below 70 K, the β value was found to increase rapidly, indicating onset of magnetic ordering. Further measurements are in progress to delineate the local manifestation of quantum critical behavior in this system.

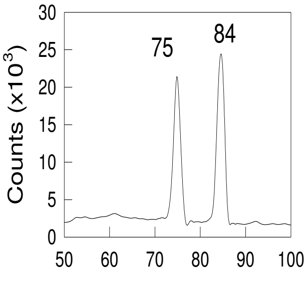

Fig. 1: γ-spectrum 24 hrs after irradiation

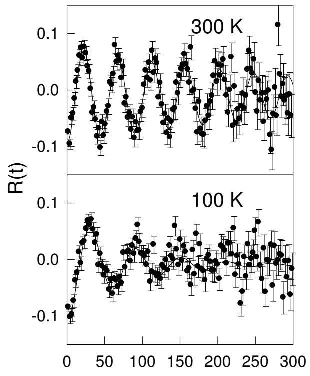

Fig. 2: Spin rotation spectra of ^{100}Rh in Bext = 0.7T

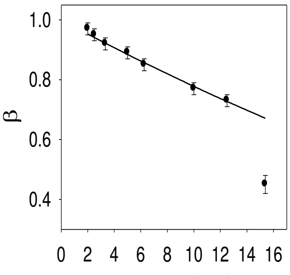

Fig. 3: $\chi_{loc}(T)$ of ^{100}Rh in $Nb_{0.95}Fe_{2.05}$

---

[1] M. Brando et al., Phys. Rev. Lett. **101**, 026401 (2008)
[2] Aftab Alam and D.D. Johnson, Phys. Rev. Lett. **107**, 206401 (2011).

Electronic address: mishra@*tifr.res.in*

P31

Molecular Orientation of Hydrogen bonded Liquid Crystal $(6BA)_2$-$(BPy)_x$ as Studied by ^{2}H NMR

Motohiro Mizuno, Yuiko Higashima, Ayaka Yamashita, Yasuyuki Ishida,
Takuma Oigawa, Ryutaro Ohashi, Tomonori Ida

Department of Chemistry, Graduate School of Natural Science and Technology,
Kanazawa University, Kakuma, Kanazawa, Ishikawa 920-1192, Japan

Hydrogen bonded liquid crystal 4-*n*-hexylbenzoicacid (6BA) forms dimer by hydrogen bonding of the acidic hydrogen and the carbonyl oxygen (Fig. 1) [1,2]. From mixture (2:1 mole ratio) of 6BA and 4,4'-bipyridine (BPy), the hydrogen bonded liquid crystal $(6BA)_2$-$(BPy)_1$, where BPy is incorporated into 6BA dimers (Fig. 1) is prepared [2]. Although 6BA is nematic liquid crystal, $(6BA)_2$-$(BPy)_1$ is smectic liquid crystal. For $(6BA)_2$-$(BPy)_x$, except for x = 1, the type of liquid crystal and the order of molecular orientation in liquid crystal phase are unknown. In the present work, the temperature range of liquid crystal phase and the order of molecular orientation in liquid crystal phase of $(6BA)_2$-$(BPy)_x$ were investigated by ^{2}H NMR and DSC.

For the measurement of DSC, thermal anomalies due to isotropic liquid (IL)-liquid crystal-I (LC-I), liquid crystal-I (LC-I)-liquid crystal-II (LC-II), liquid crystal-II (LC-II)-crystal-I (C-I), crystal-I (C-I)-crystal-II (C-II) transitions were observed at 417, 383, 340, and 317 K on cooling process, respectively.

The temperature dependence of ^{2}H NMR spectrum for $(6BA)_2$-$(BPy)_{0.5}$ was shown in Fig. 2. The quadrupole coupling constant e^2qQ/h and asymmetry parameter η estimated from the line shape of ^{2}H NMR spectrum were 170 kHz and 0.15 at 293 K. The spectra at 349 and 389 K were sharp two peaks which are caused by the orientational order of molecules in liquid crystal phase. The distribution of molecular orientation in LC-II is found to be larger than that in LC-I, since the line width of ^{2}H NMR spectrum in LC-II was broader than that in LC-I. Fig. 3 shows the order parameter in liquid crystal phase which was estimated from the peak splitting width of ^{2}H NMR spectrum. The order parameter of $(6BA)_2$-$(BPy)_{0.5}$ in LC-II decreased critically around LC-II-LC-I phase transition point. Therefore, the large fluctuation of molecular orientation is predicted to exist in LC-I.

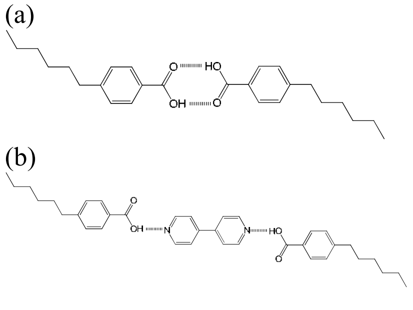

Fig.1 Structures of 6BA (a) and $(6BA)_2$-$(BPy)_1$ (b).

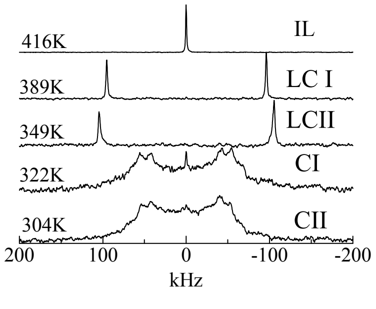

Fig. 2 Temperature dependence of ^{2}H NMR spectrum for $(6BA)_2$-$(BPy)_{0.5}$ on cooling.

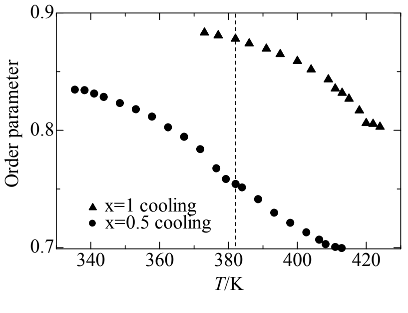

Fig. 3 Temperature dependence of order parameter in liquid crystal phase of $(6BA)_2$-$(BPy)_{0.5}$ and 6BA

---

[1] Y. Suzuki et al., *J. Phys. Chem. Solids* **71**,389 (2010)
[2] T. Kato et al., *Chem. Mater.***5**, 1094 (1993)

Electronic addrtess: *Presenting. mizuno@se.kanazawa-u.ac.jp*

P32

Evaluation of microstructure and chemical composition of low alloy steels for dry storage cask

Bohye Bak[1], Dae-Geun Nam[1*], Kyeongpil Kim[1], Jung Soo Kim[1], Byung Jun Kim[1]
[1] *Korea Institute of Industrial Technology, 618-230 Busan, South Korea*
**Corresponding author: dgnam@kitech.re.kr*

A SF (spent fuel) is a nuclear fuel material after using at the nuclear power plant. It is necessary to restrict the safety management of the SF that still has high levels of radiation and heat for a long period after putting it out from the nuclear reactors. Recently, dry storage method has used to store SF because of a little radioactive waste [1]. A low steel alloy plays an important role in metal casks for dry storage due to excellent mechanical properties, weldability and low price. However, they may suffer embrittlement by high levels of radiation and heat for a long period. Therefore, it is important to improve mechanical properties of low alloy steel for safety use. In this study, low alloy steels with Al and low C elements were fabricated to improve the mechanical properties. Mechanical properties of these steels were evaluated by tensile test, hardness test and Charpy impact test. As a result, the ductile to brittle transition temperature (DBTT) for low carbon steel is shifted to lower temperatures accompanied by the increase of upper shelf energy (USE) in Fig.1. Fracture mode is not dependent of element effects of low alloy steels and fracture surface of all steels was observed cleavage fracture at lower shelf energy (LSE) region. It was found that the reduction of the C content affects the mechanical properties to improve the tensile and Charpy impact properties of low alloy steels. The microstructure was observed using an optical microscope, SEM, EPMA and EBSD.

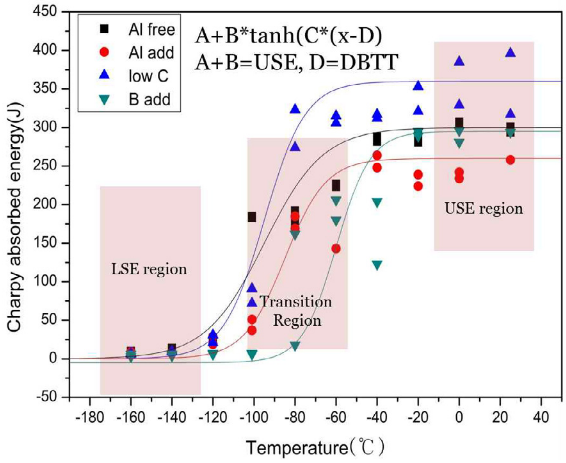

Fig 1. The Charpy impact properties of low alloy steels

[1] K.C. Chen, K. Ting, Y.C. Li, Y.Y. Chen, W.K. Cheng, W.C. Chen, C.T. Liu, A study of the probabilistic risk assessment to the dry storage system of spent nuclear fuel, International Journal of Pressure Vessels and Piping, Vol.87, pp 17-25, 2010.

Electronic addrtess: *dgnam@kitech.re.kr*

P33

Hyperfine interactions in soybean and lupin oxy-leghemoglobins studied using Mössbauer spectroscopy with a high velocity resolution

A. Kumar[1], I.V. Alenkina[2,3], A.P. Zakharova[2,3], M.I. Oshtrakh[2,3], V.A. Semionkin[2,3], S. Kundu[1]

[1]*Department of Biochemistry, University of Delhi South Campus, New Delhi, India;*
[2]*Department of Physical Techniques and Devices for Quality Control and*
[3]*Department of Experimental Physics, Institute of Physics and Technology,*
Ural Federal University, Ekaterinburg, 620002, Russian Federation.

Tetrameric hemoglobins consist of two pairs of non-identical protein subunits, mainly α- and β-subunits with similar tertiary structure but having different amino acid composition. Each protein subunit contains heme, an Fe(II)-porphyrin complex which reversibly binds oxygen molecule. In contrast, monomeric hemoglobins are similar to α-subunit of tetrameric hemoglobin. Monomeric plant hemoglobins (leghemoglobins) bind oxygen molecule with higher affinity than tetrameric hemoglobins and it is required to protect the nitrogenase enzyme complex from oxygen toxicity during the process of nitrogen fixation. Tetrameric hemoglobins with different molecular structure demonstrate different oxygen affinity related in part to the features of the heme iron electronic structure and stereochemistry. Similarly, different leghemoglobins demonstrate variations in oxygen affinity and heme iron stereochemistry.

In this work we present the first results of comparative study of the ^{57}Fe hyperfine interactions in two leghemoglobins: soybean (Lba) and lupin (LbI) using Mössbauer spectroscopy with a high velocity resolution. Mössbauer spectra of Lba and LbI in the oxy-form were measured at 90 K and fitted in two ways using one and superposition of two quadrupole doublets to reach better fits. Small variations in the hyperfine parameters revealed from the first fits for the Lba and LbI Mössbauer spectra are shown in Fig. 1. The differences in the hyperfine parameters obtained from both fits were analyzed in relation to the heme iron stereochemistry in monomeric leghemoglobins and compared with results obtained for α-subunits in some tetrameric oxyhemoglobins.

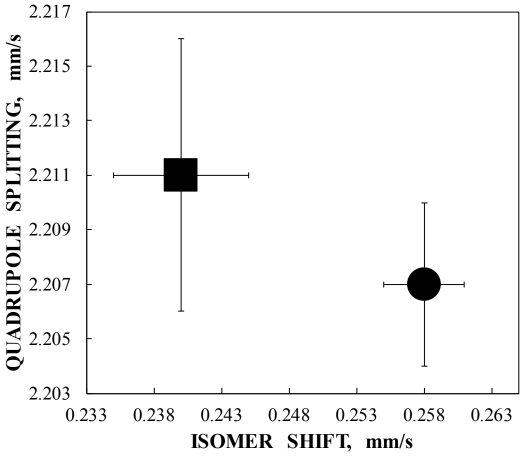

Fig. 1. Hyperfine parameters for soybean (●) and lupin (■) leghemoglobins in the oxy-form obtained from one quadrupole doublet fits of their Mössbauer spectra measured at 90 K.

Electronic address: *oshtrakh@gmail.com*

P34

A ^{57}Fe Mössbauer study of Magnetocaloric $Mn_{1-x}Fe_xCoGe$

Q. Y. Ren,[1] **W. D. Hutchison**,[1] **J. L. Wang**,[2,3] **J. M. Cadogan**[1] **and S. J. Campbell**[1]

[1]School of Physical, Environmental and Mathematical Sciences,
The University of New South Wales, Canberra, ACT 2600, Australia *
[2]Institute for Superconductivity and Electronic Materials,
University of Wollongong, Wollongong, NSW 2522, Australia
[3]Bragg Institute, Australian Nuclear Science and Technology Organisation,
Lucas Heights, NSW 2234, Australia

Materials exhibiting a large magnetocaloric effect are of interest due to their potential application as a substitute for conventional gas-compression refrigeration. Such a giant magnetocaloric effect is often associated with materials showing a magneto-structural transition. In these cases, application of an external magnetic field can induce a large change in both the magnetic and lattice entropies simultaneously [1].

MnCoGe-based compounds are intermetallics in which a magneto-structural transition can be easily obtained. Two stable phases can exist in these alloys: the nominally low-temperature orthorhombic TiNiSi-type structure, with space group *Pnma* and a ferromagnetic transition temperature T_C^{orth} ~ 345 K, and the nominally high-temperature hexagonal Ni_2In-type structure, with space group $P6_3/mmc$ and a ferromagnetic transition temperature T_C^{hex} ~ 275 K [2]. The martensitic transition temperature T_{str} from the hexagonal phase to the orthorhombic phase can be 'tuned' into the temperature range 275-345 K, resulting in a magneto-structural transition from a paramagnetic hexagonal phase to a ferromagnetic orthorhombic phase. A large magnetocaloric effect is therefore expected [3].

Substitution of Fe for Mn or Co is an effective way to achieve a magneto-structural transition as confirmed recently by neutron diffraction studies [4]. However, the exact assignments of magnetic moments at the Mn and Co sites, as well as the location of the dopant Fe, are difficult to resolve from the diffraction studies alone. ^{57}Fe Mössbauer spectroscopy, on the other hand, has the potential to reveal additional information about the local environments at both lattice sites and in this paper we present our analysis of such a study on $Mn_{1-x}Fe_xCoGe$.

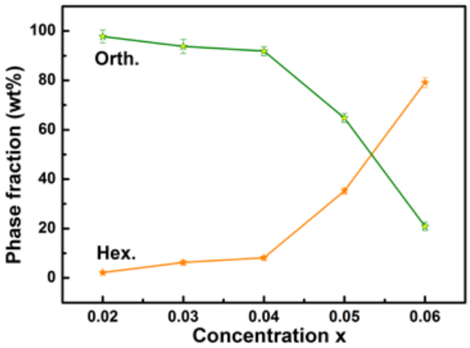

Fig. 1 The phase fraction changes (weight percentage) with increasing Fe dopant for the orthorhombic and hexagonal phases of $Mn_{1-x}Fe_xCoGe$ (0.5 wt% ^{57}Fe).

[1] J. Liu, T. Gottschall, K.P. Skokov, J.D. Moore and O. Gutfleisch, *Nat. Mater.* **11,** 620 (2012)
[2] V. Johnson, *Inorg. Chem.* **14,** 1117(1975)
[3] E.K. Liu, W. Zhu, L. Feng, J.L. Chen, W.H. Wang, G.H. Wu, H.Y. Liu, F.B. Meng, H.Z. Luo and Y.X. Li, *Europhys. Lett.* **91,** 17003 (2010)
[4] Q.Y. Ren, W.D. Hutchison, J.L. Wang, S. Muñoz-Pérez, J.M. Cadogan and S.J. Campbell, *phys. status solidi (a)* **211,** 1101 (2014)

*Electronic address: Qingyong.Ren@student.adfa.edu.au

P35

Hyperfine Interactions of Sc Impurities in Sapphire

G. N. Darriba[1] and M. Rentería[1]

[1]*Departamento de Física and Instituto de Física La Plata (IFLP, CONICET La Plata), Facultad de Ciencias Exactas, Universidad Nacional de La Plata, CC 67, 1900 La Plata, Argentina.**

In this work we present a theoretical study of structural, electronic, and hyperfine properties of α-Al_2O_3 semiconductor doped with Sc impurities using *ab initio* Density Functional Theory calculations. In recent years, we have performed similar studies in α-Al_2O_3 using acceptor or donor impurities, such as Cd and Ta atoms, respectively [1, 2]. These *ab initio* calculations were compared with Time-Differential γ-γ Perturbed Angular Correlation (PAC) experiments using (^{111}In→)^{111}Cd and (^{181}Hf→)^{181}Ta nuclides as PAC probes. On the other hand, ^{44}Sc can be used as a non-standard PAC probe using the ^{44}Ti→^{44}Sc decay. In this way, it is interesting to obtain a reliable structural, electronic, and hyperfine theoretical characterization of Sc-doped α-Al_2O_3 that could be compared with experimental results of ^{44}Sc PAC experiments, now in progress. The *ab initio* calculations were performed with the Full-Potential Augmented Plane Wave plus Local Orbitals (FP-APW+lo) method using the Wien2K code. We studied different Sc concentrations in order to simulate the isolated impurity condition ^{44}Sc has in PAC experiments. Sc is an isovalent impurity when it replaces the Al atom, nevertheless we performed calculations for different charge states of the impurity. We demonstrate that no magnetic interaction is present at Sc site and therefore a pure quadrupole hyperfine interaction is predicted. The electronic structures and the electric-field gradient are also compared with those obtained for acceptor and donor impurities in α-Al_2O_3.

[1] G.N. Darriba et al., *Physical Review B* **86,** 075203 (2012).

[2] G.N. Darriba et al., contribution to the 29th ICPS - International Conference on the Physics of Semiconductors, Rio de Janeiro, Brasil, 27 July-1 August, 2008.

---

*Electronic address: *renteria@fisica.unlp.edu.ar*

P36

A Mössbauer Spectroscopy Investigation of Orthorhombic Phase $YbMnO_3$

G. A. Stewart[1], H. A. Salama[1], C. J. Voyer[2], D. H. Ryan[2],
D. Scott[3], H. St.C. O'Neill[3]

[1] *School of Physical, Environmental and Mathematical Sciences, The University of New South Wales,*
Australian Defence Force Academy, Canberra, ACT BC 2610, Australia ✶
[2] *Centre for the Physics of Materials and Department of Physics, McGill University,*
Montreal H3A 2T8, Canada
[2] *Research School of Earth Sciences, The Australian National University,*
Canberra, ACT 0200, Australia

Metastable orthorhombic $YbMnO_3$ is interesting because of interactions observed between its magnetic and electric phases. Its Mn sub-lattice orders incommensurately at $T_N = 43$ K and commensurately at $T_N' \approx 35$ K. In this work, Mössbauer spectroscopy has been employed to probe the local magnetisation in both the Mn (doped with 0.5 % 57Fe) and Yb sub-lattices. The ^{57}Fe measurements reveal that a remnant paramagnetic component persists to well below T_N. There is also an indication of thermal magnetic hysteresis near T_N', which supports recent reports of hysteresis for the dielectric constant [1]. The orientation of the hyperfine field is consistent with the proposed low temperature E-type structure where Mn moments are aligned with the a-axis (Pnma notation). Based on recent susceptibility measurements for a single crystal specimen [2], it was proposed that the Yb sub-lattice orders in it own right at $T_{Yb} =$ 4 K. However, this is not supported by the ^{170}Yb-Mössbauer spectra, which exhibit pure quadrupole splitting down to 1.8 K. There is, nevertheless, a slight increase in line broadening with decreasing temperature, which is probably due to a weak magnetic exchange field arising out of the ordered Mn sub-lattice. The small variation in the quadrupole interaction strength requires that the Yb^{3+} electronic ground state is a well-isolated Kramers doublet.

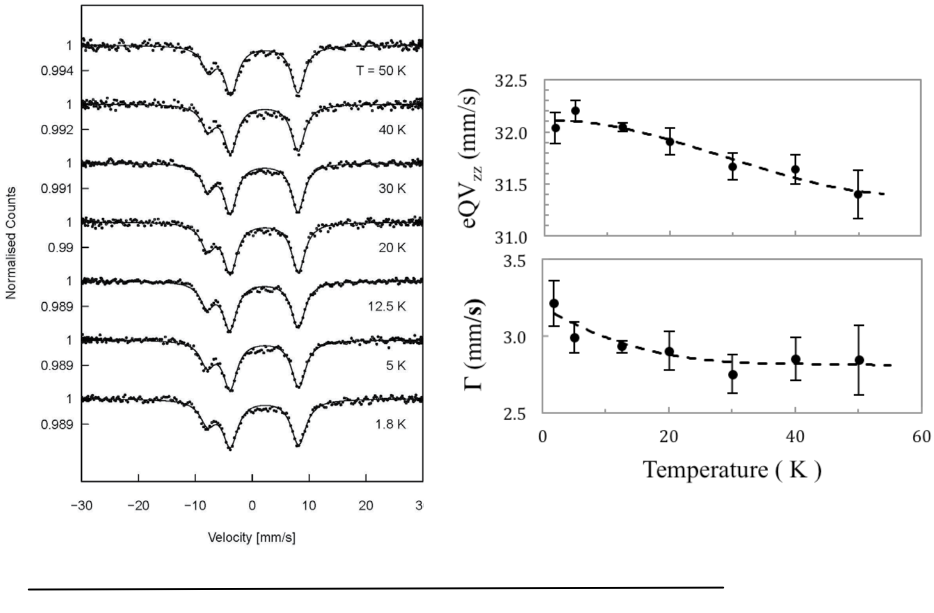

Fig. 1.
(a) ^{170}Yb-Mössbauer spectra, and
(b) fitted quadrupole interaction strength, eQV_{zz}, and line width, Γ, as a function of temperature.

[1] J.W. Wang *et al.*, *J. Appl. Phys.* **111**, 114103 (2012).
[2] Y. H. Huang *et.al.*,Chem. Mater. 18, 2130 (2006)

Electronic address: *g.stewart@adfa.edu.au*

P37

Rotation, pairing and blocking in high-K isomers explored through the rotational g-factor.

Blank line (12 points)

N.J.Stone[1]

Blank line (12 points)

[1] *Dept. of Physics and Astronomy, University of Tennessee, Knoxville TN 37996, USA*

Blank line (12 points)

Systematic analysis of experimental data on bands built on multi-quasi-particle high-K isomers in the elements Lu – Re has revealed a striking dependence of the ‘collective’ g_R parameter upon the quasi-particle make-up of the band head. This dependence is thought to be founded upon blocking of the pairing interaction in these isomers and consequent changes in the moment of inertia. Existing model calculations do not describe the observed variation of g_R well.

Ideas relating to superfluidity of the paired nucleons, and its modification through specific quasi-particle excitation, present properties of general physics interest not accessible to study in other systems such as liquid helium and electrons in metals.

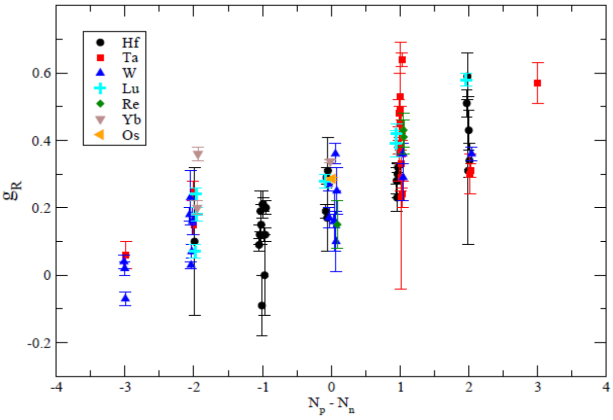

Fig. 1 Collective g-factor g_R vs difference in proton and neutron quasi-particle number.

---

[1] N.J.Stone et al., *Physics Letters* **B 726**, 675 (2013).

Electronic address: *N.Stone@physics.ox.ac.uk*

P39

Palladium-defect complexes in diamond and silicon carbide: DFT and ^{100}Pd($\rightarrow$^{100}Rh) TDPAC

A. A. Abiona[1,*], W. Kemp[1], H. Timmers[1], K. Bharuth-Ram[2]

[1] *School of Physical, Environmental and Mathematical Sciences,*
The University of New South Wales, UNSW Canberra, PO Box 7916, Canberra BC 2610, Australia
[2]*Physics Department, Durban University of Technology, Durban 4000, South Africa*

Time Differential Perturbed Angular Correlations (TDPAC) studies, supported by Density Functional Theory (DFT) modeling, have shown that palladium atoms in silicon and germanium pair with vacancies [1, 2]. Building on these results, here we present DFT predictions and some early, tentative TDPAC results on the defect integration of palladium atoms in diamond and silicon carbide host lattices.

For both, diamond and silicon carbide, the DFT calculations predict that a split-vacancy V-Pd_{BI}-V complex is favoured, with the palladium atom on a bond-centred interstitial site having a nearest-neighbour semi-vacancy on either side. Consistent with experimental results, this configuration is also assigned to palladium complexes in silicon and germanium [3, 4].

For silicon carbide the DFT modeling predicts furthermore that a palladium atom, replacing a carbon atom on a bond-centred interstitial site and pairing with a silicon vacancy is more stable than a palladium atom replacing a silicon atom on a bond-centred interstitial site pairing with a silicon vacancy. These two alternatives differ by 8.94 eV. The favourable pairing with a silicon vacancy is also supported by TRIM Monte Carlo calculations, which predict that there are more silicon vacancies than carbon vacancies following heavy ion implantation.

In order to test the modeling, the ^{100}Pd($\rightarrow$^{100}Rh) probe was synthesized via the heavy ion fusion evaporation reaction ^{92}Zr(^{12}C,4n)^{100}Pd and introduced into the host materials by recoil implantation [5]. TDPAC has shown that even after annealing at 900 °C the probe does not form a unique defect complex. This would suggest that the predicted split-vacancy complex is just one of many possible configurations. Further studies may take advantage of a new implantation technique [6] that suppresses the co-implantation of beam particles, so that the implantation damage of the host is reduced and lattice recovery by annealing is improved.

References

[1] D.A. Brett *et al*., *Phys. Rev. B* **72**, 193202 (2005).
[2] A. A. Abiona, W. Kemp and H. Timmers, *Hyperfine Interact.* **221**, 65-72 (2013).
[3] A. A. Abiona, W. Kemp and H. Timmers, *International Conference on Defects in Semiconductors 2013, Bologna, Italy, AIP Conf. Proc.***1583**, 105 (2014).
[4] A. A. Abiona, W. Kemp and H. Timmers, this conference Book of Abstracts.
[5] E. Bezakova, Ph.D. thesis, Australian National University, Canberra (1998).
[6] A. A. Abiona et al., *Heavy Ion Accelerator Symposium on Fundamental and Applied Science* 2012, Canberra, Australia, EPJ Web of Conf. **35** (2012).

Email address: *adurafimihan.abiona@gmail.com*

P41

CEMS search for magnetic cluster formation in Co/Fe implanted ZnO

Krish Bharuth-Ram

Theoretical predictions of room temperature ferromagnetism[1] (RTFM) in ZnO doped with 5 at. % Mn ions has driven the quest for experimental realisation of RTFM in wide band-gap semiconductors doped with transition metal (TM) ions. In the case of Co implanted ZnO, magnetic nanocluster formation has been reported in single crystals implanted with 5 at. % Co at 253 K and annealed at 823K [2, 3] and in Sn-doped ZnO implanted with 3-5 at.% Co [4].

To contribute to this quest we have undertaken conversion electron Mössbauer spectroscopy (CEMS) studies on ZnO implanted with 145 keV and 345 keV ^{59}Co ions followed by implantation of 60 keV Mössbauer probe ^{57}Fe ions. The implantation fluences were adjusted to yield a ‘box’ shaped implantation profile (Fig.1) and a TM ion concentration of ~2.5 at. %, thus keeping lattice damage and formation of secondary phases relatively low.

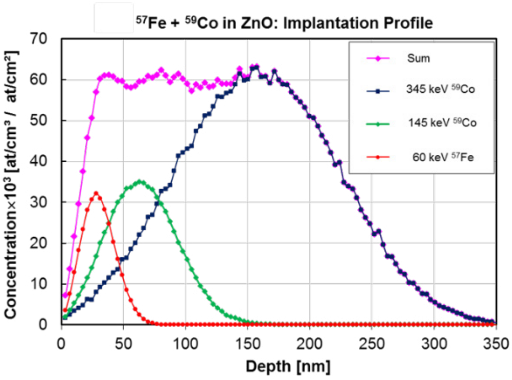

Fig 1: Implantation profile for ^{57}Fe and ^{59}Co in ZnO

CEMS measurements were perfomed on the as-implanted sample and again after annealing for 30 minutes in vacuum at 773 K and 973 K. The spectra, presented in Fig 2, show a significant change after annealing at 973K, with components due to Fe^{2+}, on Zn sites and implantation induced damage, converting to doublets with parameters characteristic of Fe^{3+}. VSM measurements on the 973 K annealed samples show ferromagnetic behaviour at 4 K, but with a very low coercive field, indicating the formation of nanoclusters of sizes below the superparamagnetic limit.

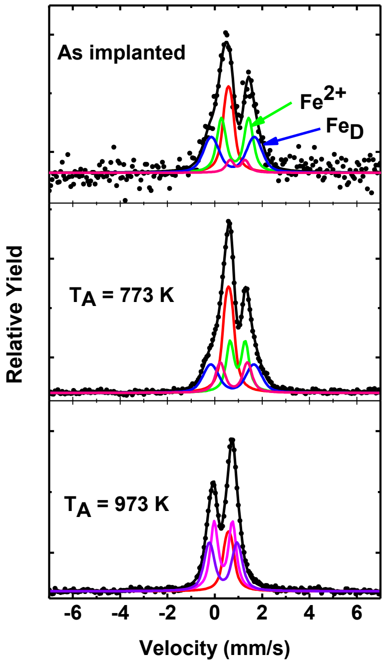

Fig. 2 CEMS spectra of Co/Fe implanted ZnO after annealing at temperatures indicated.

Acknowledgements

This project was undertaken within the DFG (Germany)-NRF (South Africa) bi-lateral research collaboration.

References

[1] Dietl, T. et al.: *Science*, **287** (2000) 1019.
[2] Zhou, S. et al.: *J. Phys. D: Appl. Phys.*, **40** (2007) 964
[3] Potzger, K., et al., *J.Appl. Phys.* 104(2008) 023510
[4] Norton, D.P., et al., *Appl. Phys. Lett.* 83 (2003) 5488

P42

Effect of cesium loading on the phase transformation of iron in iron phosphate in the oxidative dehydrogenation reactions

Blank line (12 points)

Faiza B. Khan[1], Venkata D. B. C. Dasireddy[1], K. Bharuth-Ram[1,2], H. Masenda[3] and H. B. Friedrich[1]

Blank line (12 points)

[1]School of Chemistry and Physics, University of KwaZulu-Natal, Durban, South Africa.
[2]Durban University of Technology, Durban 4000, South Africa
[3]School of Physics, University of the Witwatersrand, Johannesburg 2050, South Africa.

Blank line (12 points)

The use of promoters for $FePO_4$ catalysts has been studied for oxidative dehydrogenation (ODH) reactions involving the conversion of isobutyric acid (IBA) to methyl methacrylate (MAA) [1]. Although it was concluded that different promoters showed the most promising results, it was also reported that ODH catalysts containing alkaline elements, such as K, Rb and Cs, showed enhanced selectivities and activities. Based on these findings it was decided to synthesize a promoted $FePO_4$ catalyst for the ODH of ethyl isobutrate (EIB) to ethyl methacrylate (EMA) with the following ratios, P/Fe/Cs ~ 1.2-1.3/1/0.05-0.30, in increments of 0.05 for the cesium ions [2] . Previous reports stimulated the use of iron oxide and iron phosphate materials in the oxidative dehydrogenation of IBA to MAA [3].

Iron phosphate catalysts and cesium promoted iron phosphate catalysts were prepared using ammonia gel method illustrated in [1, 3]. The prepared catalysts were characterized by room temperature X-ray diffraction (XRD), Raman spectroscopy, and Scanning Electron Microscopy. Mössbauer spectroscopy was used to determine the phase of the iron in both catalysts, before and after the reaction conditions. The spectral parameters of the prepared iron phosphate catalyst confirm the occurrence of the $FePO_4$ tridymite-like phase which has 100 % Fe^{3+} species and is in agreement with the experimental route used [3]. Although the tridymite-like $FePO_4$ phase was the dominant phase based on the results obtained from XRD data, minor peaks were also observed. It was therefore decided to correlate the results from XRD with those obtained from Mössbauer spectroscopy for each of the cesium promoted catalysts. The isomer shift and quadrupolar splitting values obtained for the cesium promoted $FePO_4$ catalysts showed the existence of both the tridymite-like $FePO_4$ phase as well as the quartz type $FePO_4$ phase. Formation of the $CsFeP_2O_7$ phase was also observed, showing the highest concentration for the lowest cesium loading, which was also attributed to the lower P/Fe ratio. The slightly higher P/Fe ratio relative to the unpromoted $FePO_4$ catalyst resulted in the mixture of phases being formed, with the addition of an unidentified phase.

---

[1] M. Ai, *Catalysis Today* **52**, 65 (1999).
[2] M. Ai, et al., *Journal of Molecular Catalysis A: Chemical* **159**, 19 (2000).
[3] F.B. Khan, et al., *Hyperfine Interactions* **197**, 317 (2010).

Electronic address: *Dasireddy@ukzn.ac.za,Faiza.khan@sasol.com*

P43

^{57}Fe Mössbauer and Magnetic Studies of $Nd_3Fe_{24.5}Cr_{4.5}$

J.L. Wang[1,2], M.F. Md Din[1], S.J. Campbell[3,*], S.J. Kennedy[2], F.M. Yang[4], G.H. Wu[4] and S.X. Dou[1]

[1]Institute for Superconductivity and Electronic Materials, University of Wollongong, Wollongong, NSW 2522, Australia
[2] Bragg Institute, ANSTO, Lucas Heights, NSW 2234, Australia
[3]School of Physical, Environmental and Mathematical Sciences, The University of New South Wales, Canberra, ACT 2600, Australia
[4]Institute of Physics, Chinese Academy of Science, Beijing 100190, P. R. China

The structural and magnetic properties of the rare earth transition metal compound $Nd_3Fe_{24.5}Cr_{4.5}$ have been investigated by variable temperature high resolution x-ray diffraction at the Australian Synchrotron together with DC magnetization and ^{57}Fe Mössbauer effect measurements. The magnetic ordering temperature has been found to be $T_C = 423(5)$ K with spin reorientation detected below room temperature around $T_{sr} = 158(5)$ K.

Rietveld refinements indicate that $Nd_3Fe_{24.5}Cr_{4.5}$ crystallizes in the $Nd_3(Fe,Ti)_{29}$-type structure with the A2/m space group [1] and a substantial magneto-volume effect [2] is detected around T_C. As shown in Figure 1 the main features of the variable temperature Mössbauer spectra can be reproduced using five sub-spectra [3]. The temperature dependence of the average hyperfine field has been analysed in terms of different power laws of the reduced temperature [4]. The Debye temperature of $Nd_3Fe_{24.5}Cr_{4.5}$ has been determined as $\theta_D = 400\ (\pm 30)$ K from a fit to the variable temperature isomer shift IS(T).

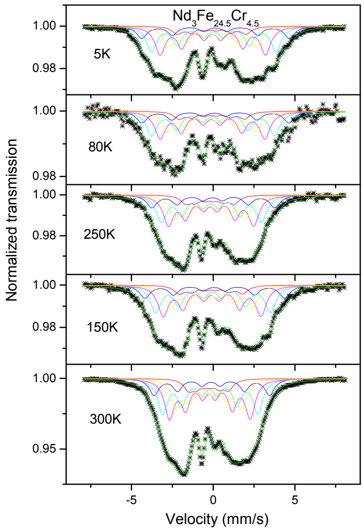

Figure 1 Mössbauer spectra of $Nd_3Fe_{24.5}Cr_{4.5}$ at selected temperatures fitted using five sub-spectra.

1] W.B. Yelon, H. Luo, M. Chen and F.P. Missell, J. Appl. Phys. **85,** 5693 (1999)
[2] J.L. Wang, C. Marquina, M.R. Ibarra, W.Q. Wang, F.M. Yang, G.H. Wu, O. Tegus, J.C.P. Klaasse, E. Brück and F.R. de Boer, J. Appl. Phys. **93,** 6924 (2003)
[3] X.F. Han, H.G. Pan, H.L. Liu, F.M. Yang and Y.W. Zheng, Physical Review B **56,** 8867 (1997).
[4] M. Venkatesan, U. V. Varadaraju, and K. V. S. Rama Rao, Phys. Rev. B **64**, 094427 (2001).

**Stewart.Campbell@adfa.edu.au*

P44

Study of effect of silicon doping in HfO_2 with perturbed angular correlation spectroscopy

Fabio Henrique de Moraes Cavalcante, Luciano Fabrício Dias Pereira, Brianna Bosch dos Santos, Rajendra Narain Saxena, Artur Wilson Carbonari

Instituto de Pesquisas Energéticas e Nucleares, IPEN, University of São Paulo, USP, Av. Prof. Lineu Prestes, 2242, São Paulo, SP, 05508-000, Brazil

In the present work, the time differential perturbed angular correlation (PAC) spectroscopy was used to study the effect of doping with 5% Si in HfO_2 bulk samples, where the presence of hafnium allows the possibility of using ^{181}Ta as a probe nucleus. The PAC method[1] is based on the hyperfine interaction of nuclear moments of the probe with extra nuclear magnetic fields or electric field gradients (EFGs). In the case of quadrupolar electric interaction, the experimental measurement gives the quadrupolar frequency ν_Q with respective distribution δ as well as the asymmetry parameter η of EFG. The γ-γ cascade of (133-482) keV, populated in the β^- decay of ^{181}Hf, was used to measure the quadrupole interaction of the 482 keV ($5/2^+$) state of ^{181}Ta, with an anisotropy coefficient A_{22}=-0.288. The γ-γ PAC measurements were carried out using a standard set up with four conical BaF_2 detector scintillators with a time resolution of 0.6 ns (FWHM). Results of previous PAC measurements in HfO_2 can be found in the literature [2, 3]. In the case of the 5 % silicon, our preliminary results indicate that dopants can induces dislocation of Hf throughout the lattice causing effects that decrease around 10 % the electric field gradient and the dielectric constant in HfO_2.

[1] G. Schatz and A. Weidenger, *Nuclear Condensed Matter Physics*, (Chichester: John Wiely \& Sons) 1996.
[2] A. Ayala, R. Alonso, and A. López García, *Phys. Rev. B*, " Temperature dependence of the hyperfine electric field gradient tensor at ^{181}Ta in HfO_2"vol. 50, p. 3547, 1994.
[3] M. Forker, P. de la Presa, W. Hoffbauer, S. Schlabach, M. Bruns, and D.V. Szabó, *Phys. Rev. B*, 77, 054108, 2008.

P45

First principles calculations of the Cd and Fe co-doped In_2O_3: a study of differences between two cation sites.

J. Mestnik-Filho, L.F.D. Pereira, Messias S. Costa, Emiliano L. Muñoz, Cleidilane O. Sena, A.W. Carbonari
Instituto de Pesquisas Energéticas e Nucleares, São Paulo, Brasil

Although several experimental and theoretical works about In_2O_3 doped with transition metals have been published since Dietl reported room temperature ferromagnetism in semiconductor oxide doped with transition metal[1], very few of them have reported results analyzing the effects of occupancy of the two possible nonequivalent cation sites (C and D) in In_2O_3 by transition metal (TM) impurities. In general, theoretical works only perform simulations for TM at sites D (which is axially symmetric) and most of magnetic experimental techniques only observed the whole sample and are not able to differentiate the preference of site occupancy by TM impurities. However recently studies using hyperfine interactions techniques (Mossbauer and Perturbed Angular Correlation spectroscopies) for Fe-doped In_2O_3, Yang [2] and Sena [3] showed that Fe ions prefer a specific site and this preference is fundamental for occurrence of ferromagnetism at room temperature. Consequently, a theoretical investigation on Fe at each sites of In_2O_3 is important to understand a possible magnetism. In this work first principles calculations using APW+lo was employed to study electronic structure and hyperfine interactions of Cd and Fe co-doped In_2O_3 systems in which Fe replaced In at each of two nonequivalent sites in individual simulations. The local correlation for Fe was treated by Hubbard model.

[1] T. Dietl, H. Ohno, F. Matsukura, J. Cibert, D. Ferrand, Science, 287, 1019, 2000 .
[2] S. Yan, W. Qiao, W. Zhong, C.-T. Au, Y. Dou, Appl, Phys. Letters, 104, 062404, 2014
[3] C. Sena, M.S. Costa, E.L. Muñoz, G.A. Cabrera-Pasca, L.F.D. Pereira, J. Mestnik-Filho, A.W. Carbonari,J.A.H. Coaquira, unpublished.

P46

Study of hyperfine interactions of Gd-doped Fe_3O_4 nanoparticles by Perturbed Gamma-Gamma Angular Correlations

Sarah D. P. Huet, Jacqueline S. Barreira, Caio Salutte, Brianna Bosch-Santos, Artur W. Carbonari

Instituto de Pesquisas Energéticas e Nucleares, Universidade de São Paulo, Av. Professor
LineuPrestes 2242, São Paulo, SP, 05508-000

In this work, nanoparticles of Fe_3O_4 doped with Gdwere investigated by PAC spectroscopy using ^{111}Cd as probe nuclei. Gd-doped Fe_3O_4 magnetic nanoparticles, which have manyapplications inbiomedicaldiagnosticsandtherapy were prepared by co-precipitation method and ^{111}In (^{111}Cd) was added to the samples by annealing of the pellet samples at 900°C. Similar samples were prepared without radioactive ^{111}In to be characterized by X-ray diffraction (XRD), Dynamic Light Scattering (DLS) and X-ray fluorescence spectrometry (XRFS). XRD results were analyzed by Rietveld method and show that samples crystallized in the Fe3O4 structure single phase. XRFS results showed that Gd-doped Fe_3O_4 samples are homogeneously doped with 4,4% of Gd. DLS results showed nanoparticles size, which is around 86 nanometers. PAC results showed that ^{111}Cd nuclei substitutes Fe.

Keywords: Perturbed Angular Correlation, nanoparticles.

PAC spectroscopy is based on the angular correlation between nuclear radiations emitted by radioactive probe nuclei, which is a well established method in nuclear spectroscopy.Perturbation occurs in this correlation by electromagnetic interactions external to the nucleus when it is inserted in a material, which can provide information on the electronic distribution of the neighborhood.

P47

The Study of hyperfine interactions on Hydroxyapatite Compounds, by Gamma Spectroscopy Perturbed Angular Correlation - PAC

Osmar Leite[1,4] F. H. M. Cavalcante[1,2] , A.W. Carbonari[2], J. T. Cavalcante[1], H. Saitovitch[1], and Ralph Santos-Oliveira[3]

[1]Centro Brasileiro de Pesquisas Físicas – CBPF/MCTI; Rio de Janeiro, Brasil
[2]Instituto de Pesquisas Energeticas e Nucleares – IPEN/CNEN; São Paulo-SP, Brasil
[3]Laboratory of Nanoradiopharmaceuticals – Brazil
[4]Instituto de Engenharia Nuclear – IEN/CNEN; Rio de Janeiro, Brasil

The use of nanoparticles in current medicine are under intense investigation. The possible advantages proposed by these systems are very impressive and the results may be quite schemer. In this scenario, the association of nanoparticles with radioactive materials (radionuclide) may be the most important step since the discovery of radioactive for nuclear medicine and radiopharmacy, especially for cancer targeting and therapy. The hyperfine interaction at ^{111}Cd probe nucleus in hydroxyapatite compounds has been investigated by perturbed angular correlation (PAC) spectroscopy at room temperature for samples prepared at temperatures of 90°C, 35°C and doped with Ho, for both thermalized and non thermalized samples. The thermalized samples were heated to T= 1273 K for 6 h. In order to add ^{111}In/^{111}Cd PAC probes to the structure of the material, samples of hydroxyapatite were sealed in evacuated quartz tubes along with the radioactive ^{111}In/^{111}Cd and heated at 1073 K for 12 h. In not thermalized samples, the PAC spectra indicate a distribution of frequency, but in the thermalized samples, the PAC spectra show the presence of β-tri calcium phosphate in the structure of this kind of Hydroxyapatites.

Electronic address: carbonar@ipen.br

P50

Knight-shift and spin-lattice relaxation of implanted ^{8}Li in the near-surface region of the strongly-correlated metal oxides Sr_2RuO_4 and $LaNiO_3$

D. L Cortie[1,2] , **G. Morris[3], Y. Maeno[4], A.V. Boris, E. Benckiser[5], G. Christiani[5], B. Keimer[5], R. Kiefl[2] ,W. A. MacFarlane[1,6]**

[1] *Quantum Matter Institute, University of British Columbia, Vancouver, BC, V6T 1Z1, Canada Columbia*
[2] *Department of Physics and Astronomy, University of British Columbia, 6224 Agricultural Road, Vancouver, BC V6T 1Z1, Canada*
[3] *TRIUMF, 4004 Wesbrook Mall, Vancouver, BC V6T 2A3, Canada*
[4] *Quantum Materials Lab, Department of Physics, Kyoto University, Kyoto 606-8502, Japan*
[5] *Max-Planck-Institut für Festkörperforschung, Heisenbergstraße 1, 70569 Stuttgart, Germany*
[6] *Chemistry Department, University of British Columbia, Vancouver, BC, V6T 1Z1, Canada*

Conventional nuclear magnetic resonance is a valuable diagnostic tool for characterizing phenomena such as exotic metallic states or high-temperature superconductivity in strongly-correlated oxides by exploiting the hyperfine coupling present in the electron-nuclear Hamiltonian. β-NMR is a variant of NMR that uses an implanted spin-polarized radioactive probe such as ^{8}Li to perform studies of interfaces and near-surface regions in thin films or crystals. Here we present β-NMR data for ^{8}Li implanted at surface depths of 1 – 200 nm in correlated oxides Sr_2RuO_4 and $LaNiO_3$. In Sr_2RuO_4 crystals, we find a quadrupole resonance consistent with a well localized non-cubic ^{8}Li site. Both the Knight-shift and the spin-lattice relaxation rate are strongly temperature dependent. This is explained via the hyperfine coupling to the anisotropic 2D-Fermi liquid transition in Sr_2RuO_4 concurrent with the increased strength of incommensurate spin fluctuations known from inelastic neutron spectroscopy. In $LaNiO_3$ thin films we report on a single dipolar-broadened resonance line and nuclear spin lattice relaxation rate at 300 K.

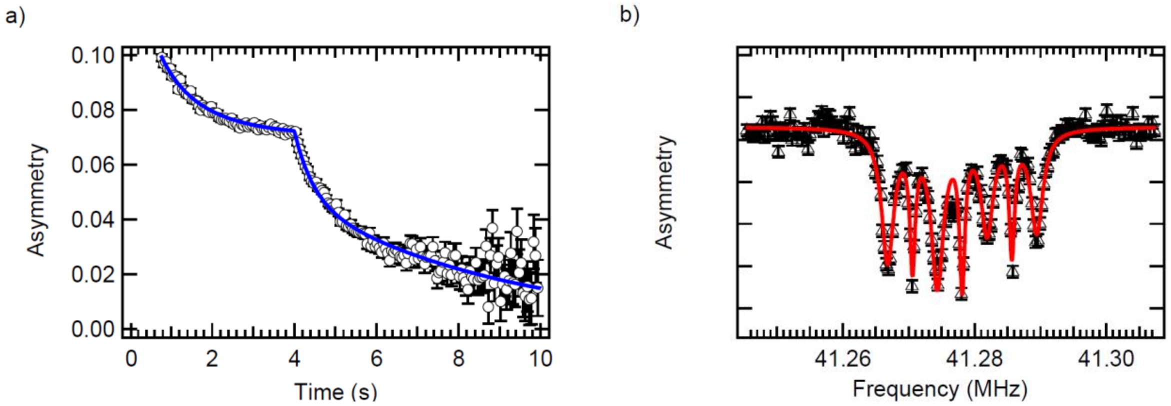

Fig. 1. a) Nuclear spin lattice relaxation rate for ^{8}Li spins injected with a 4s pulse into a $LaNiO_3$ thin film at 300 K. b) Quadrupole resonance of ^{8}Li in Sr_2RuO_4 crystal at 300 K under an applied field of 6.55 Tesla. Solid lines are fits to the data.

Electronic address: *cortie@phas.ubc.ca*

P51

The 245 keV level of ^{111}Cd: nuclear quadrupole moment and its error bar

Leo Errico,[1,2] Kurt Lejaeghere,[3] Jorge Runco,[1] Mario Rentería,[1] and Stefaan Cottenier[3,4]

[1] Departamento de Física, Instituto de Física La Plata (IFLP,
CCT-La Plata, CONICET-UNLP), Facultad de Ciencias Exactas,
Universidad Nacional de La Plata, Casilla de Correo 67, 1900 La Plata, Argentina
[2] Universidad Nacional del Noroeste de la Pcia de Buenos Aires (UNNOBA),
Monteagudo 2772, Pergamino, CP 2700, Buenos Aires, Argentina
[3] Center for Molecular Modeling, Ghent University,
Technologiepark 903, BE-9052 Zwijnaarde, Belgium
[4] Department for Materials Science and Engineering, Ghent University,
Technologiepark 903, BE-9052 Zwijnaarde, Belgium[*]

It hardly needs justification that the 245 keV level of ^{111}Cd is an important one for hyperfine interaction studies, given the prominent role of ^{111}Cd as a TDPAC probe nucleus. This makes the (re)assessment of the nuclear quadrupole moment of this level a recurrent topic at the recent editions of the HFI/NQI conferences. Nobody really challenges the experimental value of 0.83(13) b obtained by Herzog et al. back in 1980[1]. Since that time, the scene has changed and a comparison between Density Functional Theory based electric-field gradients and experimental quadrupole interaction frequencies has become the method of choice for the determination of quadrupole moments of isotopes that are relevant for hyperfine interaction methods (e.g. [2, 3]). This culminated in the value of 0.765(15) b for ^{111}Cd, presented by Haas and Correia [4] at the 2012 HFI/NQI conference.

A new trend in applied Density Functional Theory, is assessing in a quantitative way the error bar on predicted values (e.g. [5, 6]). In the present contribution we do not only try to achieve a numerically completely converged value for the ^{111}Cd quadrupole moment, we also aim at determining the error bar on this value. This is done by calculating the electric-field gradient at a Cd nucleus in 7 elemental solids (In, Sn, Hg, Sb, Cd, Zn, Ga) with extreme settings for numerical accuracy. For these solids, accurate experimental quadrupole interaction frequencies and lattice parameters are known at low temperature. Analyzing these two data sets with a proper statistical formalism, leads to (1) a 'new' prediction for the ^{111}Cd quadrupole moment (which is in good agreement with previous values), and – more importantly – (2) a statistically justified error bar on this quadrupole moment.

[1] P. Herzog, K. Freitag, M. Reuschenbach, H. Walitzki, Z. Phys. A 294 (1980) 13
[2] P. Dufek, P. Blaha, K. Schwarz, Physical Review Letters 75 (1995) 3545
[3] L. Errico, G. Darriba, M. Rentería, Z. Tang, H. Emmerich, S. Cottenier, Physical Review B 77 (2008) 195118 (2008)
[4] H. Haas and J.G. Correia, Hyperfine Interactions 198 (2010) 133
[5] K. Lejaeghere, V. Van Speybroeck, G. Van Oost, S. Cottenier, Critical Reviews in Solid State and Materials Sciences 39 (2014) 124 (open access, http://dx.doi.org/10.1080/10408436.2013.772503)
[6] K. Lejaeghere, J. Jaeken, V. Van Speybroeck, S. Cottenier, Physical Review B 89 (2014) 014304

---

[*] Electronic address: `stefaan.cottenier@ugent.be`

P56

Thermoluminescence Behaviour and Kinetics Study of Tissue-equivalent LiF Phosphors at High Exposures of Gamma-rays

A.K. Sharma[1*], **Satinder Kumar**[2], **Ankush Vij**[3], **R. Dogra**[1], **Shalendra Kumar**[4], **S. P. Lochab**[5] **and Ravi Kumar**[1]

[1]*Beant College of Engineering & Technology, Gurdaspur – India.*
[2]*Department of Physics, Government College, Hamirpur – India.*
[3]*Centre of Material Science & Engineering, National Institute of Technology, Hamirpur-India.*
[4]*Changwon National University, South Korea*
[5]*Inter-University Accelerator Centre, Aruna Asif Ali Marg, New Delhi – India.*

We report the thermoluminescence (TL) properties of pure Lithium Fluoride (LiF) phosphors synthesized at different pH values by chemical co-precipitation method and irradiated with gamma-rays of ^{60}Co radioactive source at different doses of 15 Gy – 70 kGy. Single phase nanocrystalline structure has been confimed by XRD measurements and transmission electron microscope (TEM), however FESEM images indicate microcrystalline phase having a platelet cubic structure.

TL studies show a major glow peak around 418 K (145^{o}C) in addition to other low intensity peaks. LiF phosphors synthesized at 8.00 pH have maximum TL sensitivity and single glow peak at studied gamma doses ranging from threshold to high exposures. TL-kinetics study of LiF phosphors reveals that the major peak in the TL glow curve is almost resolved from other peaks, which has been analyzed using Chen's peak shape method to determine the TL-kinetics parameters. Although TL intensity almost increases linearly, but activation energy and frequency factor has been found to be decreasing with increasing gamma dose. The observed single glow peak near 200^{o}C, high TL sensitivity from threshold to high exposures and its effective atomic number close to biological tissue identifies LiF to be potential candidate for personnel dosimetry.

*Electronic Address: arvind_bcet@yahoo.com

P57

Nuclear magnetic resonance of short-lived β-emitter ^{12}N in H_2O

M. Mihara,[1] S. Iwakiri,[1] M. Fukuda,[1] T. Minamisono,[1] J. Ohno,[1] M. Tanaka,[1]
R. Kambe,[1] S. Yamaoka,[1] K. Watanabe,[1] R. Yanagihara,[1] Y. Ishibashi,[2] K. Matsuta,[1] A. Ozawa,[2] D. Nagae,[2] T. Ohtsubo,[3] T. Izumikawa,[4] S. Momota,[5]
T. Nagatomo,[6] D. Nishimura,[7] A. Kitagawa,[8] M. Torikoshi,[8] and S. Sato[8]

*[1]Dept. Physics, Osaka Univ., 1-1 Machikaneyama, Toyonaka, Osaka 560-0043, Japan**
[2]Dept. Physics, Tsukuba Univ., 1-1-1 Tennodai, Tsukuba, Ibaraki 305-8577, Japan
[3]Dept. Physics, Niigata Univ., 8050, Ikarashi 2-no-cho, Nishi-ku, Niigata 950-2181, Japan
[4]RI Center, Niigata Univ., 1-757, Asahimachi-dori, Niigata 951-8510, Japan
[5]Kochi Univ. Technology, Tosayamada, Kami, Kochi 782-8502 Japan
[6]Riken Nishina Center, 2-1 Hirosawa, Wako, Saitama 351-0198, Japan
[7]Tokyo Univ. Science, 2641 Yamazaki, Noda, Chiba 278-8510, Japan
[8]NIRS, 4-9-1 Anagawa, Inage-ku, Chiba 263-8555, Japan

There have been very few β-NMR studies on liquid media so far, due to the difficulty of preparing liquid samples in vacuum for low energy implantation of β-NMR probe nuclei. However, spin polarized unstable nuclear beams with energies of several tens MeV/nucleon easily make it possible to implant the beam into a wrapped liquid sample placed in the atmosphere. In the present study, we have performed the β-NMR of short-lived β-emitter ^{12}N ($I = 1$, $T_{1/2} = 11$ ms) in H_2O, using a spin polarized ^{12}N beam with an energy of about 50 MeV/nucleon [1].
Figure 1 shows a β-NMR spectrum of ^{12}N in H_2O measured at room temperature together with that in Pt. The resonance was found for H_2O with a frequency shift lower by about 1500ppm than for Pt, which can not be explained with a normal chemical shift of 500ppm at most in the case of nitrogen compounds.

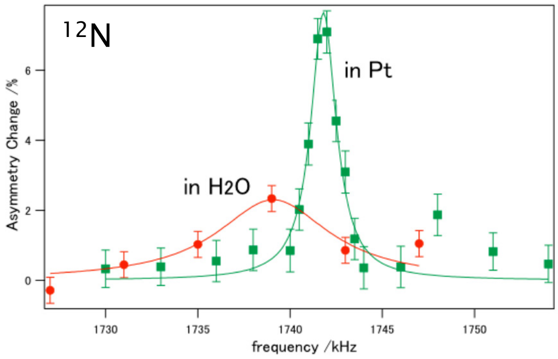

FIG. 1: β-NMR spectrum of ^{12}N in H_2O at room temperature and at $B_{\mathrm{ext}} = 0.5$ T.

[1] M. Mihara et al., Hyperfine Interactions **220**, 83 (2013).

---

*Electronic address: `mihara@vg.phys.sci.osaka-u.ac.jp`

P58

Effect of U substitution on the magnetism in the geometrically frustrated antiferromagnet YMn_2 studied through TDPAC spectroscopy.

S.K. Moshanta and S.N. Mishra

Tata Institute of Fundamenta Research, Homi Bhabha Road, Mumbai-400005, India

The Laves phase compound YMn_2 is an archetypical geometrically frustrated antiferromagnetic system with Mn moments ordering in a helical structure with T_N ~ 110 K [1]. The tetrahedrally coordinated Mn moments are known be dominated by quantum spin fluctuation giving rise to many novel behavior [2]. Addition of small quantity of Sc is known to increase spin fluctuation while, substitution of elements like Al, Fe, Co etc leads to its suppression. Here, we present our results on the magnetic behavior of $Y_{1-x}U_xMn_2$ ($0 < x < 0.1$), studied through hyperfine interaction of ^{111}Cd using TDPAC method. The hyperfine fields measured in the temperature range 20 – 300 K reveal first order magnetic transition for the undoped YMn_2, in agreement with the earlier results. With U doping, the magnetic transition rapidly decreases, becoming paramagnetic at x = 0.1. The progressive suppression of magnetism and increase in spin fluctuation behavior is also observed in the electric quadrupole interaction frequency $\nu_Q(T)$. Interestingly, our ν_Q data for the paramagnetic alloy at x = 0.1, show unconventional temperature dependence which may be due to inherent spin fluctuations arising from geometrical frustration. Details of the magnetic phase diagram will be discussed.

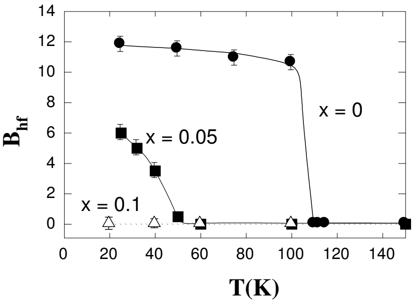

Fig. 1: Temperature dependence of ^{111}Cd magnetic hyperfine B_{hf} for in $Y_{1-x}U_xMn_2$

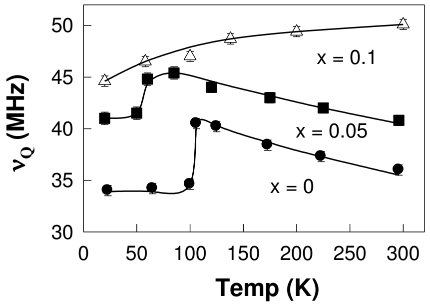

Fig. 2: Quadrupole interaction frequency ν_Q of ^{111}Cd in $Y_{1-x}U_xMn_2$

---

[1] M. Shiga, Physica B, **149**, 293 (1988).
[2] C. Lacroix, A. Solonstov and R. Ballou, Phys. Rev. B, **54**, 15178 (1996).

Electronic address: mishra@tifr.res.in

P59

Unusual temperature dependence of quadrupole interaction at ^{111}Cd in UMn$_2$.

S.N. Mishra

Tata Institute of Fundamenta Research, Homi Bhabha Road, Mumbai-400005, India

The subject of moment stability and magnetic order in geometrically frustrated Laves phase compounds RMn$_2$ (R = rare-earth and actinide elements) continues to be a topic considerable interest [1]. The compound UMn$_2$, crystallizing in the C-15 type cubic Laves phase is an interesting case as it shows stable local moment at high temperatures but lacks any magnetic ordering [2]. The compound has also been reported to show structural distortion at ~ 240K. Here, we present our results on the structural and magnetic behavior of UMn$_2$ obtained from hyperfine field measurements for ^{111}Cd probe using TDPAC method. From the quadrupole interaction pattern observed at room temperature, the probe atoms are identified to substitute at the Mn site. Upon cooling the sample, the PAC patterns continue to show pure quadrupole interaction down to 20 K, indicating the absence of magnetic order. Interestingly, the quadrupole interaction frequency $\nu_Q(T)$, displayed in Fig. 1, shows perceptible decline at low temperatures, which is opposite to the trend commonly observed in metallic alloys. We believe, this unusual temperature dependence of the quadrupole interaction frequency arise due to dynamic lattice distortion driven by spin fluctuations inherently built into the system via topological frustration.

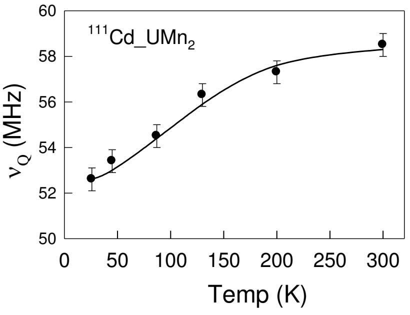

Fig.1 $\nu_Q(T)$ of ^{111}Cd in UMn$_2$.

---

[1] M. Shiga, Physica B **149**, 293 (1988)
[2] S. Giri, H. Nakamura and M. Shiga, Phys. Rev. B, **61**, 12233 (2000)

Electronic address: mishra@tifr.res.in

P60

Local Structure and Molecular Motions in Imidazolium Malonate Crystal as Studied by ^{2}H and ^{13}C NMR

Motohiro Mizuno[1], **Mizuki Chizuwa**[1], **Tsuyoshi Umiyama**[1], **Ryutaro Ohashi**[1], **Tomonori Ida**[1], **Masataka Tansho**[2], **Tadashi Shimizu**[2]

[1] *Department of Chemistry, Graduate School of Natural Science and Technology, Kanazawa University, Kakuma, Kanazawa, Ishikawa 920-1192, Japan*
[2] *National Institute for Materials Science, 3-13 Sakura, Tsukuba, Ibaraki 305-0003, Japan*

Imidazolium salts of dicarboxylic acids are known to show relatively high proton conductivity [1]. Imidazole and dicarboxylic acid are connected by the hydrogen bond and form a two-dimensional network in the crystal of these salts (Fig. 1). The proton conductivity is dominated by the continuous proton transfer in the hydrogen network between imidazolium ions and the carboxyl group and the reorientational motions of the imidazolium ion such as 180º flip and libration are predicted to play an important role [2]. In these crystals, only imidazolium malonate has the disordered imidazole ring. The proton conductivity of imidazolium malonate is above 10^{-3} S/m around room temperature. In the present work, we investigated the disorder structure and the molecular motion in imidazolium malonate using solid-state ^{2}H, ^{13}C NMR. The relation between these local structure and proton conductivity is discussed. For the measurement of ^{2}H NMR, the sample was prepared using imidazole (imidazole-d_3) in which hydrogen bonded to carbon was replaced by deuterium.

Fig. 2 shows the temperature dependence of the ^{2}H NMR Carr-Purcell-Meiboom-Gill (QCPMG) spectrum for the powder sample of imidazolium-d_3 malonate. The linewidth of each peak of QCPMG spectrum increased with increasing temperature. The temperature variation of line shape of QCPMG spectrum was well explained by 180º flip of the imidazolium ion (Fig. 1(b)). The apparent difference in mobility between ordered site and disordered site was not observed. The red lines in Fig. 2 show simulation considering 180º flip of the imidazolium ion. The rate k for the 180˚ flip of the imidazolium ion estimated from the spectral simulation was shown in Fig. 2 (c). The activation energy of the 180˚ flip of the imidazolium ion was 53 kJmol^{-1}.

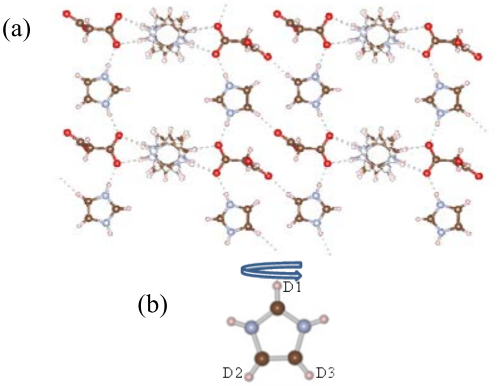

Fig.1 (a) Crystal structure of imidazolium malonate [1]. (b) 180 ˚ flip of imidazolium ion.

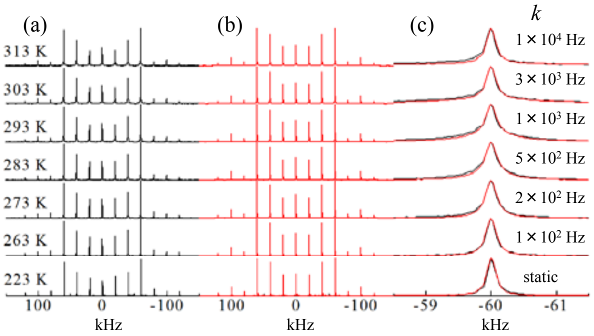

Fig. 2 Temperature dependence of the ^{2}H NMR QCPMG spectrum for imidazolium-d_3 hydrogen malonate crystal. (a) observed spectra at 45.282 MHz, (b) simulation spectra, (c)expansions of (a) and (b).

---

[1] K. Pogorzelec-Glaser, J. Garbarczyk, Cz. Pawlaczyk, E. Markiewicz, *Mat. Sci. Pol.* **24**, 245 (2006).
[2] T. Umiyama, R. Ohashi, T. Ida, M. Mizuno, *Chem. Lett.*, 42, 1323 (2013).

Electronic addrtess: *Presenting. mizuno@se.kanazawa-u.ac.jp*

P61

Fabrication and modification of nano-structure by means of ion-beam induced expansion effect

S. Momota[1], **X. Guo**[1], **N. Sato**[1], **S. Tezuchi**[1], **H. Tokaji**[1]

[1] *Kochi Univ. of Tech., Tosayamada, Kami, Kochi, 782-8502, JAPAN*

The expansion effect of crystal materials, which is irradiated by ion beams, has investigated [1] and explained by lower density in an irradiated region [2]. It is expected that this expansion effect would be hopeful candidate to develop new fabrication process for three-dimensional structures in sub-micro meter scale. Our group has performed experimental studies to confirm the feasibility of the expansion effect as a new technique to fabricate or modify structures in sub-micron scale.

Ar and Kr beams with energy E = 1~3 keV/A were irradiated on Si crystal. In this energy region, the nuclear part of dE/dx is dominant and it is evaluated that the expansion would originate in a displacement of Si atoms. In our previous studies, it was proved that a swelling height of Si surface could be controlled by changing a fluence of Ar beam [3]. Recently, we have modified cross section of a stripe structures on Si surface by irradiating Kr beam and the results indicated that the modification of cross section shows direction dependence [4].

In this paper, the direction dependence of the ion-beam induced expansion is investigated by comparing the geometrical change of nano-structure along a lateral and a normal direction. Observed expansion induced by Ar- and Kr-beam shows different behavior. The productivity of defects, created by the displacement of Si atoms, strongly depends on atomic number of irradiated ions. Observed ion-beam dependence will be discussed based on defects induced by ion beam, which was evaluated by RAMAN spectroscopy.

---

[1] O.W. Holland, B.R. Appleton, J. Narayan, *J. Appl. Phys.* **2295-2301**, 54(1983).
[2] J. S. Custer, et al., *Appl. Phys. Lett.* **437-439**, 64(1994).
[3] J. Zhang, S. Momota et al., *Nucl. Instr. and Meth.*, **17–20**, B 282(2012).
[4] to be published

Electronic address: *momota.sadao@kochi-tech.ac.jp*

P62

Studies of Ga NMR and NQR in $SrGa_4$

H. Niki [1], **N. Higa**[1], **S. Nakamura**[1], **H. Kuroshima**[1], **T. Toji**[1], **M. Yogi**[1],
A. Nakamura[1], **M. Hedo**[1], **T. Nakama**[1], **Y. Ōnuki**[1], **H. Harima**[2]

[1] *Faculty of Science, University of the Ryukyus, 1 Senbaru, Nishihara, Okinawa 903-0213, Japan*
[2] *Faculty of Science, Kobe University, Nada-ku, Kobe 657-8501, Japan*

$EuGa_4$ with the $BaAl_4$-type body center tetragonal structure orders antiferromagnetically at $T_N = 16$ K. In the paramagnetic phase, the magnetic susceptibility of $EuGa_4$ follows the Curie-Weiss law with a positive Curie-Weiss temperature $\theta_P = +3$ K. The effective magnetic moment is 7.86 μ_B, indicating Eu^{2+} electronic stae ($J = S = 7/2$) [1]. Ga atoms have two crystallographically inequivalent sites. In order to microscopically investigate the magnetic properties in $EuGa_4$, the NMR measurements of a powder sample in $EuGa_4$ were carried out [2]. In the paramagnetic phase, the nuclear relaxation times of the Ga NMR would be very fast since the fluctuation of the Eu moment is extremely large because of the large magnetic moment of Eu. Therefore, only one pair of $^{69\&71}$Ga NMR spectra at the site II can be obtained. The Knight shift shifts largely to negative side with decreasing temperature due to the RKKY interaction. The temperature dependence of the Knight shift is well consistent with that of the magnetic susceptibility. In the antiferromagnetic phase, the NMR spectra of $^{69\&71}$Ga at the site II and ^{153}Eu were obtained by the zero field NMR.

To well understand the behaviors of Ga(I) and Ga (II) sites, the NMR and NQR measurements of the $^{69\&71}$Ga in nonmagnetic $SrGa_4$ have been carried out. The crystal structure of $SrGa_4$ is the same structure as $EuGa_4$. High-quality single crystal of $SrGa_4$ was grown by the Ga-self flux method. NMR measurements using the powder sample of $SrGa_4$ have been done applying in the external magnetic field of approximately 6.5 T.

The ^{69}Ga NMR spectra corresponding to the sites I and II are obtained. The Knight shifts of the ^{69}Ga(I) and ^{69}Ga(II) shift slightly to the negative side with decreasing temperature due to the core polarization of the *d*-electrons. The values of the Knight shift of the ^{69}Ga(I) and ^{69}Ga(II) are 0.01 and -0.11 % at 4.2 K, and 0.09 and -0.08 % at 300 K, respectively. The values of the $1/T_1T$ of the NMR of both ^{69}Ga(I) and ^{69}Ga(II) are almost constant between 4.2 and 100 K, whose values are 1.5 $s^{-1}K^{-1}$ at ^{69}Ga(I) and 0.12 $s^{-1}K^{-1}$ at ^{69}Ga(II), while the $1/T_1T$ is slightly increased above 100K with increasing temperature. The value of T_1 of ^{69}Ga(I) is one order of magnitude less than that of ^{69}Ga(II). The nuclear relaxation time at Ga(I) is very faster than that at Ga(II) in $SrGa_4$. The same situation would occur in the case of Ga(I) site in $EuGa_4$. Therefore, the Ga(I) NMR spectra could not be detected due to the very fast nuclear relaxation time in $EuGa_4$.

The NMR spectrum of $^{69\&71}$Ga (a spin $I = 3/2$) in the powder sample of $SrGa_4$ does not take a typical powder pattern caused by the NQR interaction because of the very strong anisotropy of the Knight shift, which indicates that the nonuniform distribution of crystal orientation in the powder sample occurs. From the analysis of the Ga NMR spectrum, it is found that the *ab* plane of the crystal is parallel to the external magnetic field, which would be attributed to the anisotropy of the magnetic susceptibility with the easy axis parallel to the *ab* plane. This result is also confirmed by the ^{69}Ga NQR in $SrGa_4$.

[1] S. Bobev *et al.*, J. Magn. Magn. Mater. **277** 236 (2004).
[1] M. Yogi *et al.*, J. Phys. Soc. Jpn. **82,** 103701 (2013).

Electronic addrtess: *niki@sci.u-ryukyu.ac.jp*

P63

The ^{57}Fe hyperfine interactions in iron storage proteins in liver and spleen tissues from normal human and two patients with mantel cell lymphoma and acute myeloid leukemia: a Mössbauer effect study

M.I. Oshtrakh[1,2], **I.V. Alenkina**[1,2], **A.V. Vinogradov**[3], **T.S. Konstantinova**[3],
V.A. Semionkin[1,2]

[1]*Department of Physical Techniques and Devices for Quality Control and*
[2]*Department of Experimental Physics, Institute of Physics and Technology,*
Ural Federal University, Ekaterinburg, 620002, Russian Federation;
[3]*Ural State Medical University, Repin str., 3, Ekaterinburg, 620028, Russian Federation*

Liver and spleen tissues contain a large amount of iron deposited in iron storage proteins ferritin and hemosiderin. Ferritin consists of a nanosized ferrihydrite iron core surrounded with 24 protein subunits shell. The cavity for the iron core is about 8 nm and the largest amount of iron atoms may be of about 4500. Hemosiderin is considered as denatured ferritin. In the case of pathologies related to the iron status disorder in the body the iron core structure and size may vary from more amorphous to more crystalline and from smaller to larger size. The variations in the iron core structure may be reflected by the ^{57}Fe hyperfine parameters. Therefore, in the present work we studied samples of human normal and patients' liver and spleen tissues using Mössbauer spectroscopy with a high velocity resolution.

Fresh spleen and liver tissues were obtained from normal human and from two patients with mantel cell lymphoma and acute myeloid leukemia. Samples were lyophilized and powdered, then measured using Mössbauer spectrometric system with a high velocity resolution at 295 K. The Mössbauer spectra of spleen and liver tissues were fitted using two quadrupole doublets 1 and 2 related to the iron core. The residual amount of hemoglobin was found in some tissues. Small variations in the ^{57}Fe hyperfine parameters for corresponding quadrupole doublets for normal and patient's tissues (Fig. 1) as well as different areas of these quadrupole doublets were found. The results obtained indicated different small changes in the iron cores of iron storage proteins in liver and spleen tissues from two patients with mantel cell lymphoma and acute myeloid leukemia in comparison with those in normal human liver and spleen tissues.

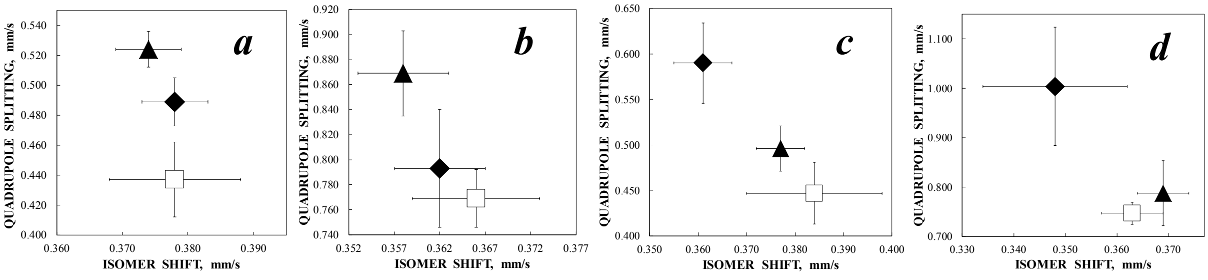

Fig. 1. Plots of the ^{57}Fe hyperfine parameters for normal human tissues (☐), patients with mantel cell lymphoma (◆) and acute myeloid leukemia (▲): liver tissues, quadrupole doublet 1 (***a***) and quadrupole doublet 2 (***b***); spleen tissues, quadrupole doublet 1 (***c***) and quadrupole doublet 2 (***d***).

Electronic address: *oshtrakh@gmail.com*

P64

Phase transformation of iron in hydroxyapatite in the activation of *n*-octane

D. Padayachee[1], **Venkata D. B. C. Dasireddy**[1], **K. Bharuth-Ram**[1,2], **S. Singh**[1] **and H. B. Friedrich**[1]

[1]*School of Chemistry and Physics, University of KwaZulu-Natal, Durban, South Africa*
[2]*Physics department, Durban University of Technology, Durban 4000, South Africa*

Great demand for olefins exists in the chemical industry worldwide [1]. A promising route for the production of these olefins is through the activation of *n*-octane over hydroxyapatites [2]. Catalytic performance in the activation of *n*-octane relies on the acid-base properties of the material or on the isolated cations capable of activating C-H bonds [3]. Previous reports stimulated the use of iron oxide and iron phosphate materials in the activation of C-H bonds [4].

Iron (3 wt%) substituted hydroxyapatite catalysts, used in the activation of *n*-octane, were prepared using two methods. Firstly, using a co-precipitation technique and secondly, using a wet impregnation technique. This was done to compare the effect of iron substitution into hydroxyapatite and supporting iron on the surface of hydroxyapatite. By doing so, its corresponding influence on catalytic activity and the phase transformation of iron was established. The fresh, reduced, re-oxidised and used catalysts were characterized by room temperature X-ray diffraction (XRD), Raman spectroscopy, and Scanning Electron Microscopy. Rietveld refinement, performed on the XRD patterns of the catalysts, suggested that iron was substituted for calcium in hydroxyapatite, using the co-precipitation technique. However, iron was found on the surface of hydroxyapatite when the catalyst was prepared using the wet-impregnation technique.

Mössbauer spectroscopy was used to determine the phase of the iron in both catalysts, before and after the reaction conditions. The Mössbauer spectra showed the presence of an iron (III) oxide phase for both catalysts. After reduction, the iron substituted catalyst showed the presence of an iron (II) pyrophosphate ($Fe_2P_2O_7$) phase; the iron supported on hydroxyapatite catalyst showed the presence of iron (II) oxide phase. Upon re-oxidation, both catalysts showed the presence of iron (III) oxide. The same pattern was also observed in variable temperature XRD measurements which showed the reduction of Fe^{3+} to Fe^{2+}. Thus, a redox mechanism is followed by the catalysts in the activation of C-H bonds in the activation of *n*-octane as evidenced by Mössbauer spectroscopy and XRD.

[1] S. Albonetti, et al., *Catalysis Reviews* **38**, 413 (1996).
[2] V.D.B.C. Dasireddy, et al., *Applied Catalysis A: General* **467**, 142 (2013).
[3] V.D.B.C. Dasireddy, et al., *Applied Catalysis A: General* **456**, 105 (2013).
[4] F.B. Khan, et al., *Hyperfine Interactions* **197**, 317 (2010).

Electronic address: *Dasireddy@ukzn.ac.za, 207513702@stu.ukzn.ac.za*

P65

DFT Study of Electric-Field Gradients and Magnetic Fields at Dilute Cd Atoms Doping Al_2O_3 Near the (001) Surface

G. N. Darriba[1], R. Faccio[2] and M. Rentería[1]

[1]*Departamento de Física and Instituto de Física La Plata (IFLP, CONICET La Plata), Facultad de Ciencias Exactas, Universidad Nacional de La Plata, CC 67, 1900 La Plata, Argentina.**
[2]*Cryssmat-Lab, DETEMA, Facultad de Química, Universidad de la República, Gral. Flores 2124, P.O. Box 1157, Montevideo, Uruguay.*

In this work we present an electronic structure calculation study from first principles of Cd atoms located at and near the (001) α-Al_2O_3 semiconductor surface. In particular, we focus at the origin of the magnetic interaction that appears at Cd impurities located at this surface. For this, we studied the total and partial density of states projected at Cd and their nearest oxygen neighbors, as a function of the depth of the Cd atom from the (001) α-Al_2O_3 surface. Two methods with different basis set were used: the Full-Potential Augmented Plane Wave plus local orbitals (FP-APW+lo), using the WIEN2k code, and a linear combination of numerical localized atomic orbital basis sets, using the SIESTA code. The Cd impurity is located at Al substitutional sites in the reconstructed α-Al_2O_3 surface and as a function of the depth from the surface. Besides the appearance of the magnetic interaction, the electric-field gradient (EFG) at the topmost Cd atom at the equilibrium positions in the reconstructed surface is 4 times larger than the EFG at dilute Cd atoms located in bulk, in agreement with the experimental EFG ratio for ^{111}Cd atoms located at the surface and at bulk of metallic indium. Through these comparisons we demonstrated the large sensitivity of ^{111}Cd probe atoms for evaluating surface and bulk properties on Al_2O_3.

---

*Electronic address: *renteria@fisica.unlp.edu.ar*

P67

Optimum discretization of velocity scale in Mossbauer spectrum measurements

V.G.Semenov[1,2], S.M.Irkaev[2], V.V. Panchuk[1,2], A.A. Goydenko[2]

[1] *St.Petersburg State University,198504, St.Petersburg, Russia*
[2]*Institute for Analytical Instrumentation, St. Petersburg, Russia*

In modern spectroscopy is widely used representation of spectral information in discrete form. In this procedure becomes important signal digitization and selection discretization step Δ. For small values of Δ the number of points in the observed spectrum will be large and therefore accuracy of reproduction of the spectral function containing necessary analytical information is high. On the other hand a reduction Δ will decrease interval of time of each channel, which would reduce the number of accumulated pulses and this require increasing the time required for accumulating the spectrum with the necessary statistical accuracy. The accuracy is the value equal to the ratio of the signal amplitude to the average level of noise. For large values of the discretization step Δ number of channels is reduced, consequently, accuracy of reproduction of the spectral function is reduced due to the strong averaging of this function within the interval Δ. So this is the optimal discretization provides a representation of the desired spectral function with the required precision and a minimum number of channels. In this case, all points of the spectrum are significant to restore the original function and requires minimum time for their accumulation. Optimal sampling step is estimated by mistake restoration of of the spectral function.

The immediate aim of the Mossbauer experiment is the registration intensity of gamma rays connected with the processes of resonance absorption or scattering in a certain energy range. For the process of energy scanning is used Doppler modulation the energy of gamma rays emitted by the source. Modulation is performed using a mechanical motion of the source relative to investigated sample in the required velocity range.

In the work describes the main approaches for selecting the optimum width channels at a discretization of the velocity scale in the accumulation of the Mössbauer spectra by means of multi-channel накопитель. One is based on an analysis of the Kotel'nikov-Shannon's frequency criterion, the second - is based on an analysis of errors that arise in the case of a differential representation of the spectrum. In this case, the analysis is conducted in two phases: the first phase is considered the ideal shape distortion of the spectrum due to the sampling velocity of the scale and the second takes into account the influence of the statistical spread in the spectrum. At the second stage, the notion of quality of the spectrum (S / N). To estimate the width of the channel in each approach the mathematical expression.

The reported study was partially supported by RFBR, research project No. 13-08-00623-a.

P68

Calibration of Recoil-In-Vacuum attenuations from first principles: comparison with recent experimental data on Fe isotopes.

Blank line (12 points)

N.J.Stone[1,2], **J.R.Stone**[1,2], **A.E.Stuchbery**[3] **and P. Jönsson**[4]

Blank line (12 points)

[1] *Dept. of Physics and Astronomy, University of Tennessee, Knoxville, TN 37996, USA*
[2] *Dept. of Physics, Oxford University, Oxford, OX1 3PU, U.K.*
[3] *Dept. of Nuclear Physics, Australian National University, Canberra ACT 0200 Australia*
[4] *Malmo University, 20506 Malmo, Sweden*

Blank line (12 points)

Precession of aligned nuclear spin systems in ions recoiling from the target into vacuum (RIV) with consequent attenuation of angular distributions of emitted radiation is, in principle, a versatile method for measurement of *g* factors of nuclear excited states of lifetimes in the picosecond range [1,2]. Calibration of the observed attenuations has been achieved in favourable cases through comparison with measurements on states having known *g* factors and lifetimes. The lack of suitable known *g*-factor states, and the considerable effort required to perform empirical calibrations, have limited the application of the RIV method.

This paper sets forth the present status of efforts to describe the states of excited ions recoiling into vacuum in detail so that the average hyperfine interaction can be estimated with useful precision from a-priori theory. The calculations use the GRASP2K package [3] to obtain, for each recoiling ion change state, the individual possible electronic states, their configurations, lifetimes and hyperfine interactions. It is assumed that all possible ionic states are produced, up to a chosen excitation energy. This energy is selected to approximate the energy at which all states have lifetimes far shorter than the nuclear state of interest. It is further assumed that the ionic state total electron angular momenta are randomly oriented in space.

The first estimates of the average attenuation of emission distributions, as a function of the product $g\tau$ of the nuclear state *g* factor and lifetime, used an averaged precession frequency obtained neglecting transitions between electronic states. Improved calculations, which include decay of electronic states having lifetimes shorter than the lifetime of the nuclear state, will be described and compared with recent experimental results on recoiling Fe ions.

[1] N.J. Stone et al., Phys. Rev. Lett. **94,** 192501 (2005)
[2] A.E. Stuchbery and N.J. Stone, Phys Rev C **76**, 034307 (2007)
[3] P. Jönsson et al., Comp. Phys. Comm. **177**, 597 (2007) and **184**, 2197 (2013)

Electronic address: *n.stone@physics.ox.ac.uk*

P69

The influence of Joule heating on the structural properties of $Fe_{73}Al_5Ga_2P_8C_5B_4Si_3$ amorphous ribbons

R. A. Susilo[1], **J. M. Cadogan**[1], **D. Triyono**[2]

[1] *School of Physical, Environmental and Mathematical Sciences, UNSW Canberra at the Australian Defence Force Academy, Canberra BC 2610, Australia*
[2] *Departemen Fisika – FMIPA, Universitas Indonesia, Depok, 16424, Indonesia*

The structural properties of Joule heated $Fe_{73}Al_5Ga_2P_8C_5B_4Si_3$ amorphous ribbons have been studied using x-ray diffraction, differential scanning calorimetry (DSC) and ^{57}Fe Mössbauer spectroscopy. DSC measurements on the as-cast sample show that this alloy undergoes a two-step crystallization process in the temperature range between 700 K and 850 K, consistent with resistivity measurements [1]. The first crystallization process starts after Joule heating with a current of 2.0 A, leading to the formation of crystalline α-Fe-like precipitates (bcc), and the second crystallization process occurs after Joule-heating with a current of 2.5 A. The occurrence of the minimum coercive field of this material after Joule heating with a current of 1.5 A ($J \sim 12$ A/mm^2), which was attributed to the structural relaxation caused by heat treatment [1], is confirmed by our Mössbauer measurements. As seen in Figure 1, there is no noticeable change in the hyperfine field distribution between the as-cast and the sample Joule heated with a current of 1.5 A. This observation, along with the absence of crystallinity in the sample, suggests that the magnetic softness of this alloy upon heat treatment is indeed caused by stress-relief or structural relaxation.

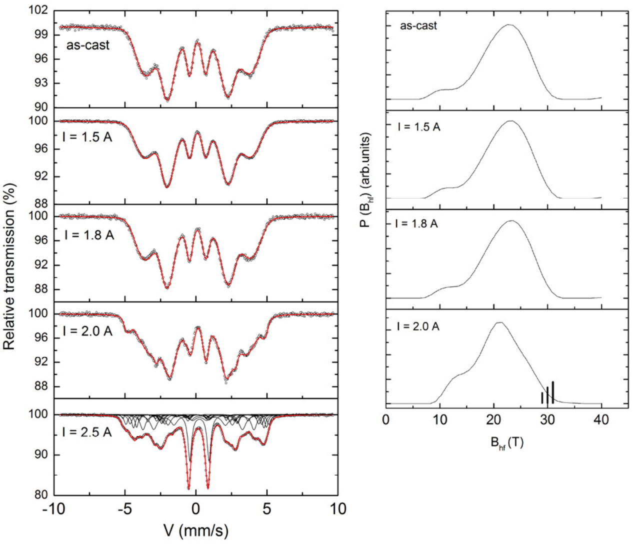

Fig. ^{57}Fe Mössbauer spectra (295 K) of the as-cast and Joule heated $Fe_{73}Al_5Ga_2P_8C_5B_4Si_3$ amorphous ribbon.

[1] R.S. Turtelli, D. Triyono, G. Badurek, M. Schönhart, R. Grössinger, C.D. Dewhurst, H. Sassik and C. Bormio-Nunes. J. Magn. Magn. Mater. **281**, 364 – 371 (2004).

Electronic address: *resta.susilo@student.adfa.edu.au*

P70

TDPAC studies of interaction between He and *A* = 140 elements in Fe

Y. Ohkubo, A. Taniguchi, Q. Xu, M. Tanigaki, K. Sato

Research Reactor Institute, Kyoto University, Kumatori, Sennan, Osaka 590-0494, Japan

As far as we know, the state of impurities He and Ce in Fe was not studied experimentally until our previous work [1]. This knowledge is important in materials science related to nuclear fusion reactor materials. With the TDPAC method on ^{140}Ce as probe nuclei arising from ^{140}Cs via ^{140}Ba and then ^{140}La, we obtained the result that the parent atoms (La and Ba) of ^{140}Ce very efficiently trap He both doped in Fe and they form complexes in Fe, which do not have a definite geometrical structure.

This time, we prepared an Fe sample by implanting 4-keV He and then 100-keV ^{140}Cs, this doping order being opposite to the case in [1]. Figure 1 shows room-temperature TDPAC spectra for (a) ^{140}Ce in Fe (as a reference) and (b) ^{140}Ce in He-doped Fe, subjected to no annealing, 0.5-h annealing in vacuum at 473 K, 673 K, 773 K, and 1073 K (after annealed at 873 K and 973 K). The oscillation pattern seen in Fig. 1 is due to a unique static magnetic hyperfine interaction at ^{140}Ce occupying the Fe substitutional site with no lattice defects nearby [2]. With annealing, the oscillation amplitude gets reduced. This is because in case of (a) vacancies bonded to these ^{140}Ce and in case of (b) both He and vacancies did so. However, in He-doped Fe, these ^{140}Ce are not susceptible to defects below around 700 K.

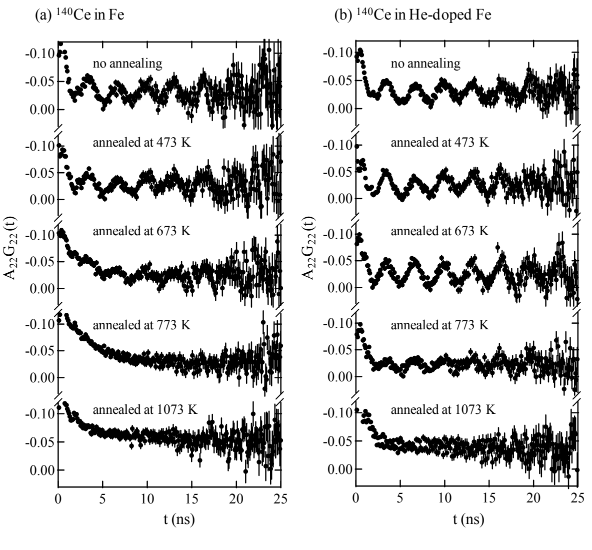

Fig. 1 Room-temperature TDPAC spectra for (a) ^{140}Ce in Fe and (b) ^{140}Ce in He-doped Fe, subjected to no annealing, 0.5-h annealing in vacuum at 473 K, 673 K, 773 K, and 1073 K.

---

[1] Y. Ohkubo et al., accepted for publication in *Phi. Mag. Lett.*

[2] Y. Ohkubo et al., *Phys. Rev. C* **87**, 044324 (2014).

Electronic address: *tanigaki@rri.kyoto-u.ac.jp*

P71

TDPAC measurement of hyperfine fields at Pm impurities in Fe

M. Tsuneyama[1], M.Tanigaki[2], A.Taniguchi[2], Q. Xu[2] and Y. Ohkubo[2]

[1] *Graduate School of Science, Kyoto University, Sakyo-ku, Kyoto, 606-8502, Japan*
[2] *Research Reactor Institute, Kyoto University, Kumatori, Osaka, 590-0494, Japan*

The magnetic hyperfine fields B_{HFF} at impurities in materials are useful in evaluating first-principle calculations in condensed matter physics. Recently, Torumba *et al.* derived values of B_{HFF} at lanthanide impurities in Fe by first-principle calculations and compared the results with experimental B_{HFF} values [1]. However, the comparison is not sufficient because of the limited number of reliable experimental B_{HFF} results. In the case of Pm impurities in Fe, although two experimental results are reported, $B_{\mathrm{HFF}} = 406 \pm 100$ T [2] and 284 ± 35 T [3], these values were obtained using the low-temperature nuclear orientation (LTNO) method with an unreliable two-site model which assumes that impurities are only located at sites either full or no B_{HFF}.

This time, we attempted to measure a reliable room-temperature experimental value of B_{HFF} at Pm impurities in Fe by means of the time-differential perturbed-angular-correlation (TDPAC) method. The TDPAC method does not need such an unreliable assumption as the two-site model. In addition, TDPAC is free from the skin effect which is critical for NMR measurements.

The sample used is an Fe foil irradiated with 100-keV ^{147}Nd ($I^{\pi} = 5/2^{-}$, $T_{1/2} = 10.98$ d), a parent nuclide of ^{147}Pm, available at the ISOL of Kyoto University Research Reactor Institute (KUR-ISOL). The Larmor precession for the 91-keV state in ^{147}Pm ($I^{\pi} = 5/2^{+}$, $\mu = 3.22 \pm 0.16\ \mu_{\mathrm{N}}$, $T_{1/2} = 2.50$ ns) was observed through the 440−91-keV γ−γ cascade. TDPAC measurements were performed in two geometries of $\theta = \pm 135°$ and $\theta = 90°$ and 180° correlations. In the $\theta = \pm 135°$ correlations, three $\mathrm{BaF_2}$ scintillation counters were used and a 3 kG magnetic field was applied perpendicularly to the detector plane. In $\theta = 90°$ and 180° correlations, four $\mathrm{BaF_2}$ counters were used and a 8 kG magnetic field was applied similarly to the case of $\theta = \pm 135°$ correlations.

In the present experiment, the statistical errors in the TDPAC spectra were so large that a reliable value could not be obtained for B_{HFF} at Pm impurities in Fe. Possible improvements will be presented in the Conference.

References

[1] D. Torumba, P. Novak and S. Cottenier, *Phys. Rev. B* **77**, 155101 (2008).
[2] B. D. D. Singleton *et al.*, *Hyp. Interact.* **75**, 471 (1992).
[3] J. Goto *et al.*, *Hyp. Interact.* **136/137**, 561 (2001).

Electronic address: m.tsuneyama@rri.kyoto-u.ac.jp

P72

Iron (III) sulfide particles produced by a polyol method

Ryo Shimizu,[1] Ippei Kubono[1], Yoshio Kobayashi[2, 3], Yasuhiro Yamada[1]

[1] *Tokyo University of Science, 1-3 Kagurazaka, Shinjuku-ku, Tokyo 162-8601, Japan*
[2] *The University of Electro-Communications, 1-5-1 Chofugaoka, Chofu, Tokyo 182-8585, Japan*
[3] *RIKEN, 2-1 Hirosawa, Wake, Saitama 351-0198, Japan*

Iron (III) sulfide Fe_2S_3 has been studied for a long time, but the structure and nature of metastable Fe_2S_3 are still unclear. Unstable phase has chance to be stabilized in a nanoparticle shape. We have produced various iron sulfide particles using a polyol method, and obtained the mixture of FeS, Fe_3S_4 and Fe_2S_3 varying the mixture ratio of the starting materials [1]. We found the best condition to maximize the yields of Fe_2S_3. A mixture of ferrocene (2 mmol), 1, 2-hexadecanediol (8 mmol), 1-octadecanethiol (8 mmol), and oleylamine (15 mL) was stirred for 1 h at room temperature and then refluxed for 2 h at 320 °C under an Ar flow. The resultant particles were investigated by Mössbauer spectroscopy, X-ray diffraction (XRD), and scanning electron microscopy (SEM).

SEM image of the particles was observed (Fig. 1), showing that the particles had rugged shape with sizes of 100-200 nm. The Mössbauer spectrum of the particles measured at 293 K (Fig. 2a) had two sets of doublet, which were assigned to FeS and Fe_2S_3. The Mössbauer spectrum measured at 6 K (Fig. 2b) showed the sextet of FeS (H = 32 T) with 11% of area intensity. Another sextet (H = 25 T) was assigned to Fe_2S_3. The broad absorptions having distributed hyperfine magnetic field was due to the small Fe_2S_3 crystalline size. The doublet was still observed at 6 K, and this doublet is Fe(III) species in the particles. XRD patterns of the iron sulfide particles (Fig.3) showed the combination of Fe_2S_3 and FeS.

It was shown that the metastable Fe_2S_3 particles were successfully produced by the polyol method. Though the Fe_2S_3 particles indicated sharp XRD peaks, the Mössbauer spectra showed a magnetic distribution and superparamagnetic nature due to its small crystallite size. The structure of Fe_2S_3 will be discussed based on density functional calculations.

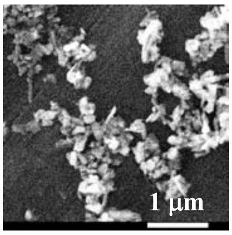

Fig. 1. SEM image of the iron sulfide particles

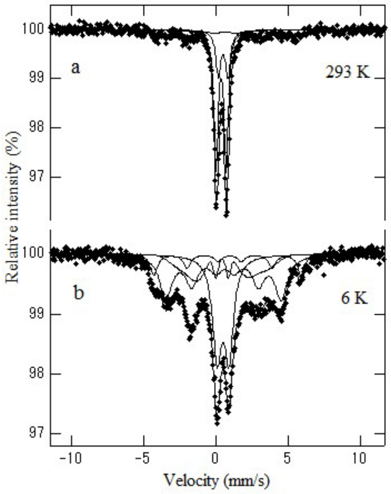

Fig. 2. Mössbauer spectra of the iron sulfide particles measured at 293 and 6 K.

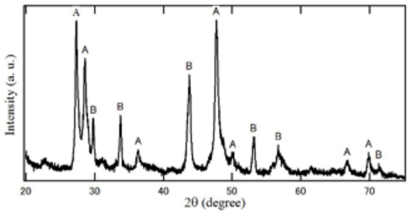

Fig. 3. XRD patterns of the iron sulfide particles. Fe_2S_3 (A) and FeS (B) were observed simultaneously.

---

[1] S. Shimizu et al., *J. Radioanal. Nucl. Chem.* (2013), submitted.

Electronic address: *yyasu@rs.kagu.tus.ac.jp*

P74

Ab initio calculations of electric field gradient and magnetic hyperfine field in Fe-doped SnO_2

Qiaoli Zhang, Daqing Yuan, Ping Fan, Yi Zuo, Yongnan Zheng, Xiaoqiang Ma, Juncheng Liang, Huanqiao Zhang and Shengyun Zhu

China Institute of Atomic Energy, PO Box 275-50, Beijing 102413, China

Much attention has been paid to study the diluted ferromagnetic semiconductors with a Curie temperature well above room temperature, which have potential applications in spin electronics. For a better understanding of the origin of the ferromagnetism, especially in the presence of O vacancies, the microscopic electronic structure and hyperfine fields are required. These can be obtained theoretically by an *ab initio* calculation.

In this paper, the *ab initio* calculations of the electric field gradients (EFG) and magnetic hyperfine fields in the Fe doped SnO_2 were performed by the Wien2k code embodying the full-potential linearized augmented plane-wave method for two charge states of the Fe impurity that occupies a substitutional site of Sn atom, which are related to two different cases of the neutral impurity state Fe^0 and the charged acceptor state Fe^{1-} or Fe^{2-}. The Fe doped SnO_2 system can provide one or two electrons via oxygen donor vacancies. Listed in the Table 1 are the calculated electric field gradients and their asymmetry parameters and the magnetic hyperfine fields at the Fe sites.

Table 1 Calculated electric field gradients, asymmetry parameters and magnetic hyperfine fields

Supercells	V_{33}(10^{21} V/m^2)	V_{33}direction	η	magnetic hyperfine field (T)
$(SnO_2)_{15}FeO_2$	15.03	Z	0.27	22.8
$(SnO_2)_{15}FeO$ (V_{O1})	10.36	Z	0.20	-45.2
$(SnO_2)_{15}FeO$ (V_{O2})	-4.68	X	0.64	-45.1
$(SnO_2)_{15}FeO$ (V_{O3})	3.15	Y	0.05	-49.4
$(SnO_2)_{15}FeO_2$+1e	2.85	Y	0.09	-45.5
$(SnO_2)_{15}FeO_2$+2e	7.30	X	0.11	-43.9

The present results illustrate clearly that the energy level splitting of the Fe-3*d* orbit with O vacancies and without O vacancies for the $(SnO_2)_{15}FeO_2$+1e and $(SnO_2)_{15}FeO_2$+2e valences resulted in increasing the unpaired electron number and leading the Fe atoms to the high spin states, causing the giant magnetic moment. Also, our calculation yields the ferric moment of 5 μ_B per ion for $(SnO_2)_{15}FeO_2$+1e. The details will be given.

Electronic address: *zql@ciae.ac.cn*

NOTES

UNSW
AUSTRALIA
Canberra

Don't let your brain drain.

Never Stand Still | Research Student Unit

Be involved in cutting edge research.
Study alongside high profile academic staff.
Scholarships available.

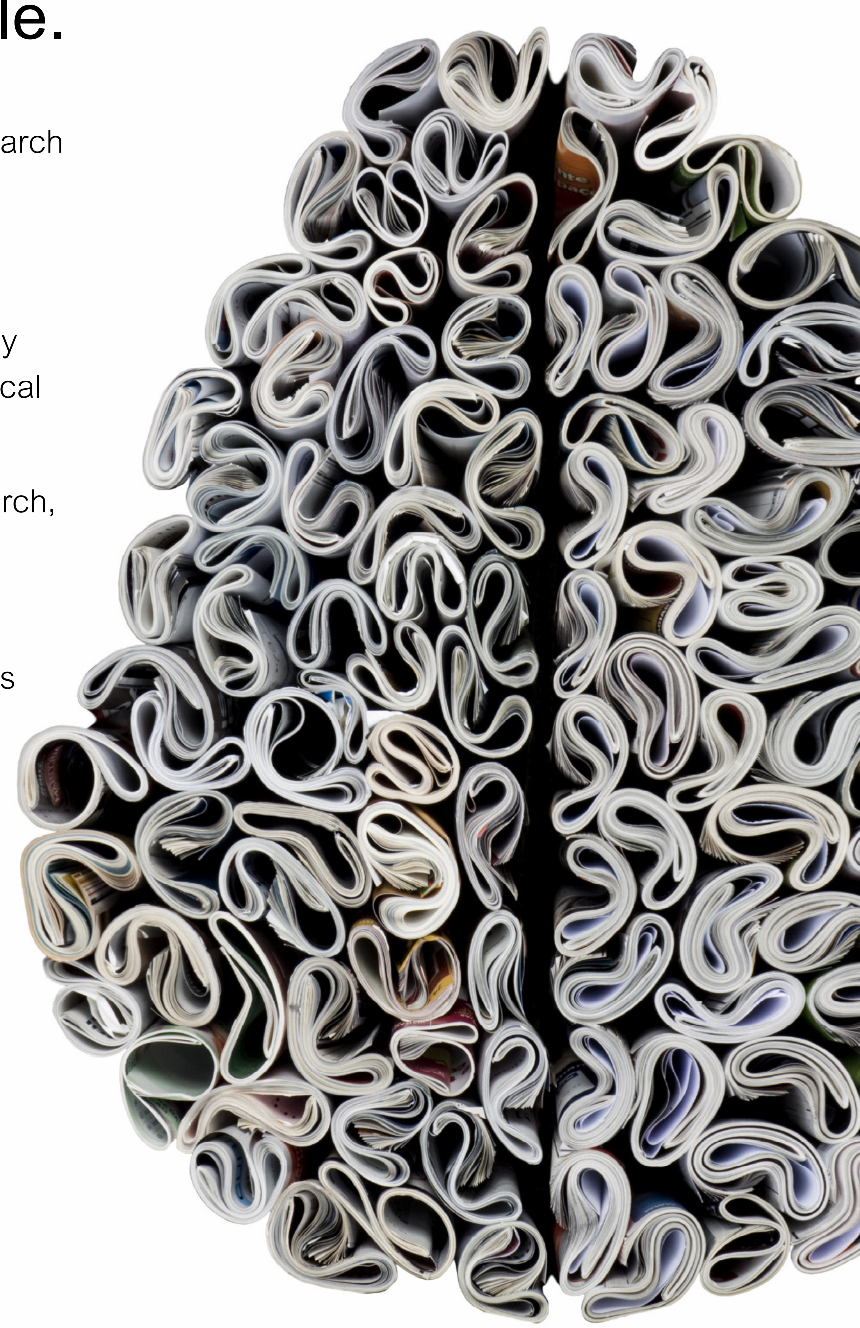

UNSW Canberra offers postgraduate research scholarships in the following disciplines:

- Humanities and Social Sciences
- Business
- Engineering & Information Technology
- Physical, Environmental & Mathematical Sciences

If you are considering postgraduate research, contact:

Research Student Unit
Ph: 02 6268 8597
W: sas.unsw.adfa.edu.au/rsu/scholarships

for more information and to learn about current and emerging research themes.

Enquire today for 2015 applications!

GROUP
OF EIGHT
AUSTRALIA

CRICOS Provider Number: 00100G

hfi nqi 2014 Canberra

JOINT INTERNATIONAL CONFERENCE ON
Hyperfine Interactions
AND SYMPOSIUM ON
Nuclear Quadrupole Interactions 2014

21–26 SEPTEMBER 2014 **THE SHINE DOME** CANBERRA AUSTRALIA